



THE HONG KONG
POLYTECHNIC UNIVERSITY

香港理工大學

Pao Yue-kong Library

包玉剛圖書館

Copyright Undertaking

This thesis is protected by copyright, with all rights reserved.

By reading and using the thesis, the reader understands and agrees to the following terms:

1. The reader will abide by the rules and legal ordinances governing copyright regarding the use of the thesis.
2. The reader will use the thesis for the purpose of research or private study only and not for distribution or further reproduction or any other purpose.
3. The reader agrees to indemnify and hold the University harmless from and against any loss, damage, cost, liability or expenses arising from copyright infringement or unauthorized usage.

IMPORTANT

If you have reasons to believe that any materials in this thesis are deemed not suitable to be distributed in this form, or a copyright owner having difficulty with the material being included in our database, please contact lbsys@polyu.edu.hk providing details. The Library will look into your claim and consider taking remedial action upon receipt of the written requests.

**A NOVEL MUCOSAL VACCINE FORMULATION AGAINST
TUBERCULOSIS BY EXPLOITING THE ADJUVANT
ACTIVITY OF S100A4—A DAMAGE-ASSOCIATED
MOLECULAR PATTERN MOLECULE**

OLIFAN ZEWDIE ABIL

PhD

The Hong Kong Polytechnic University

2023

The Hong Kong Polytechnic University

Department of Health Technology and Informatics

**A novel mucosal vaccine formulation against tuberculosis by
exploiting the adjuvant activity of S100A4—a damage-associated
molecular pattern molecule**

Olifan Zewdie Abil

A thesis submitted in partial fulfilment of the requirements for the
degree of Doctor of Philosophy

June 2023

CERTIFICATE OF ORIGINALITY

I hereby declare that this thesis is my own work and that, to the best of my knowledge and belief, it reproduces no material previously published or written, nor material that has been accepted for the award of any other degree or diploma, except where due acknowledgement has been made in the text.

_____ (Signed)

Olifan Zewdie Abil (Name of Student)

ABSTRACT

Tuberculosis (TB) is a disease that has afflicted humans for much of the recorded history. *Mycobacterium tuberculosis*, the causative agent of TB, is the world's leading cause of death by a single infectious agent, second only to SARS-CoV-2, which causes the COVID-19 infection during the pandemic. Vaccination is the most cost-effective strategy for preventing infectious diseases. Currently, the only vaccine approved for human use against TB is the bacillus Calmette-Guerin (BCG), which has a protective efficacy against extrapulmonary forms of TB in children. However, BCG is notoriously variable in protecting adolescents and adults, who account for the majority of pulmonary TB transmission. Therefore, new TB vaccine formulations that can elicit improved protective immunity for adults against the pulmonary form of TB are desperately needed.

In the first part of my thesis, it is demonstrated that S100A4 effectively augmented durable antigen-specific immune responses to the model vaccine antigen ovalbumin (OVA). S100A4, which could reach the pulmonary tissues and spleen after intranasal instillation, was capable of promoting the migration of dendritic cells and maturation of CD8 T cells. S100A4 facilitated antigen transport to nasal tissues and lymph nodes. Importantly, it is worth noting that S100A4 did not induce inflammation of the olfactory bulb, an organ that transmits smell information from the nose to the brain, which is vulnerable to the inflammatory stimulation by most microbial toxin-based adjuvants. In the second part of my work, a clinically relevant vaccine antigen derived from *Mycobacterium tuberculosis*, or ESAT-6, was admixed to S100A4 for intranasal immunization. S100A4 remarkably augmented the levels of anti-ESAT-6 IgG in serum and IgA in mucosal sites, including lung exudates, nasal mucosa, and bronchoalveolar lavage fluid (BALF). Furthermore, in both the lungs and the spleen, S100A4 strongly promoted ESAT-6-specific expansion of CD4 T cells. Upon reencounter with the immunizing antigen, CD8 T cells from S100A4-treated mouse spleen and lung tissues expressed higher levels of granzyme B, a toxic substance critical for cytotoxicity exhibited by these killer T cells. Both CD4 and CD8 T cells from these tissues expressed increased levels of IFN- γ , TNF- α , and IL-17, cytokines critical for antimicrobial activity. Antigen-reencounter-induced T cell proliferative responses, a key vaccine performance indicator, were augmented in the spleen of S100A4-adjuvanted mice.

In the current thesis work, I have sufficiently advanced our understanding of S100A4 as a potential mucosal adjuvant. I have provided compelling experimental evidence demonstrating that S100A4 can induce remarkable *Mycobacterium tuberculosis*-specific adaptive immune responses after intranasal immunization with a *Mycobacterium tuberculosis*-derived vaccine antigen with defined mechanisms. Thus, my work has laid a solid foundation for further exploration of the translational value of this molecule as a clinically applicable mucosal adjuvant for infectious diseases including TB.

RESEARCH OUTPUT

Conference presentations

1. **Olifan Zewdie**, Yu-Wen Yeh, Yuxuan WU, Arka Sen Chaudhuri, Nga Shan Li, Shuwei Liu and Zou Xiang. A novel mucosal vaccine formulation against tuberculosis by exploiting the adjuvant activity of S100A4—a damage-associated molecular pattern molecule. 4th ABCT Research Postgraduate Symposium, August 18, 2023, Hong Kong. (Shortlisted for oral presentation).
2. **Olifan Zewdie**, Yu-Wen Yeh, Yuxuan WU, Arka Sen Chaudhuri, Nga Shan Li, Shuwei Liu and Zou Xiang. A novel mucosal vaccine formulation against tuberculosis by exploiting the adjuvant activity of S100A4—a damage-associated molecular pattern molecule. Postgraduate symposium organized by the Department of Health Technology and Informatics, June 14, 2023, Hong Kong. (Shortlisted for oral presentation).
3. **Olifan Zewdie**, Yu-Wen Yeh, Yuxuan WU, Arka Sen Chaudhuri, Nga Shan Li, Shuwei Liu and Zou Xiang. A novel mucosal vaccine formulation against tuberculosis by exploiting the adjuvant activity of S100A4—a damage-associated molecular pattern molecule. The Hong Kong Polytechnic University Research Student Conference (PRSC-2023). May 8-9, 2023, Hong Kong. (Shortlisted for oral presentation).
4. Yu-Wen Yeh, Shuwei Liu, **Olifan Zewdie**, Nga Shan Li, Chujun Deng, Yuxuan Wu and Xiang Zou. Naturalization of laboratory mice for creating mouse asthma models that better mimic human asthmatic immune responses. The Hong Kong Polytechnic University Research Student Conference (PRSC-2023). May 8-9, 2023, Hong Kong. (Shortlisted for poster presentation)
5. Yuxuan Wu, **Olifan Zewdie**, Yu-Wen Yeh, Arka Sen Chaudhuri, Nga Shan Li, Yuxuan WU and Zou Xiang. A novel immunotherapy that outwits tumor cells. The Hong Kong Polytechnic University Research Student Conference (PRSC-2023). May 8-9, 2023, Hong Kong. (Shortlisted for oral presentation).

6. **Olifan Zewdie**, Yu-Wen Yeh, Yuxuan WU, Arka Sen Chaudhuri, Nga Shan Li, Shuwei Liu and Zou Xiang. A novel mucosal vaccine formulation against tuberculosis by exploiting the adjuvant activity of S100A4—a damage-associated molecular pattern molecule. Korean Association of Immunologists (KAI) international meeting. November 3-5, 2022, Songdo Convensia, Incheon, Korea. (International travel award from the meeting organizer).
7. Yu-Wen Yeh, Shuwei Liu, **Olifan Zewdie**, Nga Shan Li, Chujun Deng, Yuxuan Wu and Xiang Zou. Mouse naturalization—an effective approach for shaping mast cell tissue distribution. The Hong Kong Polytechnic University Research Student Conference (PRSC-2023). Korean Association of Immunologists (KAI) international meeting. November 3-5, 2022, Songdo Convensia, Incheon, Korea. (International travel award from the meeting organizer).
8. **Olifan Zewdie**, Yu-Wen Yeh, Yuxuan WU, Arka Sen Chaudhuri, Nga Shan Li, Shuwei Liu and Zou Xiang. Exploration of the adjuvant activity of S100A4 by flow cytometry for elucidating its impact on T cell activation in a mouse vaccination model. 26th Annual General and Scientific Meeting of the Hong Kong Society of Flow Cytometry. October 15, 2022, Hong Kong. (Shortlisted for poster presentation).

Publications

1. **Olifan Zewdie**, Yu-Wen Yeh, Yuxuan WU, Arka Sen Chaudhuri, Nga Shan Li, Shuwei Liu and Zou Xiang. A novel mucosal vaccine formulation against tuberculosis by exploiting the adjuvant activity of S100A4—a damage-associated molecular pattern molecule. (Manuscript for submission).
2. Arka Sen Chaudhuri, Yu-Wen Yeh, **Olifan Zewdie**, Nga Shan Li, Jia-Bin Sun, Tao Jin, Bin Wei, Jan Holmgren, Zou Xiang. S100A4 exerts robust mucosal adjuvant activity for co-administered antigens in mice. *Mucosal Immunol.* 2022; 15(5):1028–39.

ACKNOWLEDGEMENTS

First and foremost, I would like to express my gratitude to Almighty God for His protection and strength throughout my entire PhD journey. He always has a solution to every problem, a light in every shadow, and solace during every sorrowful moment. I will continue to put my faith in Him for my future. Thank you, Lord, for giving me favor in Your sight.

After a difficult and challenging journey, this PhD work becomes a reality. I could not have finished it without the kind support and assistance of many people who have been instrumental in my success.

I would like to express my profound gratitude to my supervisor Professor Zou Xiang. The tremendous support I received from the moment I contacted you about joining The Hong Kong Polytechnic University PhD program until the very end is exceptional. Your care has been palpable from the moment you welcomed me to The Hong Kong Polytechnic University until the end of my studies. Words cannot express how grateful I am for your exceptional academic supervision, knowledge, meticulous comments, and encouragement, all of which have contributed to my personal and professional growth during my PhD journey. Your office was always open for productive meetings and discussions, sometimes until late at night, as we worked on the articles and the PhD thesis. Professor Zou Xiang taught me not only advanced immunology and immunologic techniques, but also the rigorous scientific writing approach and the dedication to work. I can assure you that only the most fortunate students will have such an opportunity, and it has been a great privilege to work under your supervision. I cannot thank you enough for being such a wonderful mentor to me over the years. The difficult journey of my thesis would not have happened without your encouragement and supervision.

My heartfelt thanks go to all of the faculty members at Hong Kong Polytechnic University Department of Health Technology and Informatics. I would especially like to thank Professor Shea-ping Yip, Dr. Gilman SIU, Dr. Kenneth Cheng, Dr. Chi Ming Wong, Dr. Liang-Ting Lin, Dr. Chien-Ling Huang, and Dr. CAI, Yin David for their encouragement and support. Meanwhile, I hope to express my heartfelt gratitude to those who helped me as my assessors, listening to my work several times and providing me with valuable feedback and advice.

I want to express my gratitude to The Hong Kong Polytechnic University in particular for providing me the all-around assistance I needed to effectively complete my studies. The staff at the Centralized Animal Facility (CAF), The Hong Kong Polytechnic University, in particular Dr. Au Lai Shan, Alice, Mr. Tang Wang Him, Vincent, and Mr. Ho Hei Man, deserve my sincere gratitude for their unwavering support and assistance throughout my entire small animal experimental model. I would also like to thank The Hong Kong Polytechnic University's University Research Facility in Life Sciences (ULS) staff, particularly Dr. Ryan Chow Ho-yin, Clara Hung Hiu-ling, and Rachel Li Wai-sum, who gave me the technical training. I would also like to acknowledge the NIH Tetramer Core Facility, USA, for provision of the tetramer reagent.

I am truly grateful to all of my colleagues for their kind support during all of my laboratory experiments. Eden, please accept my heartfelt gratitude for your valuable contribution to this thesis and for generously devoting your time to providing me with guidance, encouragement, suggestions, and comments during all of my large-scale experiments. You have made a significant contribution to my long and difficult journey with this work, and I found you to be softhearted and genuine. I would also like to thank Maple, Yuxuan, Sylvia, Chujun and Arka. Your valuable comments, friendliness, patience, understanding, and encouragement were unforgettable. May the Almighty God richly bless all of you!

I want to express my gratitude to all of my friends for making my time at PolyU so enjoyable by continuously motivating, cheering me on, and encouraging me in all circumstances. I am extremely grateful to all of my families who supported me and prayed for me during the course of my study. I value your unwavering support, inspiration, and affection forever.

Finally, but definitely not least, “Hawwoo Koo!”, my wife, the ultimate price you paid for me was never substantiated. Your loving words act as catalysts, giving me confidence each day when I am feeling down. I am so proud of you for always being supportive, understanding, and loving while taking on full accountability for our future.

Booranaan yeroo seenaa qabeessa keessa dhalate. Kanaaf maqaan “Booranaa” jedhamu moggafameef. Ati mucaa warra seenaati! Jaalala onnee koo irraa siif qaba! Naaf guddadhu!

TABLE OF CONTENTS

Contents	page
ACKNOWLEDGEMENTS	VI
LIST OF FIGURES	XI
LIST OF TABLES	XIII
LIST OF ABBREVIATIONS	XIV
1 GENERAL INTRODUCTION	1
1.1 The global burden of tuberculosis (TB)	1
1.2 Basic microbiology and immunopathogenesis of <i>Mycobacterium tuberculosis</i>	2
1.3 Immune responses to <i>Mycobacterium tuberculosis</i>	3
1.3.1 Innate immune responses	3
1.3.2 Adaptive immune responses	6
1.4 General introduction to vaccination	7
1.5 Mode of action of vaccines	8
1.6 Route of administration for vaccines	8
1.6.1 Parenteral vaccination	8
1.6.2 Mucosal vaccination	10
1.7 Advantages of mucosal vaccination	10
1.8 Challenges in designing mucosal vaccines	11
1.9 Mucosal adjuvant – a tool for overcoming the challenges in mucosal vaccine design	11
1.10 Mechanisms underlying adjuvanticity	12
1.11 Major types of adjuvants	13
1.12 The calcium-binding protein S100A4	15
1.13 TB vaccine development	16
1.14 Antigen used in TB vaccine development	17
1.15 ESAT-6 as an immunodominant protective peptide antigen for formulating the TB vaccine	17
1.15.1 TB vaccine strategies	19
1.15.2 Adjuvants for TB subunit vaccines	21
1.16 Significance of the study	22
2 OBJECTIVES	23

3	MATERIALS AND METHODS	24
3.1	Experimental animals	24
3.2	Mouse immunization	24
3.3	Sample harvesting and preparation	24
3.3.1	Blood	24
3.3.2	Bronchoalveolar lavage fluid (BALF) and vaginal washing	24
3.3.3	Single-cell preparation	25
3.3.4	Antigen recall responses	25
3.3.5	Tissue collection for exudate preparation	25
3.3.6	Preparation and stimulation of bone marrow-derived dendritic cells (BMDCs)	26
3.4	Tissue and cell analysis	26
3.4.1	Measurement of antigen-specific antibodies	26
3.4.2	Measurement of released cytokines and chemokines	27
3.4.3	Flow cytometry	27
3.4.4	Extraction of total RNA, cDNA synthesis and reverse transcription quantitative real-time polymerase chain reaction (RT-qPCR)	28
3.4.5	Antigen transport and dendritic cell migration assay	29
3.4.6	Immunohistochemistry	29
3.5	Statistical analysis	30
4	RESULTS	31
4.1	S100A4 is a potent mucosal adjuvant and elicits durable adaptive immune responses	31
4.2	S100A4 enhances antigen recall responses of cytotoxic T cells	32
4.3	S100A4 provokes greater mucosal and cellular immune responses than subcutaneous immunization adjuvanted with alum	35
4.4	S100A4 migrates to the spleen and lung tissues following intranasal administration	35
4.5	S100A4 facilitates antigen transport to secondary lymphoid organs and mucosal tissues	36
4.6	S100A4 does not induce olfactory bulb inflammation following intranasal delivery	36
4.7	S100A4 potentiates antigen-specific antibody production after intranasal immunization with the <i>Mycobacterium tuberculosis</i> -derived antigen ESAT-6	41
4.8	S100A4 expands antigen-specific CD4 T cell responses after intranasal immunization with the <i>Mycobacterium tuberculosis</i> -derived antigen ESAT-6	43

4.9	S100A4 upregulates cytokine secretion in the blood circulation in response to intranasal immunization with the <i>Mycobacterium tuberculosis</i> -derived antigen ESAT-6	43
4.10	S100A4 enhances immune memory-associated T cell activation and proliferation after re-stimulation ex vivo with the immunizing antigen ESAT-6 derived from <i>Mycobacterium tuberculosis</i>	46
4.11	S100A4 enhances immune memory-associated B cell activation and proliferation after re-stimulation ex vivo with the immunizing antigen ESAT-6 derived from <i>Mycobacterium tuberculosis</i>	47
4.12	S100A4 enhances activation of antigen-specific Th1 memory cells after re-stimulation ex vivo with the immunizing antigen ESAT-6 derived from <i>Mycobacterium tuberculosis</i>	53
4.13	S100A4 induces antigen-specific memory CD4 helper T cells and CD8 cytotoxic T cells that express pro-inflammatory cytokines upon re-stimulation with the immunizing antigen ESAT-6 derived from <i>Mycobacterium tuberculosis</i>	53
4.14	S100A4 promotes production of granzyme B in cytotoxic T cells after re-stimulation ex vivo with the immunizing antigen ESAT-6 derived from <i>Mycobacterium tuberculosis</i>	55
4.15	S100A4 augments cytokine and chemokine secretion by splenocytes after re-stimulation ex vivo with the immunizing antigen ESAT-6 derived from <i>Mycobacterium tuberculosis</i>	55
4.16	S100A4 induces the expression of cytokines in the lung tissues after immunization with the <i>Mycobacterium tuberculosis</i> -derived antigen ESAT-6	59
4.17	S100A4 enhances the expression MHC class II and costimulatory molecules by dendritic cells in vitro	61
4.18	S100A4 promotes secretion of pro-inflammatory cytokines by dendritic cells in vitro	63
4.19	S100A4 enhances the expression of TLR2 on dendritic cells in vitro	63
5	DISCUSSION	71
6	REFERENCES	78

LIST OF FIGURES

Figure 1.1	Immunopathogenesis and immune responses generated in response to <i>Mycobacterium tuberculosis</i> infection	4
Figure 1.2	A naïve T cell requires two signals for activation	9
Figure 4.1	S100A4 is a potent mucosal adjuvant and elicits durable humoral immune responses	32
Figure 4.2	S100A4 expands antigen-specific cytotoxic T cell immune responses	33
Figure 4.3	S100A4 induces H-2K ^b /OVA-specific memory cytotoxic T cells that express granzyme B and pro-inflammatory cytokines upon re-stimulation with immunizing antigen	34-35
Figure 4.4	S100A4 provokes greater mucosal and cellular immune responses in intranasal immunization compared to subcutaneous immunization adjuvanted with alum	37
Figure 4.5	S100A4 migrates to the spleen and lung tissues following intranasal administration	38
Figure 4.6	S100A4 facilitates antigen transport to nasal tissues and lymph nodes	39
Figure 4.7	S100A4 facilitates antigen transport to lung tissues	40
Figure 4.8	S100A4 promotes transport of antigen delivered at the footpad to draining lymph nodes	41
Figure 4.9	S100A4 does not induce olfactory bulb inflammation following intranasal administration	42
Figure 4.10	S100A4 enhances immune memory-associated T cell activation and proliferation after re-stimulation ex vivo with the immunizing antigen ESAT-6 derived from <i>Mycobacterium tuberculosis</i>	44
Figure 4.11	S100A4 expands antigen-specific CD4 T cell responses after intranasal immunization with the <i>Mycobacterium tuberculosis</i> -derived antigen ESAT-6	45
Figure 4.12	S100A4 upregulates cytokine secretion in the blood circulation in response to intranasal immunization with a <i>Mycobacterium tuberculosis</i> -derived antigen ESAT-6	46
Figure 4.13	S100A4 enhances the proliferation of spleen T cells after re-stimulation ex vivo with the immunizing antigen ESAT-6 derived from <i>Mycobacterium tuberculosis</i> based on the cell proliferation marker Ki-67	48
Figure 4.14	S100A4 enhances the activation of spleen T cells after re-stimulation ex vivo with the immunizing antigen ESAT-6 derived from <i>Mycobacterium tuberculosis</i> based on the cell activation marker CD69	49

Figure 4.15	S100A4 enhances the activation of spleen T cells after re-stimulation ex vivo with the immunizing antigen ESAT-6 derived from <i>Mycobacterium tuberculosis</i> based on the cell activation marker CD25	50
Figure 4.16	S100A4 enhances the proliferation/activation of spleen T cells after re-stimulation ex vivo with the immunizing antigen ESAT-6 derived from <i>Mycobacterium tuberculosis</i> based on both Ki-67 and CD69 expression	51
Figure 4.17	S100A4 enhances the proliferation/activation of spleen B cells after re-stimulation ex vivo with the immunizing antigen ESAT-6 derived from <i>Mycobacterium tuberculosis</i> based on both Ki-67 and CD69	52
Figure 4.18	S100A4 enhances activation of antigen-specific Th1 memory cells after re-stimulation ex vivo with the immunizing antigen ESAT-6 derived from <i>Mycobacterium tuberculosis</i>	54
Figure 4.19	S100A4 induces antigen-specific memory CD4 helper T cells that express pro-inflammatory cytokines upon re-stimulation with the immunizing antigen ESAT-6 derived from <i>Mycobacterium tuberculosis</i>	56-57
Figure 4.20	S100A4 induces antigen-specific memory CD4 T cells that express a combination of different pro-inflammatory cytokines upon re-stimulation with the immunizing antigen ESAT-6 derived from <i>Mycobacterium tuberculosis</i>	58-59
Figure 4.21	S100A4 induces antigen-specific memory CD8 cytotoxic T cells that express pro-inflammatory cytokines upon re-stimulation with the immunizing antigen ESAT-6 derived from <i>Mycobacterium tuberculosis</i>	60-61
Figure 4.22	S100A4 induces antigen-specific memory CD8 cytotoxic T cells that express a combination of different pro-inflammatory cytokines upon re-stimulation with the immunizing antigen ESAT-6 derived from <i>Mycobacterium tuberculosis</i>	62-63
Figure 4.23	S100A4 promotes production of granzyme B in cytotoxic T cells after re-stimulation ex vivo with the immunizing antigen ESAT-6 derived from <i>Mycobacterium tuberculosis</i>	64
Figure 4.24	S100A4 augments cytokine and chemokine secretion by splenocytes after re-stimulation ex vivo with the immunizing antigen ESAT-6 derived from <i>Mycobacterium tuberculosis</i>	65-66
Figure 4.25	S100A4 induces the expression of cytokines in the lung tissues after immunization with the <i>Mycobacterium tuberculosis</i> -derived antigen ESAT-6	66
Figure 4.26	S100A4 enhances the expression of MHC class II and costimulatory molecules by dendritic cells in vitro	67-68
Figure 4.27	S100A4 promotes secretion of pro-inflammatory cytokines by dendritic cells in vitro	68-69
Figure 4.28	S100A4 enhances the expression of TLR2 on dendritic cells in vitro	69-70

LIST OF TABLES

Table 1	Currently licensed mucosal vaccines	12
Table 2	Promising mucosal adjuvants	14
Table 3	Antigens used in experimental subunit TB vaccines	19
Table 4	List of TB vaccine candidates in human clinical trials	20
Table 5	Adjuvants used for TB vaccines	21
Table 6	Antibodies used in this study	28
Table 7	PCR primers used in this study	30

LIST OF ABBREVIATIONS

Abbreviation	Full term
Alum	Aluminum salt
APC	Antigen-presenting cell
BALF	Bronchoalveolar lavage fluid
BCG	Bacillus Calmette-Guerin
BMDC	Bone marrow-derived dendritic cell
CT	Cholera toxin
DAMP	Damage-associated molecular pattern
ELISA	Enzyme-linked immunosorbent assay
ESAT-6	Early secreted antigenic target 6
ESX-1	ESAT-6 secretion system 1
LT	heat-labile toxin
MHC	Major histocompatibility complex
OVA	Ovalbumin
PAMP	Pathogen-associated molecular pattern
PCR	Polymerase chain reaction
PBS	Phosphate-buffered saline
RT-qPCR	Reverse transcription quantitative real-time PCR
TB	Tuberculosis
TLR	Toll-like receptor
WHO	World Health Organization

1. GENERAL INTRODUCTION

1.1. The global burden of tuberculosis (TB)

Mycobacterium tuberculosis is a pathogen responsible for a contagious disease called TB. It spreads by inhalation of fine droplets containing the bacilli from an infected individual and primarily affects the lungs in addition to other parts of the body. This disease has been harassing humankind throughout much of the known human history. TB is estimated to infect one-third of the world's population, who have a high risk of developing the disease. Globally TB remains one of the top ten causes of death and is responsible for 4000 lives a day (1). Of the total TB cases, majority are from the World Health Organization (WHO) list of 30 high-TB burden countries in which South-East Asian and African countries are over-represented, suggesting that this disease is highly associated with poverty (1). More than half of the global cases come from the top eight high-TB burden countries, including India, Pakistan, Bangladesh, South Africa, Nigeria, China, Philippines, and Indonesia (2). This indicates that TB is a severe contagious disease that still has a significant global impact.

If well-managed, the majority of the drug-susceptible TB cases are curable with combined first-line drugs, namely, isoniazid, rifampicin, pyrazinamide, and ethambutol (3). However, if these first-line antibiotics fail to effectively control the disease, it opens the door for the development of the multi-drug resistant strain of *Mycobacterium tuberculosis* (3). In many countries, the development and spread of multi-drug resistant-TB strains have been alarmingly increasing, and these strains have even evolved to be extensively drug-resistant TB. In terms of the costs and the time it takes, the treatment of TB-associated diseases is substantial (4). Treatment of all forms of drug-resistant TB requires a combination of multiple anti-TB drugs for a sustained duration, which may unfortunately engender side effects (5). Multi-drug resistant-TB and extensively drug-resistant-TB strains remain public health threats due to the difficulties associated with treatment. Individuals infected with multi-drug resistant-TB and extensively drug-resistant TB who do not receive proper treatment may experience life-threatening risks, which leads to disastrous consequences if the community-wide spread of these dreadful, difficult-to-treat strains happens (6). Approximately 450 000 people worldwide have been diagnosed with multi-drug resistant or rifampicin-resistant TB. Worldwide, China, India, and Russia account for nearly half of all multi-drug resistant-TB cases (1).

According to the new agenda of WHO's End TB Strategy set for 2030 and 2035, concerted efforts are required to focus on the prevention of new infections of *Mycobacterium tuberculosis* and their progression to TB disease to reduce mortality and morbidity (7). If the new WHO agenda is well implemented, TB incidence is expected to see a reduction by 80% and 90% by 2030 and 2035, respectively, which requires exceptionally accelerated efforts in the abatement and control of TB incidence after 2025. A prerequisite for achieving this target is an effective interruption of the progression from latent TB infection to active TB disease among those who are already infected, which constitutes a third of the global population (8). Essentially, it is critical to develop reliable diagnostic tools and cutting-edge effective therapies for people with latent TB infection, as well as to develop high-quality vaccination modalities (9).

1.2. Basic microbiology and immunopathogenesis of *Mycobacterium tuberculosis*

A distinguishable feature of the mycobacterium species apart from the majority of other prokaryotes is the presence of remarkable molecular complexity in their cell wall. The envelope of these species shares some of the features of the gram-negative cell wall, although they are traditionally classified as gram-positive bacteria (10). The cell wall structure is composed of an inner layer, which is formed by the mycolyl-arabinogalactan-peptidoglycan complex (10), and an outer layer, which is comprised of different proteins and lipids with long chains of carbons attached to the mycolic acid of the mycolyl-arabinogalactan-peptidoglycan complex (11). Generally, the high lipid feature of the cell wall structure of mycobacterium along with the presence of several other components, namely, phenolic glycolipid, phosphatidylinositol mannosides, and lipoarabinomannan, accounts for the immunomodulatory activity of the mycobacterium species that contributes to resistance against antimicrobial agents (11).

The immunopathogenesis of *Mycobacterium tuberculosis* infection is determined by the inter-talk between the bacteria and the host's immune system. TB is an air-borne disease transmitted through inhalation of aerosol droplets expelled by infected individuals. A small dose of bacilli (1-200) is enough to establish infection. It is expected that a single droplet can carry approximately 1-400 bacilli. Alveolar macrophages engulf the bacilli after encountering them at alveoli in the distal airways of the lung (12,13). A possible outcome of phagocytosis is that phagocytized bacilli are subjected to degradation after phagolysosomal fusion. This highly

regulated event is an important antimicrobial mechanism by phagocytic cells (14). Furthermore, phagocytized bacilli induce alveolar macrophages to produce inflammatory mediators, which alert the immune system to the infection. However, even though numerous polymorphonuclear immune cells and lymphocytes can migrate to the focal site of infection as a consequence of macrophage-mediated inflammatory responses, they are unable to kill the organism effectively. In fact, the bacteria can rely on a number of mechanisms, such as prevention of phagosomal maturation, inhibition of inflammasome activation, and suppression of macrophage apoptosis, to evade immune surveillance (15). If the bacilli successfully resist the bactericidal mechanisms of the macrophage, they start to multiply inside the phagosomes, which may lead to necrosis of the macrophages. The successfully released bacilli are further phagocytized by another macrophage and such a cycle can be continued if the host immune system fails to control the growth of the organism (15).

The accumulation of macrophages together with numerous host immune cells leads to the formation of granuloma at the site of infection. The bacilli can hide within the granuloma for a long time, which may cause chronic infection. Clinical signs may appear after reactivation of the dormant bacteria, or when the bacilli from the granuloma are disseminated to the environment after granuloma necrosis and formation of cavitation (Fig. 1.1). If the infection is successfully stopped because of the granuloma formation, the granuloma shrinks and finally disappear, leaving only a small scar. When all the mechanisms for controlling the bacterial infection fail, fibrosis represents the final defense mechanism of the host (16).

1.3. Immune responses to *Mycobacterium tuberculosis*

The disease progression pattern of *Mycobacterium tuberculosis* is determined by the host's ability to mount a robust immune response to the infection (17). Both innate and adaptive immune responses contribute to the immune defense against *Mycobacterium tuberculosis* (18).

1.3.1. Innate immune responses

Innate immune responses to *Mycobacterium tuberculosis* are initiated by the activation of the innate immune cells, which is important for the subsequent recruitment of the adaptive immune cells (14). The role of innate immune cells is critical in early anti-mycobacterial responses,

which determine the progression of infection by activating the proper adaptive immune responses through regulating inflammation (14).

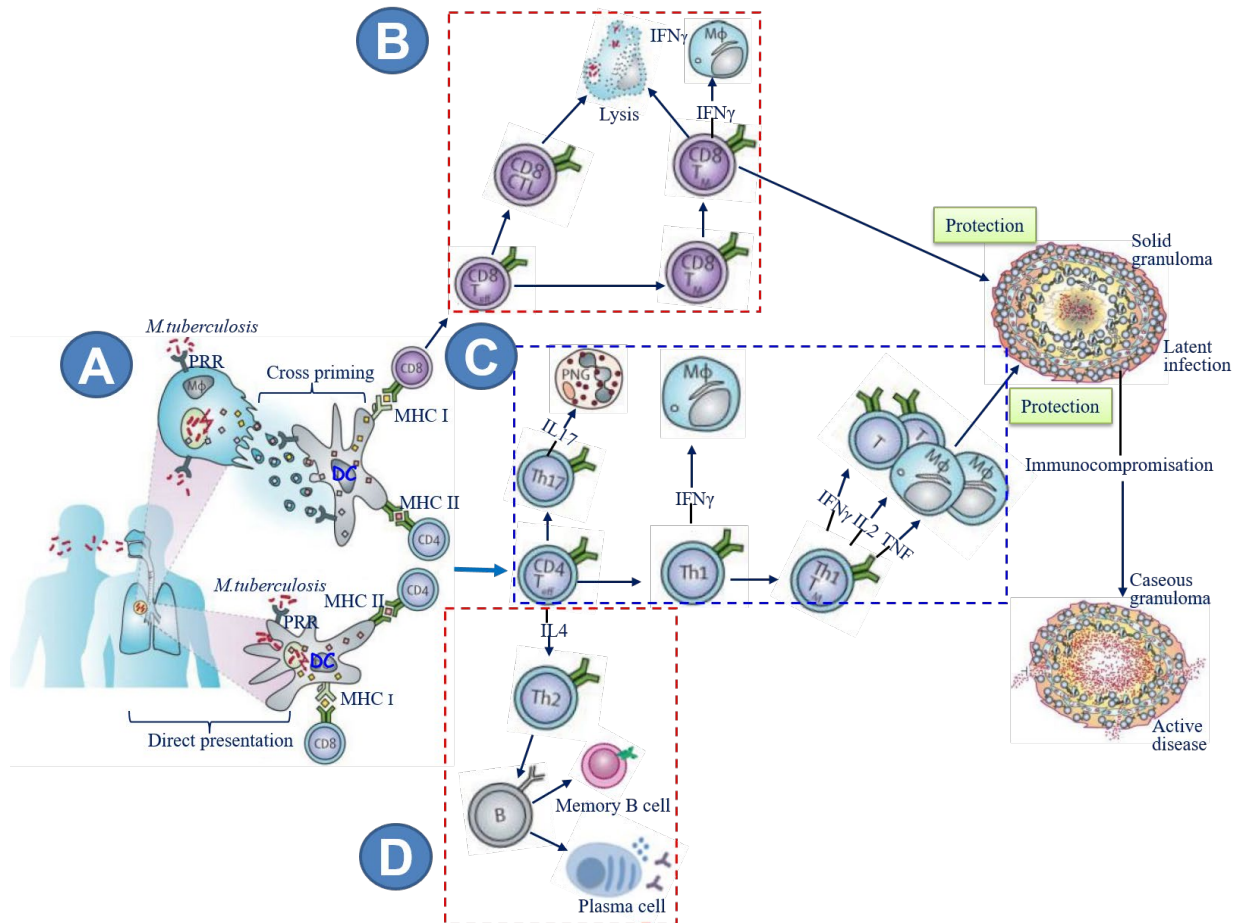


Figure 1.1. Immunopathogenesis and immune responses generated in response to *Mycobacterium tuberculosis* infection. Following infection of *Mycobacterium tuberculosis*, antigen-presenting cells (APCs), such as dendritic cells (DCs), take up the pathogen and present the digested peptides on major histocompatibility complex (MHC) class I and class II to activate naïve CD8 and CD4 T cells, respectively (A). Next, CD8⁺ T cells are polarized into different effector functional cells to activate macrophages and kill the target cells by secreting various types of granular products and cytokines (B). Similarly, CD4⁺ T cells are activated and polarized toward Th1, Th2, or Th17 cells. IFN- γ , IL-2, and TNF- α are produced by Th1 cells to activate macrophages; IL-17 is secreted by Th17 cells to activate polymorphonuclear granulocytes (PNG) (C); CD4⁺ T cells also secrete IL-4 after being polarized into Th2 cells, which is an essential step in activating B cells (D). If the bacteria cannot be cleared, the accumulation of bacillus-containing macrophages along with numerous activated immune cells results in the formation of granuloma. Adapted from Kaufmann (17).

Different immune cells, namely, macrophages, dendritic cells, neutrophils, natural killer cells, B-lymphocytes, and several other epithelial and endothelial cells, can recognize structural components and secreted proteins from *Mycobacterium tuberculosis* through various pattern recognition receptors, which is critical in the control of the infection (19). Of these pattern recognition receptors, the toll-like receptor (TLR) family has a prominent role in recognizing a wide range of microbial molecules. The expression of TLRs on antigen-presenting cells (APCs) is critical for initiating innate immunity and enhancing adaptive immune responses. Among the TLR family members, TLR2 and TLR4 are critically important in the recognition of various *Mycobacterium tuberculosis*-derived antigens including early secreted antigenic target 6 (ESAT-6) (20).

The prominent APCs, in *Mycobacterium tuberculosis* infections include macrophages and dendritic cells (21). Macrophages are the primary cells that determine the survival and growth of the engulfed bacteria. In addition to this direct role in bacterial clearance, macrophages also participate in the activation of both innate and acquired protective immune responses, which is crucial in facilitating the elimination of the bacilli (22). The alveolar macrophages are the first-line defenders who meet the bacilli in the lungs (23).

Dendritic cells are the most critical professional APCs, which coordinate innate and adaptive immune responses against the bacilli. They processed and present antigen to naïve T cells in secondary lymphoid organs and initiate adaptive immune responses through their multiple capacities, including interacting with naïve T cells via their costimulatory molecules and secreting the T-helper cell polarizing cytokines (24,25). The process and presentation of antigen by dendritic cells to naïve T cells depend on the nature of the pathogen endocytosed through their respective major histocompatibility complex (MHC) class I or class II (26). Mature dendritic cells are capable of stimulating specific T cell responses after migrating to secondary lymphoid organs, which are richly populated with T cells (27). Within secondary lymphoid organs, dendritic cells efficiently secrete polarizing cytokines for inducing CD4⁺ T cell differentiation into various subtypes (27). The secretion of IL-12 is induced when dendritic cells are exposed to an intracellular pathogen that results in the differentiation of CD4 T cells into Th1 cells. After this differentiation, IFN- γ secreted by the Th1 cells further sensitizes dendritic

cells to produce IL-12 that reinforces Th1 cell development (27). Dendritic cells also secrete IL-6, which facilitates the differentiation of activated CD4⁺ T cells to the Th2 cell lineage. This differentiation further enhances the activation of Th17 cells by secreting IL-1 β and IL-23 (28). In these ways, the activation of dendritic cells, along with the activation of various T cells subsets, promotes the clearance of pathogens in addition to inducing tissue inflammation (29).

1.3.2. Adaptive immune responses

Adaptive immunity is composed of humoral immune responses mediated by antibodies and cellular immune responses initiated by T cells (30). The primary immunologic axis for developing protective vaccines against TB has been predicted to be cell-mediated immune responses. Despite the fact that less contribution of humoral immunity to *Mycobacterium tuberculosis* infection is assumed, the involvement of antibodies in controlling *Mycobacterium tuberculosis* infection has been suggested (31). It is reported that *Mycobacterium tuberculosis*-specific antibody contributes to host defense mechanisms against this bacterium. The specific antibodies produced are also able to recognize the bacterial components and exert antimicrobial activity (32). Moreover, secretory IgA plays a prominent role in immune defense, such as immune exclusion, at the mucosal sites (33). IgA can also form immune complexes with bacterial cell wall components resulting in bacterial-host cell interactions to block the entrance of pathogens (33).

The substantial contribution of cell-mediated immune response in controlling *Mycobacterium tuberculosis* infection is well established. Following aerosol challenge of the mouse with *Mycobacterium tuberculosis*, highly activated antigen-specific CD4⁺ T cells accumulated in the lungs (34). Primarily, the specific cytokines released by Th1-cells are critical in containing *Mycobacterium tuberculosis* infection. Antimycobacterial activities of the macrophages are enhanced by IFN- γ , which mediates the maintenance of the granuloma architecture and inhibition of *Mycobacterium tuberculosis* growth (35). TNF- α co-operates with IFN- γ to activate macrophages, which inhibits the replication of intracellular bacteria (36). The expansion of T cells is promoted by the production of IFN- γ , TNF- α , and IL-2 in the intracellular pathogen infection model (36). The polyfunctional T cells are mainly associated with the increased immune response to specific pathogens and the production of multiple

cytokines (36). In *Mycobacterium tuberculosis* infection, Th17 cells play a critical role to control the growth of the bacteria. The production of IL-17 is pronounced following bacillus Calmette-Guerin (BCG) vaccination, although the specific roles of Th17 cells are less characterized (37). It is also reported that the recruitment of activated neutrophils to the site of the infection is enhanced by IL-17 (38).

Lysis and apoptosis of the infected macrophages and the subsequent killing of the intracellular *Mycobacterium tuberculosis* are mainly mediated by CD8 T cells through the production of cytotoxic molecules, such as granulysin and perforin. Furthermore, CD8 T cells participate in long-term protective immunity against TB (39). Helper T cells enhance CD8 T cells to differentiate into cytotoxic T lymphocytes (CTLs) and CTLs further promote the activation of macrophages by secreting IFN- γ (40).

1.4. General introduction to vaccination

Vaccination refers to the process whereby an individual develops protective immune responses against a pathogen after receiving a vaccine specific to this pathogen. The pioneers of vaccinology, Edward Jenner and Louis Pasteur, paved the way for modern vaccination (41). Their work laid the groundwork for significant progress in vaccine development, which has proven to be the most successful and cost-effective public health campaign, as demonstrated by the global eradication of smallpox (42). The explosive growth in our understanding of the immune system helps to develop vaccines that may protect us from a variety of diseases. In particular, vaccines are critical in controlling infectious diseases and reducing the rapidly rising antimicrobial resistance that jeopardizes the effectiveness of antibiotics (43). Despite considerable improvement achieved in recent decades in vaccinology for various global public health issues, the vaccine community is still in the early stages of understanding how vaccines can achieve better protective efficacy. In particular, the mucosal route for vaccine delivery has attracted substantial attention (44). Infectious diseases transmitted through mucosal surfaces remain unacceptably high that are threatening humankind. Recently, the SARS-CoV-2 that causes the COVID-19 pandemic has provided a cruel reminder of the ongoing, and probably never-ending threat of new mucosal infectious challenges. The need for mucosal vaccines

against respiratory pathogens, as well as numerous pathogens transmitted through other mucosal and non-mucosal routes, is ever more pressing (44).

1.5. Mode of action of vaccines

When an individual undergoes a natural exposure to a pathogen, the pathogen will trigger adaptive immune responses and the immune system will elicit possibly lifelong immunological memory. Vaccines containing antigenic epitopes shared by the pathogen can mimic the pathogen and similarly mobilize the body's immune system to launch adaptive immune responses against that particular pathogen (45). Therefore, the basic working mechanisms of a vaccine are similar to those after a natural infection. The primary effector cells against pathogens are B cells, which are responsible to produce antibodies that specifically bind the pathogen or its products for elimination. Cytotoxic T cells, which play an important role in the clearance of intracellular pathogens or target cells, are also among the most effective cells. Helper T cells play an important role in the production of high-affinity antibodies, memory B cells, and effector T cells by secreting various cytokines.

1.6. Route of administration for vaccines

The route of vaccine administration is crucial in affecting the outcome of the vaccination efficacy. A proper route of administration enables the vaccine antigen to efficiently drain to secondary lymphoid organs relevant for the nature of the pathogen that the vaccine antigen mimics (46).

1.6.1. Parenteral vaccination

Currently, the majority of the vaccines have been administered through the parenteral route whereby injection is required for delivering the vaccine into or under the skin. The innate immune response is activated to a greater extent through intradermal vaccination administration as exemplified in vaccination against influenza and yellow fever (47). Despite the fact that the subcutaneous tissue is comprised of not only connective and adipose tissues but also blood vessels and nerve bundles, which poses a threat to safe vaccination, one of the advantages of subcutaneous delivery is the possibility of administering large volumes of the vaccine compared to the intradermal delivery. Therefore, most licensed vaccines such as measles, mumps, rubella,

varicella, yellow fever, zoster, typhoid, and Japanese encephalitis are delivered subcutaneously (46). Intramuscular injection is another commonly used route of vaccine administration (48).

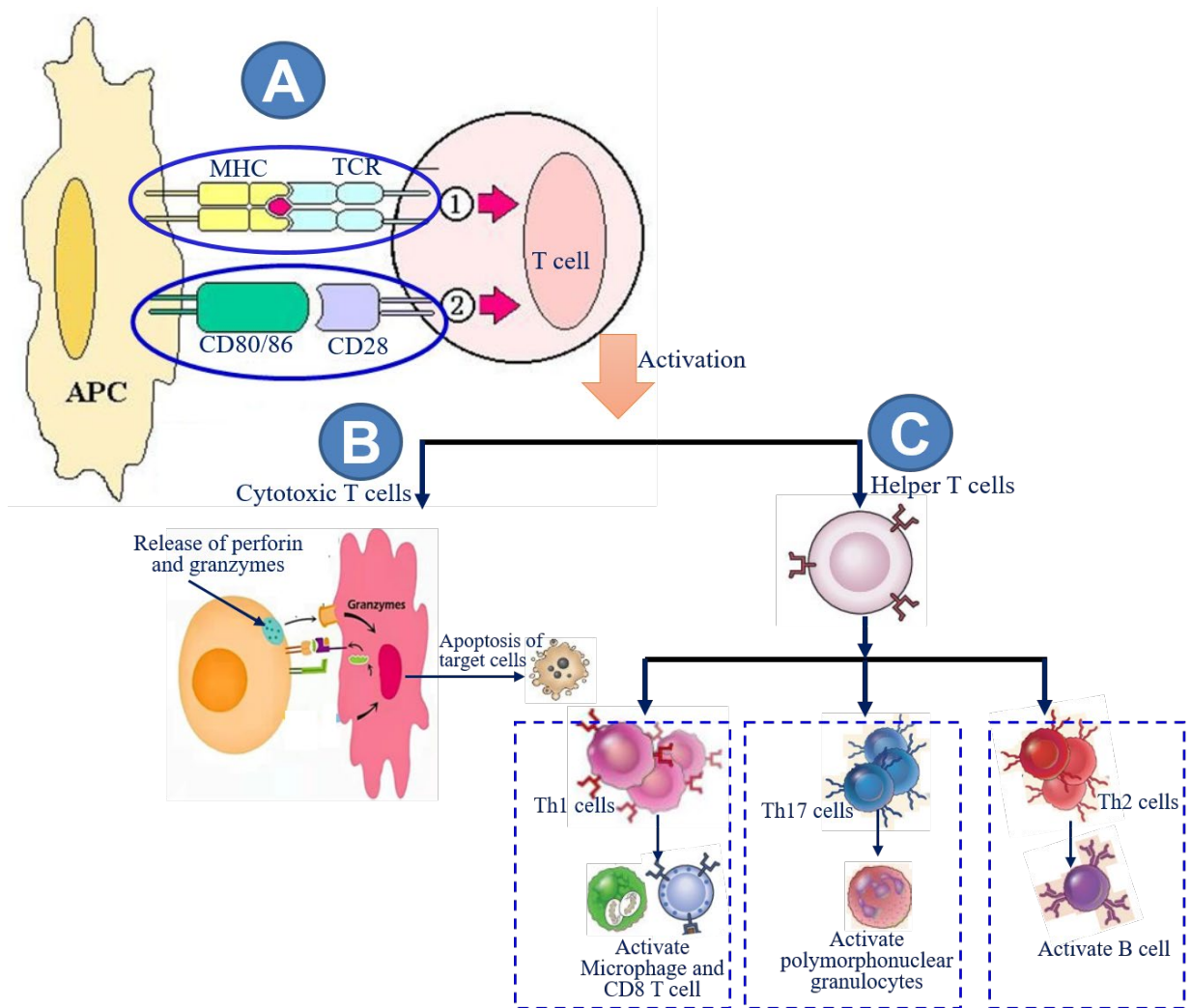


Figure 1.2. A naïve T cell requires two signals for activation. The first signal is the formation of an immune complex between an antigen-presenting cell (APC) and a T cell through the interaction between the MHC molecule and T cell receptor (TCR). The second signal is the interaction of co-stimulatory molecules, such as CD80 and CD86 on the surface of specialized APCs, and CD28 on the surface of T cells (A). Both signals eventually lead to the differentiation of the T cell into different effector T cell subtypes, including cytotoxic T cells (B) and helper T cells (C). T helper cells can be differentiated into Th1, Th17, and Th2 cells, which are required for the activation of macrophages and CD8 T cells, polymorphonuclear granulocytes, and B cells, respectively.

The vastus lateralis muscle (anterolateral thigh) and the deltoid muscle (upper arm) are the two most popular sites for intramuscular vaccine administration. As these sites are free from neuronal or vascular structures, the risks are reduced compared to other routes of vaccine administration (46).

1.6.2. Mucosal vaccination

In contrast to the parenteral vaccination, various mucosal delivery routes for vaccines have been attempted and these include mainly oral, nasal, and sublingual routes. An optimal mucosal delivery route is expected to activate antigen-specific humoral and cell-mediated immune responses both at the systemic and mucosal compartments (44). The first successful mucosal vaccine was the famous Sabin oral poliovirus vaccine which is a live attenuated vaccine, and it has contributed substantially to the worldwide control and management of the devastating disease poliomyelitis (49). Another attractive mucosal site for vaccine delivery is the nasal mucosa, where the nasopharyngeal-associated lymphoid tissue (NALT) is an effective induction site for generating robust immune responses (50). Compared with oral vaccination, the intranasal vaccination approach requires much lower antigen and adjuvant doses. Thus, research efforts have also focused on vaccination through the nasal cavity (50). However, the disadvantage of the nasal route lies in the fact that nasal delivery of vaccines can target olfactory neurons which have a direct neuronal connection to the olfactory bulb, part of a neural circuit associated with the central nervous system. This has raised substantial safety concerns for exploiting pathogen-derived substances, e.g., bacterial toxins (even after detoxification), as adjuvant (51).

1.7. Advantages of mucosal vaccination

Given that quite a number of pathogens enter the host through the mucosal surfaces, which cover a large area and provide first-line immune defense, vaccines that target mucosal surfaces become attractive as mucosal delivery of vaccines is expected to provide high-quality mucosal protection, e.g., through blocking the attachment of the pathogen at the portal of entry (52,53). In contrast, parenteral vaccination may be ineffective in stimulating immune responses at the mucosal site. Of note, vaccines administered via mucosal routes can promote immune responses both at mucosal sites and in circulation (54), as the mucosal surfaces cover a vast area, the

biodistribution of the vaccine antigen administered through mucosal surfaces is easily facilitated in both the systemic and mucosal tissues (55). In general, vaccine administration via the mucosal route is safer because it avoids the use of needles and eliminates needle-related risks. Mucosal vaccine administration has better user compliance than the parenteral injection, particularly for children. Yet one more advantage of mucosal vaccination is that it can obviate the requirement for trained personnel for vaccine delivery, which not only enhances user-friendliness, but also significantly lowers the cost of mass vaccination (53,56). Importantly, mucosal vaccine production and storage do not require strict sterile procedures, necessitating simpler technology than parenteral vaccines (53,56). Table 1 lists currently licensed mucosal vaccines.

1.8. Challenges in designing mucosal vaccines

Despite all of the benefits mentioned above, only a limited number of mucosal vaccines are licensed and commercially available. Among these, FluMist/Fluenz® and Nasovac™ are nasal vaccines against influenza types A and B, and H1N1 influenza viruses, respectively. Other examples include a few oral vaccines, such as Vaxchora®, and Dukoral® against *Vibrio cholera*; Rotarix™, RotaTeq® vaccine for rotavirus, Vivotif® for *Salmonella typhi*, and oral polio vaccine (OPV) for poliovirus (57,58). The limited number of approved mucosal vaccines available demonstrates substantial challenges involved in the development of mucosal vaccines (59). The primary challenge for developing mucosal vaccines lies in the fact that there exist mucosal barrier effects because of mucosal tolerance (59). Mucosal tolerance is evolved as an essential beneficial mechanism for preventing harmful inflammatory reactions to innocuous environmental antigens. Obviously, mucosal tolerance is a hurdle for launching productive immune responses upon vaccine delivery at the mucosal surface (60,61). The development of tolerogenic dendritic cells and regulatory T cells at mucosal sites, among others, is the proposed mechanism of mucosal tolerance (62). Co-administration of the vaccine antigen with a mucosal adjuvant is proposed as a solution for overcoming mucosal immune tolerance.

1.9. Mucosal adjuvant – a tool for overcoming the challenges in mucosal vaccine design

Adjuvant refers to a substance, when formulated together with a vaccine antigen, that is capable of enhancing and/or shaping the immune responses of the vaccine antigen to elicit better protective immunity (63). The use of an adjuvant is particularly important for mucosal

vaccination, as the default immune response at the mucosal sites is tolerance instead of active immunity (64).

Table 1. Currently licensed mucosal vaccines

Pathogen	Trade name	Composition	Route & Dosage	Immunological mechanism	Efficacy
Rotavirus	Rotarix, RotaTeg	Live attenuated, mono or pentavalent rotaviruses	Oral, 3 doses	Mucosal IgA and systemic IgG	70%-90%
Poliovirus	Orimune, OPV	Live attenuated mono, bi and trivalent polioviruses	Oral, 3 doses	Mucosal IgA and systemic IgG	Over 90%
<i>Salmonella typhi</i>	Vivotif, Ty21A	Live attenuated <i>Salmonella typhi</i> bacteria	Oral, 3-4 doses	Mucosal IgA and systemic IgG and CTL responses	Over 50%
<i>Vibrio cholera</i>	Dukoral, ORC-Vax, Shanchol	Inactivated <i>Vibrio cholera</i> O1 classical and El Tor biotypes with/without CTB	Oral, 2-3 doses	Antibacterial, toxin-specific, and LPS-specific IgA	Over 85%
Influenza type A and B	FluMist	Live viral reassortant with trivalent mix of H1, H3, and B strains	Nasal, 2 doses	H and N-specific mucosal IgA and systemic IgG	Over 85%
H1N1 influenza (swine flu)	NASOVA C (Serum Institute of India)	Monovalent live attenuated vaccine	Nasal spray, 1-2 doses	H1 and N1-specific mucosal and systemic antibody and CTL responses	Unavailable

Adapted from Correa et al. (65). Abbreviations: OPV, oral polio vaccine; CTL, cytotoxic T lymphocyte; CTB, cholera toxin B subunit; LPS, lipopolysaccharide.

1.10. Mechanisms underlying adjuvanticity

Multifactorial mechanisms of action of vaccine adjuvants in enhancing immune responses have been described. A common adjuvant mechanism of action is depot formation at the injection or delivery site. By facilitating the slow release of antigens at the delivery site, depot-inducing vehicle adjuvants ensure localized and consistent immune cell stimulation (63). Furthermore, the formation of a depot at the delivery site prolongs antigen accessibility to APCs (66). Another major mechanism underlying adjuvanticity is the stimulation of APCs by the adjuvant, facilitating vaccine antigen uptake and processing by the APCs. For example, the

experimentally tested adjuvant system chitosan and its derivatives can enhance both local delivery and immunostimulation (67).

1.11. Major types of adjuvants

The choice of adjuvants is as critical as the selection of the vaccine antigen for preparing a vaccine formulation that can achieve robust protective immunity. Compelling experimental evidence has demonstrated that both the immediate immune response and the long-term protective effect of a vaccine can be dramatically augmented by a robust adjuvant (68,69). Although aluminium salt (alum) has been included in the formulations of most injectable vaccines with reliable adjuvant activity and a good safety record, alum is not effective in boosting mucosal immunization (70). Various strategies have been suggested for developing effective adjuvants for mucosal vaccination (44).

Among all the mucosal adjuvants under development, TLR agonists have attracted much attention. TLR agonists mobilize the key innate immune system by activating APCs (71). ESAT-6, a *Mycobacterium tuberculosis*-derived antigen, is a TLR2 agonist that can augment immune responses by inducing the production of pro-inflammatory cytokines (72). Various types of cytokines, including interferons and interleukins, have all been exploited as potential mucosal adjuvants for enhancing immune responses (67).

Another major category of mucosal adjuvants belongs to a family of bacterial toxins or their detoxified products. The major enterotoxins produced by *Escherichia coli* and *Vibrio cholerae* are heat-labile toxin (LT) and cholera toxin (CT), respectively. These two toxins have been identified as the most powerful immunomodulators (73,74). Therefore, both of these two toxins have been classically used as experimental mucosal adjuvants. However, they cannot be used directly in human mucosal vaccine formulations because of their substantial toxicity. Non-toxic and modified forms of CT and LT have been developed to remove toxicity while maintaining adjuvanticity (75,76), which has not been convincingly successful. For example, nasal administration of LTK63 (a mutant form of LT), despite being effective in providing adjuvanticity, still poses a safety risk as a few cases of facial paralysis were observed after marketing for vaccination. Despite relentless efforts, there is still a scarcity of effective mucosal

vaccine adjuvants that can potentiate the immune response while minimizing toxicity. Hence, the identification of novel classes of mucosal adjuvants that meet clinical safety standards is an active research topic. Table 2 lists different promising mucosal adjuvants.

Both TLR ligands and bacterial toxins can be regarded as a class of molecules that are related to substances derived from pathogens. In fact, many of the molecules associated with pathogens are grouped into a family called pathogen-associated molecular pattern (PAMP) molecules which are themselves potent immunostimulators. In contrast to PAMP, another category of immunostimulators is a group of molecules known as damage-associated molecular pattern (DAMP) molecules. This is a family of heterogeneous molecules composed of proteins, lipids, nucleic acids, and small-molecule compounds that are normally confined within cells but are released in response to tissue injury and stress (77,78). Therefore, DAMP molecules are invisible under a steady state to the immune system. However, upon stress stimulation these molecules are released into the extracellular environment, thus providing a danger signal to alert the immune cells.

Table 2. Promising mucosal adjuvants

Adjuvant	Characteristics	Target site	Licensed vaccine
Enterotoxins	CTB	GM1	Yes
	LT	GM1 and other gangliosides	No
	Mutants of CT and LT	GM1 and other gangliosides	No
	CTA1-DD	Immunoglobulin binding fragment	No
TLR agonist	Monophosphoryl Lipid A	TLR-4	No
	CpG-ODN	TLR-9	No
	Flagellin	TLR-5	No
Cytokines	Interleukin-1	IL-1R	No
	Interleukin-12	IL-12R	No

Adapted from Srivastava A. et al. (79).

However, upon stress stimulation these molecules are released into the extracellular environment, thus providing a danger signal to alert the immune cells. DAMP molecules can activate innate immune cells that express receptors for the respective DAMP molecule in question, including dendritic cells which are important orchestrators in the coordination of the

innate and adaptive immune responses (80). Furthermore, DAMP molecules are human internal molecules and therefore are likely to present a better safety profile.

1.12. The calcium-binding protein S100A4

S100A4 is originally defined as a calcium-binding protein that exhibits biological functions in many cell types (81,82). The binding of calcium to S100A4 plays an important role in regulating its biological functions in different cell types. This can lead to a variety of biological effects, depending on the specific context and the other molecules involved. For example, the binding of calcium to S100A4 can promote its interaction with cytoskeletal proteins, which has an impact on cell migration and invasion. Such binding can also affect the ability of S100A4 to interact with other signaling molecules, such as enzymes or receptors, which can modify cellular processes, such as proliferation and differentiation (82). Taken together, S100A4 has been shown to regulate a variety of cellular processes such as growth, survival, differentiation, and motility (81).

S100A4 also fulfills the definition of a DAMP family molecule as it is typically released upon tissue injury (83). It interacts with cellular targets via at least the receptor for advanced glycation endproducts (RAGE) and TLR4 (84). The interaction of these receptors on immune cells with S100A4 profoundly amplifies various cell signaling pathways, resulting in cell differentiation, activation, and inflammatory mediator production (82). RAGE is a cell surface receptor that is involved in inflammation. S100A4 has been shown to bind to RAGE and activate downstream signaling pathways that are implicated in various inflammatory conditions (85). TLR4 is another cell surface receptor that is involved in innate immune responses and inflammation. S100A4 has been shown to activate TLR4 signaling, leading to the production of pro-inflammatory cytokines (86).

S100A4 is originally characterized as exerting its regulatory functions intracellularly, especially during oncogenesis (82). The immune regulatory function of S100A4 was first revealed in 2014 when the roles of this protein in allergic inflammation were identified based on the use of bioinformatics approaches and experimental validation (87). Consistently, it has recently been reported that S100A4 is required for mast cell activation (88). The potential role of S100A4 in

immunization was hinted when this protein was found to be required for maintaining the functionality of dendritic cells (89). This finding is supported mechanistically by the observation that S100A4 is critical for the maturation and development of microfold cells (M cells) (90), which play a key role in the antigen capture at mucosal surfaces and initiation of mucosal immune responses. Our group has recently demonstrated that intranasal administration of S100A4 admixed to OVA remarkably enhanced antigen-specific adaptive immune responses both at the mucosal compartment and circulation (84).

It can be also expressed in many normal cells whereby it has been found to regulate many normal cellular processes such as cell growth and survival, differentiation, and motility (91). Although most of the clinically-oriented research on S100A4 has focused on its ability to promote cancer metastasis (91), this does not preclude the use of S100A4 as an adjuvant. First of all, no documented evidence has shown that S100A4 can induce oncogenesis. Tumors develop as a result of multiple factors. After tumor cells are formed, they upregulate their own production of S100A4 to facilitate motility.

1.13. TB vaccine development

Currently, the only vaccine approved for human use against *Mycobacterium tuberculosis* is the BCG vaccine. Although it is inefficient in protecting against pulmonary TB, it has demonstrated protective efficacy against severe and extra pulmonary forms of TB in infants and young children (92). On the other hand, one-third of the world's population currently harbors latent TB infection and around three in every 1000 people carry latent MDR-TB infection globally (1). Furthermore, TB incidence is increasing among young adults in high-TB-burden countries (93). One possible explanation for this consequence is assumed to be the lack of long-lived T effector memory cells (94). One common feature of all the BCG strains is the absence of ESAT-6 secretion system 1 (ESX-1), owing to the deletion of region of difference one (RD1). ESAT-6 antigen is a key virulence factor, which is absent in BCG, providing a probable mechanistic explanation for this weakened parenteral vaccine (95).

1.14. Antigen used in TB vaccine development

Approximately 4000 proteins are expressed by *Mycobacterium tuberculosis*, many of which contain predicted antigenic epitopes that can be recognized by either CD4 or CD8 T cell receptors (96). For developing novel vaccines against TB, the major challenge is the absence of antigen diversity. The antigen selection is critical for successful vaccination (97). A study has shown that secreted proteins of *Mycobacterium tuberculosis* can be used as the potential vaccine antigen for formulating an effective vaccine against *Mycobacterium tuberculosis* infection (98). Currently, subunit vaccine antigens are selected according to their immunodominance in animal and human studies. Some secreted proteins, including ESAT-6, MPT64, and Ag85 complex, as well as cell wall proteins, such as heat shock proteins, are well-known *Mycobacterium tuberculosis* proteins that have potent immune stimulatory potential (99). ESAT-6 is always expressed during *Mycobacterium tuberculosis* infection, while Ag85B is expressed mainly in the early stage of infection (100). Screening adequate antigens in *Mycobacterium tuberculosis* for subunit vaccine preparation is challenged by the complexity of various infection models of this bacillus as it induces chronic/persistent/latent infection. Table 3 lists some antigens frequently used in TB subunit vaccine development in both preclinical and clinical research (98).

1.15. ESAT-6 as an immunodominant protective peptide antigen for formulating the TB vaccine

Mycobacterium tuberculosis has a hydrophobic outer layer composed of glycolipids and mycolic acids, and its secretion system differs from that of many gram-positive bacteria. Instead, *Mycobacterium tuberculosis* utilizes a series of five different type VII secretion system complexes unique to mycobacteria, namely ESX-1 through ESX-5 (101). Shortly after *Mycobacterium tuberculosis* is phagocytosed, ESAT-6 is secreted as a tight heterodimer from the ESX-1-specialized membrane, one of the five-secretion system complexes of the organism (102). ESAT-6 is suggested to be important for *Mycobacterium tuberculosis* to evade the immune system and persist in the body of the host. ESAT-6 can form a heterodimer complex with CFP-10 that plays a crucial role in the virulence of mycobacteria (103). The complex works together to disrupt host cell membranes in several ways. After being released, this complex has the ability to disrupt and break down cell membranes by creating pores through the formation

of a channel in the cell membrane. The channel allows ions and other small molecules to pass through the membrane, causing the osmotic imbalance and disrupting cellular processes. The pore-forming activity of the complex can have significant implications for the pathogenesis of tuberculosis and the host immune response to the infection (102). However, the ESAT-6-CFP-10 complex is known to be relatively unstable and can readily dissociate into its individual components, ESAT-6 and CFP-10 (103). Furthermore, ESAT-6 can disrupt the membrane of phagosomes, which are compartments within immune cells that are responsible for engulfing and destroying the invading pathogens. By breaking down the phagosomal membrane, ESAT-6 allows *Mycobacterium tuberculosis* to escape from the phagosome and enter the cytosol of the host cell, where it can replicate and spread (104). ESAT-6 has also been found to induce cell death in infected macrophages, which helps to promote the spread of *Mycobacterium tuberculosis* (104). In addition, it can also interfere with the presentation of MHC class I molecules on the surface of infected cells, a process necessary for the recognition and elimination of infected cells by cytotoxic T cells. This can help the bacterium evade the host's immune system and establish a persistent infection (105). ESAT-6 is therefore considered a virulence factor of *Mycobacterium tuberculosis*, as it plays a crucial role in the pathogenesis of the bacterium.

Meanwhile, the immune system can make use of ESAT-6 and launch antigen-specific immune responses against the bacterial invasion. ESAT-6 is recognized by TLR2 on the APCs, resulting in the upregulation of a number of downstream response genes leading to inflammatory responses. ESAT-6 is a highly immunogenic protein, and recognition of this protein is an important step in the immune response to *Mycobacterium tuberculosis* (106). Therefore, ESAT-6 is considered a potential vaccine antigen candidate in formulating a subunit *Mycobacterium tuberculosis* vaccine infection (105).

Table 3. Antigens used in experimental subunit TB vaccines

Vaccine	Antigen	Description
M72	Rv1196 Rv0125	Proline–proline–glutamate (PPE) family member Peptidase
H1	ESAT-6 Ag85B	Prominent antigen of <i>Mycobacterium tuberculosis</i> encoded in the region of difference 1 Mycolyl transferase
H4	TB10.4 Ag85B	Prominent TB antigen Mycolyl transferase
H56	H1 + Rv2660c	Dormancy antigen
ID93	Rv2608 Rv3619 Rv3620 Rv1813	PPE family member Virulence factor Virulence factor Dormancy antigen
Ad5Ag85A	Antigen 85A	Mycolyl transferase
MVA85A	Antigen 85A	Mycolyl transferase
Ad35	Antigen 85A TB10.4	Mycolyl transferase Prominent TB antigen
Ag85B	Antigen 85B	Mycolyl transferase
TB-FLU-04L	Antigen 85A	Mycolyl transferase

Adapted from Kaufmann SHE, et al. (98).

1.15.1. TB vaccine strategies

The target populations for TB vaccination are expected to include both uninfected (pre-exposure) and infected (post-exposure) individuals. The latter group comprises people with latent infection, symptomatic patients, and patients after treatment. For the uninfected population, prevention of infection and prevention of disease are the two major targets of TB vaccination. Furthermore, TB vaccines should ideally be able to, as a post-exposure strategy, prevent progression to TB disease for those carriers of *Mycobacterium tuberculosis*, and, as a treatment strategy, to relieve the disease symptoms for TB patients (107). Most of the vaccines for other infections primarily aim for achieving prevention of infection.

Table 4. List of TB vaccine candidates in human clinical trials

Type	Candidate	Description	Company	Status*
Adjuvanted Subunit vaccines	M72/AS01E	Contains Mtb39a and Mtb32a proteins with AS01E microbial-derived adjuvant	GSK, Aeras	Phase 2b
	H56/IC31	Contains MTB antigens Ag85B, ESAT-6, and Rv2660c with IC31 adjuvant	SSI, Valneva, Aeras	Phase 2b
	ID93/GLA-SE	Contains MTB virulence antigens (Rv2608,Rv3619c/EsxV, and Rv3620c/EsxW) or latency (Rv1813) in GLA-SE adjuvant	IDRI, Aeras	Phase 2a
Viral vectored	ChAdOx1-85A/MVA85A	Replication-deficient Chimpanzee/modified vaccinia Ankara virus expressing Ag85A	University of Oxford	Phase 1
	TB/FLU-04L	Attenuated influenza viral vector expressing Mtb Ag85A and ESAT-6/EsxA	RIBSP	Phase 2a
Live-attenuated mycobacterial	MTBVAC	Live attenuated MTB with <i>phop</i> and <i>fadb26</i> deletions	Biofabri, TBVI	Phase 2a
	VPM1002	Live attenuated BCG with urease C deletion and lysteriolysin insertion	SII, MPIIB, TBVI	Phase 3
Inactivated whole-cell mycobacterial	RUTI®	A liposomized killed MTB fragments	Archivel Farma	Phase 2a
	DAR-901	Heat killed <i>M. abvensse</i>	Dartmout, GHIT	Phase 2b
	Vaccae™	An injectable form of heat-inactivated <i>M. vaccae</i>	AZL	Phase 3

*Aeras Global Clinical Pipeline (latest revision: August 2018)

Abbreviations: MTB, *Mycobacterium tuberculosis*; IDRI, Infectious Disease Research Institute; GSK, Glaxo Smith Kline plc.; SSI, Statens Serum Institute; RIBSP, Research institute for Biological Safety Problems; TBVI, Tuberculosis Vaccine Initiative; SII, Serum Institute of India; MPIIB, Max Planck Institute for Infection Biology; GHIT, Global Health Innovative Technology Fund; AZL, Anhui Zhifei Longcom Biologic Pharmacy Co. Ltd.; ICMR, Institute of Leprosy and Other Mycobacterial Diseases.

However, a major issue in TB control and management is to achieve prevention of disease in already infected people. Therefore, designing a vaccine that can efficiently achieve prevention of disease is warranted. Of course, vaccines that can be given both pre- and post-exposure to protect uninfected people as well as to prevent the progression of disease in infected individuals would be more desirable (108,109). Table 4 lists TB vaccine candidates currently under human clinical trials. TB vaccine candidates in clinical trials can be classified into two types in terms of the vaccine antigens they contain: whole-cell or subunit vaccines. Whole-cell vaccines include live attenuated *Mycobacterium tuberculosis* strains, *Mycobacterium bovis* (i.e., BCG) or recombinant BCG, and killed mycobacterial vaccines derived from *Mycobacterium tuberculosis* or other saprophytic mycobacterial species (110). In humans, attenuated live vaccines based on *Mycobacterium tuberculosis* are predicted to stimulate specific host-immune responses that mimic natural TB infection without causing disease (111).

1.15.2. Adjuvants for TB subunit vaccines

Subunit vaccines often require a strong adjuvant for potentiating immune responses. Most of the potent vaccine adjuvants that help to enhance the innate immune response are ligands or agonists that can interact with and stimulate pattern recognition receptors. Recently, a significant number of novel adjuvants have been developed that act either as immunomodulators or as robust delivery systems (112). Some of these adjuvants are currently tested for formulating TB vaccines in both preclinical and clinical development (Table 5) (98). Apart from interacting with the cellular receptors and initiating downstream inflammatory signaling cascade responses, some of the adjuvants may work through currently unknown mechanisms (113).

Table 5. Adjuvants used for TB vaccines

Vaccine	Adjuvant	Composition
H1, H4, H56	IC31	Cationic peptides/TLR9 agonist
H1	CAF01	Cationic liposome/immunomodulatory glycolipid
ID93	GLA-SE	Oil in water emulsion/TLR4 agonist
M72	AS01E	Liposomes/TLR4 agonist

Adapted from Kaufmann SHE, et al. (98).

1.16. Significance of the study

The strong interest of WHO in the development of vaccines against TB demonstrates that the disease is a global public health concern. However, currently, only the BCG vaccine is available for infants and small children to control disseminated TB. The first-ever clinical trial of a new TB vaccine that was expected to strengthen the efficacy of BCG has been concluded recently with unsatisfactory results (114). Over 20 vaccine candidates have been vigorously evaluated in clinical trials in the last two decades. Unfortunately, several candidates, using both parenteral and mucosal vaccination modalities, failed to advance through clinical evaluation (115,116). Therefore, we are still faced with challenges in developing a vaccine that can elicit reliable protective immunity. Bearing in mind the disappointing results of the recent clinical trials of several TB vaccine candidates and the limitations of the BCG vaccine, a new TB vaccine formulation with a relevant immunodominant TB antigen, a strong and safe adjuvant, and an appropriate delivery method is warranted.

In this thesis work, I designed a mucosal TB vaccine formulation by combining the well-characterized *Mycobacterium tuberculosis* vaccine candidate ESAT-6 with the novel mucosal adjuvant S100A4. I have provided compelling evidence that this formulation can remarkably potentiate ESAT-6-specific antibody and T cell responses in the respiratory mucosal tissues and in the circulation after intranasal immunization of mice. I also characterized the mechanisms underlying the adjuvant activity of S100A4 in greater detail using both ESAT-6 and OVA as an experimental model antigen. My work has significantly broadened the knowledge base for further preclinical evaluation of S100A4 as a robust mucosal adjuvant in augmenting vaccine responses not only for TB but also for other disease models.

2. OBJECTIVES

This thesis work is composed of mainly two sections. The first part focuses on the evaluation of the mucosal adjuvant activity of S100A4, a novel mucosal adjuvant identified by our group, using the model vaccine antigen OVA. The second part aimed to provide proof-of-concept evidence using a clinically relevant pathogen-derived vaccine antigen, ESAT-6, which is an immunodominant protective vaccine antigen against *Mycobacterium tuberculosis*.

Specific objectives:

- ◆ To investigate the long-term adjuvant activity of S100A4 in augmenting humoral and cellular immune responses after nasal co-administration with OVA.
- ◆ To examine the adjuvant activity of S100A4 in augmenting humoral and cellular immune responses after intranasal immunization of mice with the clinically relevant vaccine antigen ESAT-6 admixed to S100A4.
- ◆ To investigate the mechanisms underlying the adjuvant activity of S100A4 using either OVA or ESAT-6 as a vaccine antigen.
- ◆ To determine the safety profile of S100A4 as a nasal vaccination adjuvant.

3. MATERIALS AND METHODS

3.1. Experimental animals

Female C57BL/6 mice (6-8 weeks old) were used for this study. Animals were bred in-house at the Centralised Animal Facilities at the Hong Kong Polytechnic University with unrestricted access to food and water. The animal research was approved by the Animal Subject Ethics Subcommittee of the Research Committee at The Hong Kong Polytechnic University. All animal procedures were carried out in accordance with institutional animal and bio-safety guidelines.

3.2. Mouse immunization

Mice were anesthetized with isoflurane before receiving the vaccine preparation for intranasal immunization. A 20- μ l phosphate-buffered saline (PBS) solution containing the *Mycobacterium tuberculosis* antigen ESAT-6 (5 μ g; MyBioSource; MBS204541) or OVA (10 μ g; Sigma-Aldrich; grade V) alone or in the presence of S100A4 (10 μ g; Gentaur Molecular Products; 01-2081A4M; with His-tag) was administered dropwise to the external nares of the mice (10 μ l per nostril). Some mice were immunized with ESAT-6 (5 μ g) or OVA (10 μ g) admixed to CT (1 μ g; List Biological Labs; 100B), as a control adjuvant. Alternatively, mice were immunized subcutaneously (s.c.) with OVA (10 μ g) alone or adsorbed to 40 μ g alum. Each mouse was immunized three times at 10-day intervals.

3.3. Sample harvesting and preparation

3.3.1. Blood

The blood sample was collected from the jugular vein of the mouse. Next, the whole blood was centrifuged at $2500 \times g$ for 15 min at 4°C for harvesting the serum followed by aliquoting and being stored at -80°C until further analysis.

3.3.2. Bronchoalveolar lavage fluid (BALF) and vaginal washing

The procedure for BALF collection was performed as described before (117). Briefly, the trachea of the mouse was surgically exposed, and a syringe catheter was used to intubate deep into the lower respiratory tract. One ml cold PBS was used to lavage the lungs to obtain the BALF and the retained fluid was centrifuged at $400 \times g$ for 5 min at 4°C before collecting the

supernatant for further investigation. Vaginal secretion was collected by inserting a saline-filled pipette tip into the vaginal opening and repeated washing with cold PBS.

3.3.3. Single-cell preparation

Lungs were collected after circulating blood was removed by cardiac perfusion with cold PBS. Briefly, the mouse lung tissue was minced into small pieces and incubated in RPMI 1640 medium containing collagenase type II (0.5 mg/ml; Sigma-Aldrich; 420302) at 37°C for 1 hr. The lymph nodes and spleen tissues were dissociated with gentle pressing using a 1-ml syringe plunger. The nasal tissue was collected after carefully removing skins from the snout. Next, the nasal tissue was digested for 20 min at 37°C with 400 U/ml DNase I (Roche; 11284932001) and Liberase™ (Roche; 05401119001). For processing all the above-mentioned tissues, a 70-µm cell strainer (Thermo Fisher Scientific; T_70122363548) was used to prepare single-cell suspensions after erythrocytes were lysed using red blood cell lysis buffer (Biolegend; 420302).

3.3.4. Antigen recall responses

Lung and spleen cells (2×10^6 cells/ml) were seeded in a 96-well round-bottom plate in complete RPMI 1640 medium supplemented with 10% heat-inactivated fetal bovine serum, 2.5 mM 4-(2-hydroxyethyl)-1-piperazineethanesulfonic acid (HEPES), 4 mmol/l L-glutamine, 50 µmol/l 2-mercaptoethanol, 100 µg/ml penicillin/streptomycin (all from Sigma-Aldrich). ESAT-6 (2 µg/ml) or OVA (10 µg/ml) was added for stimulating antigen-specific lymphocytes. Brefeldin A (eBioscience; 00-4506-51) was added for blocking the protein transport to facilitate intracellular protein measurement according to the manufacturer's instructions. After 6 hr of antigen re-stimulation, the cells were harvested and washed with PBS for further analysis. In some assays, splenocytes were incubated with concanavalin A (ConA; 5 µg/ml) as a positive control for T cell activation. In some experiments, splenocytes were incubated with the ESAT-6 antigen for 72 hr followed by downstream analysis.

3.3.5. Tissue collection for exudate preparation

Tissue samples including the lungs and nasal mucosa were harvested and homogenized for 45 sec at 4°C in the presence of the radioimmunoprecipitation assay buffer (Thermo Fisher Scientific; 89900) and the protease inhibitor (Life Technologies; 89900) for the measurement

of antigen-specific antibodies in the lung and nasal exudates. Exudates were obtained by centrifugation at $10,000 \times g$ for 20 min at 4°C.

3.3.6. Preparation and stimulation of bone marrow-derived dendritic cells (BMDCs)

Mouse femurs and tibiae were collected and bone marrow cells were harvested under sterile conditions by flushing with cold PBS using a syringe with a 23-gauge needle. A 70- μm cell strainer (Thermo Fisher Scientific; T_70122363548) was used for obtaining single-cell suspensions. Cells were centrifuged at $300 \times g$ for 5 min at 4°C. A red blood cell lysis buffer (Biolegend; 420302) was used to remove erythrocytes. Cells were cultured in complete RPMI 1640 medium (Thermo Fisher Scientific; 61870127) as described above together with 200 ng/ml recombinant Flt3-L (PeproTech; 250-31L). Cells were cultured for nine days at 37°C in 5% CO₂. For activation, cells were treated in vitro with ESAT-6 (1 $\mu\text{g}/\text{ml}$) alone or in the presence of S100A4 (1 $\mu\text{g}/\text{ml}$) or positive control stimuli as indicated at 37°C in 5% CO₂.

3.4. Tissue and cell analysis

3.4.1. Measurement of antigen-specific antibodies

ESAT-6-specific antibody levels were measured using the enzyme-linked immunosorbent assay (ELISA). A 96-well flat-bottom ELISA microtiter plate (Nunc-Thermo Fisher Scientific; 467320) was coated overnight at 4°C with 100 μl PBS containing ESAT-6 (1.5 $\mu\text{g}/\text{ml}$) or OVA (100 $\mu\text{g}/\text{ml}$). After overnight incubation, the ELISA plate was washed twice with a washing buffer containing 0.01% Tween-20. The plate was blocked by the addition of a blocking buffer (100 $\mu\text{l}/\text{well}$) containing 1% fetal bovine serum, followed by incubation for 1 hr at 37°C. After washing, an appropriate volume of the sample was added, and the plate was incubated for 2 hr at 37°C. The unbound primary antibody was removed after vigorous washing. Next, goat anti-mouse secondary antibodies for IgG (Southern Biotech; 1030-05), IgG1 (Southern Biotech; 1070-05), IgG2c (Southern Biotech; 1079-05) or IgA (Southern Biotech; 1040-05) conjugated with horseradish peroxidase was added, followed by incubation for 1 hr at 37°C. The ortho-phenylenediamine dihydrochloride (OPD; Thermo Fisher Scientific; 34006) substrate was added for color development after rigorous washing of the plates. The reaction was stopped by the addition of 100 μl of 2.5 M H₂SO₄. The absorbance was read using a spectrophotometer (BMG SPECTROStar Nano microplate reader) at 492 nm.

3.4.2. Measurement of released cytokines and chemokines

For the measurement of the production of cytokines and chemokines, cell-free culture supernatants were analyzed using the Bio-Plex multiplex system (Bio Plex™, Bio-Rad Laboratories; M60009RDPD) according to the manufacturer's protocol. The target cytokines and chemokines include TNF- α , IFN- γ , IL-4, IL-5, IL-10, IL-13, IL-6, IL-17, IL-1 β , GM-CSF, G-CSF, RANTES, MIP-1 β , MIP-1 α , MCP-1 (MCAF), eotaxin, CXCL1 (KC), IL-9, IL-1 α , IL-2, and IL-3. The data were acquired using a Bio-Plex 200 reader (Bio-Rad). The concentrations of each of the cytokines and chemokines were determined based on comparing with a standard curve, and the results were analyzed using Bio-Plex Manager software (Bio-Rad). Cytokines including IFN- γ , IL-12, IL-1 β , IL-4, IL-5, and IL-6 in the blood circulation were measured using ProcartaPlex™ Multiplex Immunoassay (Thermo Fisher Scientific; EPX110-20820-901) according to the manufacturer's instructions.

3.4.3. Flow cytometry

Cultured cells or single-cell suspensions prepared from various tissues were collected for flow cytometric analysis. CD4 T cells that could recognize the ESAT-6 peptide (QQWNFAGIEAAASA) presented by MHC class II were detected using a BV421-conjugated I-A^b/ESAT-6 tetramer (NIH tetramer core facility, Atlanta, USA). Cells were stained for 30 min at 37°C in darkness with the I-A^b/ESAT-6 tetramer. Similarly, cells were stained on ice with BV421-conjugated H-2K^b/SIINFEKL tetramer (MBL International) to detect cytotoxic T cells that could recognize OVA peptide (SIINFEKL). For staining cell surface markers, cells were incubated for 30 min on ice in darkness with the fluorescent antibodies listed in Table 6. A dye (BD Horizon™ Fixable Viability 620) for discriminating live and dead cells was used to facilitate proper cell gating. For the measurement of intracellular molecules, cells were first stained with antibodies against surface markers as described above, followed by fixation and permeabilization using the fixation buffer set (eBioscience™; 00-5523-00, or Thermo Fisher Scientific; 88882400) according to the manufacturer's instructions. Cells were then incubated for 30 min at room temperature in darkness with the fluorescent antibodies listed in Table 6. The stained cells were analyzed using a flow cytometer (BD FACSAria III), and data were analyzed using FlowJo software (Tree Star).

Table 6. Antibodies used in this study

Antibody	Fluorochrome	Source	Clone
CD11c	PE	Life Technologies-eBioscience™	N418
MHC class II	APC	Life Technologies-eBioscience™	AF6-120.1
CD86	FITC	Life Technologies-eBioscience™	GL1
CD80	PercP-Cy7	Life Technologies-eBioscience™	16-10A1
CD40	Brilliant Violet 520™	Life Technologies-eBioscience™	3/23
F4/80	PE	Life Technologies-eBioscience™	BM8
CD25	APC-Cy7	BD Pharmingen™	PC61
CD44	FITC	Life Technologies-eBioscience™	IM7
CD69	PE-Cy7	BD Pharmingen™	H1.2F3
Ki-67	FITC	BD Pharmingen™	B56
CD45	APC-Cyanine7	Life Technologies-eBioscience™	30-F11
CD4	APC-H7	BD Pharmingen™	GK1.5
CD3	Brilliant Violet 421™	Bio-gene	17A2
CD8	Brilliant Violet 510™	Biolegend	53-6.7
B220	PercP Cy5.5	BD Pharmingen™	RA3-6B2
IFN- γ	Alexa Fluor® 700	Biolegend	XMG1.2
IL-17	PercP5.5	Life Technologies-eBioscience™	eBio17B7
TNF- α	PE-Cy7	Life Technologies-eBioscience™	TN3-19.12
IL-2	APC	Life Technologies-eBioscience™	JES6-5H4
IL-6	PE	Life Technologies-eBioscience™	MP5-20F3
IL-1 β	PE-Cy7	Life Technologies-eBioscience™	NJTEN3
T-bet	PE-Cy5	Life Technologies-eBioscience™	eBio4B10 (4B10)
Granzyme B	PE	Invitrogen	GB12

3.4.4. Extraction of total RNA, cDNA synthesis and reverse transcription quantitative real-time polymerase chain reaction (RT-qPCR)

Total RNA was extracted according to the manufacturer's instructions using the RNeasy Mini Kit (Qiagen; 74106). cDNA was synthesized using the Thermo Scientific™ RevertAid™ First Strand cDNA Synthesis Kit (Thermo Fisher Scientific; K1622). The synthesized first-strand cDNA was used as a DNA template for RT-qPCR, which was carried out using the PowerTrack™ SYBR™ Green Master Mix (Applied Biosystems) in the ViiA7 real-time PCR system (Thermo Fisher Scientific; A25776). Briefly, the PCR reaction (10 μ l) including the

template and relevant primers was started with incubation for 2 min at 50°C and another 2 min at 95°C, followed by 40 cycles of 95°C for 15 sec for denaturation, and 60°C for 1 min for annealing/extension. Melt curve analysis was employed to confirm the specificity of the PCR reaction. The double delta Ct ($2^{-\Delta\Delta Ct}$) method was used to calculate the gene expression levels of various samples. Glyceraldehyde 3-phosphate dehydrogenase (GAPDH) was used as an endogenous reference control. Details of the primers used in this study are listed in Table 7.

3.4.5. Antigen transport and dendritic cell migration assay

To examine whether S100A4 could facilitate vaccine antigen transport, mice were given a single intranasal administration of a 20- μ l PBS solution containing Alexa Fluor 647-conjugated OVA (OVA-AF647; 10 μ g) with or without S100A4 (20 μ g) or CT (1 μ g). Naïve mice were also examined for background control. Flow cytometric analysis was performed as described above. To determine whether S100A4 promotes dendritic cell migration, BMDCs were treated in the presence or absence of S100A4 (1 μ g/ml), followed by an overnight incubation at 37°C in 5% CO₂. Next, S100A-treated cells were stained with CellTracker™ green (5-chloromethylfluorescein diacetate [CMFDA]; Thermo Fisher Scientific) according to the manufacturer's instructions. A total of 2×10^6 BMDCs, either primed with S100A4 or treated with vehicle control, was injected into the footpad of a mouse. The popliteal lymph nodes were harvested 24 hr later for detecting fluorescent dendritic cells that had migrated into the lymph nodes using flow cytometry.

3.4.6. Immunohistochemistry

The mouse spleen, lungs, and olfactory bulb tissues were fixed in 10% neutral buffered formalin for 24 hr at room temperature followed by paraffin embedding. Next, the tissues were processed with a tissue processor (Thermo Fisher Scientific; Excelsior AS Tissue Processor). A standard microtome blade was used to generate 5- μ m consecutive sections from each paraffin-embedded tissue block, and the sections were fixed onto microscopic slides. After deparaffinization and rehydration, sections were stained at 4°C overnight with a mouse monoclonal antibody against His-tag (clone 1B7G5; Proteintech) or a rat monoclonal antibody against CD45 (BD Biosciences; 557659) for recognizing S100A4 and leukocytes, respectively. After washing, an anti-mouse IgG secondary antibody (Proteintech; SA00001-1) or an anti-rat IgG secondary antibody (Cell Signaling

Technology; 7077S) was added followed by incubation at room temperature for 2 hr. The slides were mounted with an anti-fade mounting medium (Thermo Fisher Scientific).

3.5. Statistical analysis

Statistical analysis was performed using GraphPad Prism 8.00. $P < 0.05$ was determined by Student's *t*-test, Mann-Whitney *U* test or ANOVA with a multiple comparison test.

Table 7. PCR primers used in this study

Target Gene	Forward primer sequence (5'-3')	Reverse primer sequence (5'-3')
GAPDH	GGTGAAGGTCGGTGTGAACGGA	TGTTAGTGGGGTCTCGCTCCTG
CD80	GGTATTGCTGCCTTGCCGTT	TCCTCTGACACGTGAGCATC
CD86	TCCTGTAGACGTGTTCCAGA	TGCTTAGACGTGCAGGTCAA
CD40	GTTTAAAGTCCCGGATGCGA	CTCAAGGCTATGCTGTCTGT
IL-1 β	GGAGAACCAAGCAACGACAAAATA	TGGGGAActCTGCAGACTCAAAC
IL-6	CCACTTCACAAGTCGGAGGCTTA	CCAGTTTGGTAGCATCCATCATTTC
TNF- α	AAGCCTGTAGCCACGTCGTA	AGGTACAACCCATCGGCTGG
IFN- γ	TAGCCAAGACTGTGATTGCGG	AGACATCTCCTCCCATCAGCAG
IL-4	ACGGGAGAAGGGACGCCAT	GAAGCCCTACAGACGAGCTCA
IL-23	TGCCCAGCCTGAGTTCTAGT	AGACAGAGTTGCTGCTCCGT
IL-10	GCCAGAGCCACATGCTCCTA	GATAAGGCTTGGCAACCCAAGTAA
IL-12	TGGGAGTACCCTGACTCCTG	GGAACGCACCTTTCTGGTTA
TLR2	GCTGGAGGACTCCTAGGCT	GTCAGAAGGAAACAGTCCGC
TLR4	GCTTTCACCTCTGCCTTAC	GAAACTGCCATGTTTGAGCA

4. RESULTS

4.1. S100A4 is a potent mucosal adjuvant and elicits durable adaptive immune responses

A good adjuvant is expected to induce long-term immune responses. Together with my colleagues, we attempted to investigate the durability of antigen-specific antibody production after mucosal immunization with S100A4 as an adjuvant at a late time point (about 6 months post-last immunization). To this end, mice were nasally administered with OVA, a model vaccine antigen, alone or admixed to S100A4 or CT three times at a 10-day interval. Next, various samples were harvested for the measurement of OVA-specific antibody levels (Fig. 4.1A). Overall, the use of S100A4 substantially augmented antigen-specific antibody levels in various compartments 6 months after the last immunization (Fig. 4.1). Anti-OVA total IgG, IgG1, and IgG2c antibody levels remained high in the serum of S100A4-adjuvanted mice (Fig. 4.1B). The production of IgA antibody in the mucosal tissues is critical for the first-line defense against many infectious diseases. Thus, OVA-specific IgA antibody production in mucosal tissue secretions, such as the lung tissue exudate (Fig. 4.1C), BALF (Fig. 4.1D), vaginal secretion (Fig. 4.1E), and fecal extract (Fig. 4.1F) remained substantially high in S100A4-adjuvanted mice at this late time point. Notably, the antibody durability induced by S100A4 was comparable to that obtained with CT, which is described as a gold standard mucosal adjuvant (Fig. 4.1). These late time point antibody levels were comparable to earlier time points, suggesting good durability of the adjuvant effect of S100A4 (84).

Antigen-specific CD8 T cells are critical in controlling infection caused by intracellular pathogens (118). To assess whether S100A4 could promote the expansion of cytotoxic T cells that could recognize the immunizing antigen OVA, an MHC class I-associated OVA peptide (SIINFEKL) tetramer (H-2K^b/OVA) was employed for detecting OVA-specific CD8 T cells in mice that were immunized with OVA (Fig. 4.2A and B). S100A4 robustly induced the expansion of OVA-specific CD8 T cells in the lungs (Fig. 4.2C) measured at both 10 days and 196 days after last immunization. These antigen-specific T cell responses in lymph nodes (Fig. 4.2D) and spleen (Fig. 4.2E) were also augmented 10 days after the last immunization. Of note, S100A4 outperformed CT with respect to promoting the clonal expansion of antigen-specific CD8 T cells (Fig. 4.2).

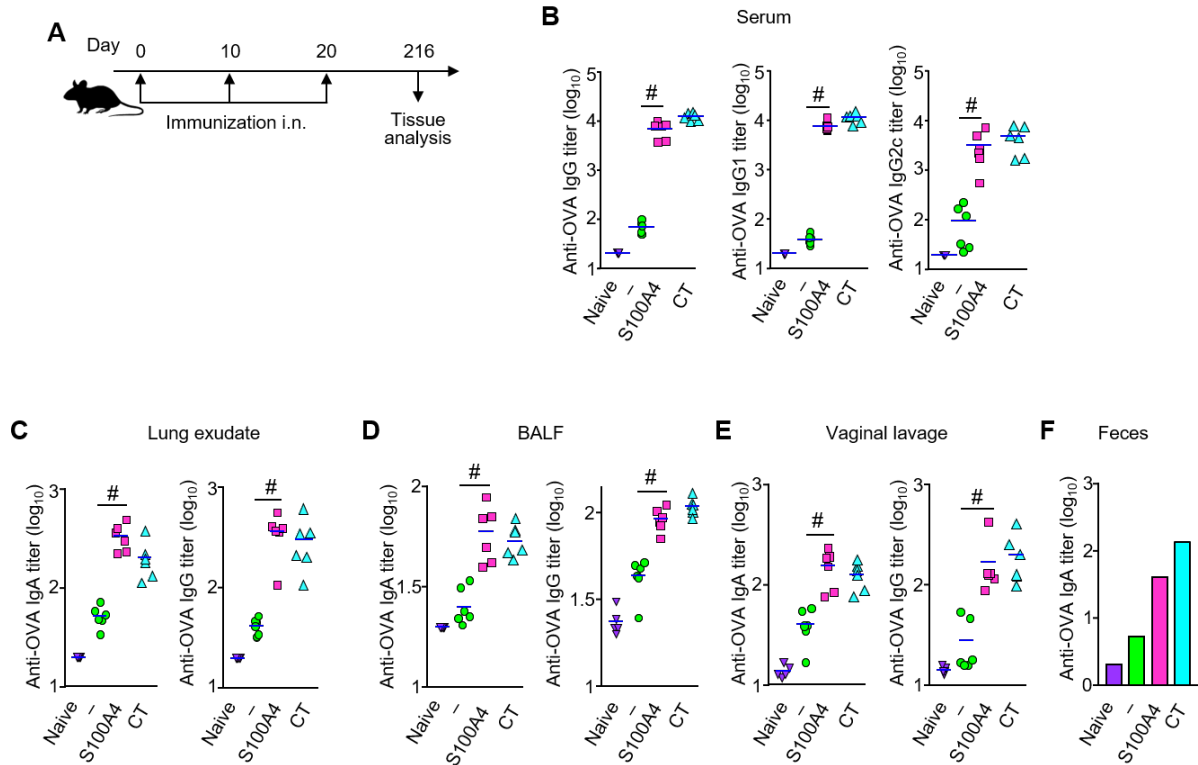


Figure 4.1. S100A4 is a potent mucosal adjuvant and elicits durable humoral immune responses. Mice were immunized three times intranasally (i.n.) with ovalbumin (OVA; 10 μ g) in the absence or presence of S100A4 (10 μ g) or cholera toxin (CT; 1 μ g) at an interval of 10 days. For baseline control, unmanipulated naive mice were used. Various tissue samples were harvested 196 days after the last immunization (A). Levels of OVA-specific total IgG, IgG1 and IgG2c in serum (B), OVA-specific IgA and total IgG in lung exudates (C), bronchoalveolar lavage fluid (BALF) (D), and vaginal lavage (E), as well as OVA-specific IgA in pooled feces (F) were measured using ELISA. Each symbol represents measurement from a single mouse, and blue lines indicate the average values. # $P = 0.002$ is determined by Mann-Whitney U test. (Adapted from reference No. 84).

Taken together, these results demonstrate that intranasal immunization adjuvanted with S100A4 is effective in promoting cytotoxic T cell responses, in addition to humoral immune responses. S100A4 as a mucosal adjuvant is demonstrated to be capable of sustaining durable protective immunity (84).

4.2. S100A4 enhances antigen recall responses of cytotoxic T cells

Granzyme B, together with cytokines, are among the immune defensive toolkit by which cytotoxic T cells eliminate infection (119). To confirm if S100A4 could induce the production of granzyme B and pro-inflammatory cytokines by antigen-specific cytotoxic T cells upon antigen re-encounter, mice were immunized three times with OVA adjuvanted with S100A4 or CT, followed by

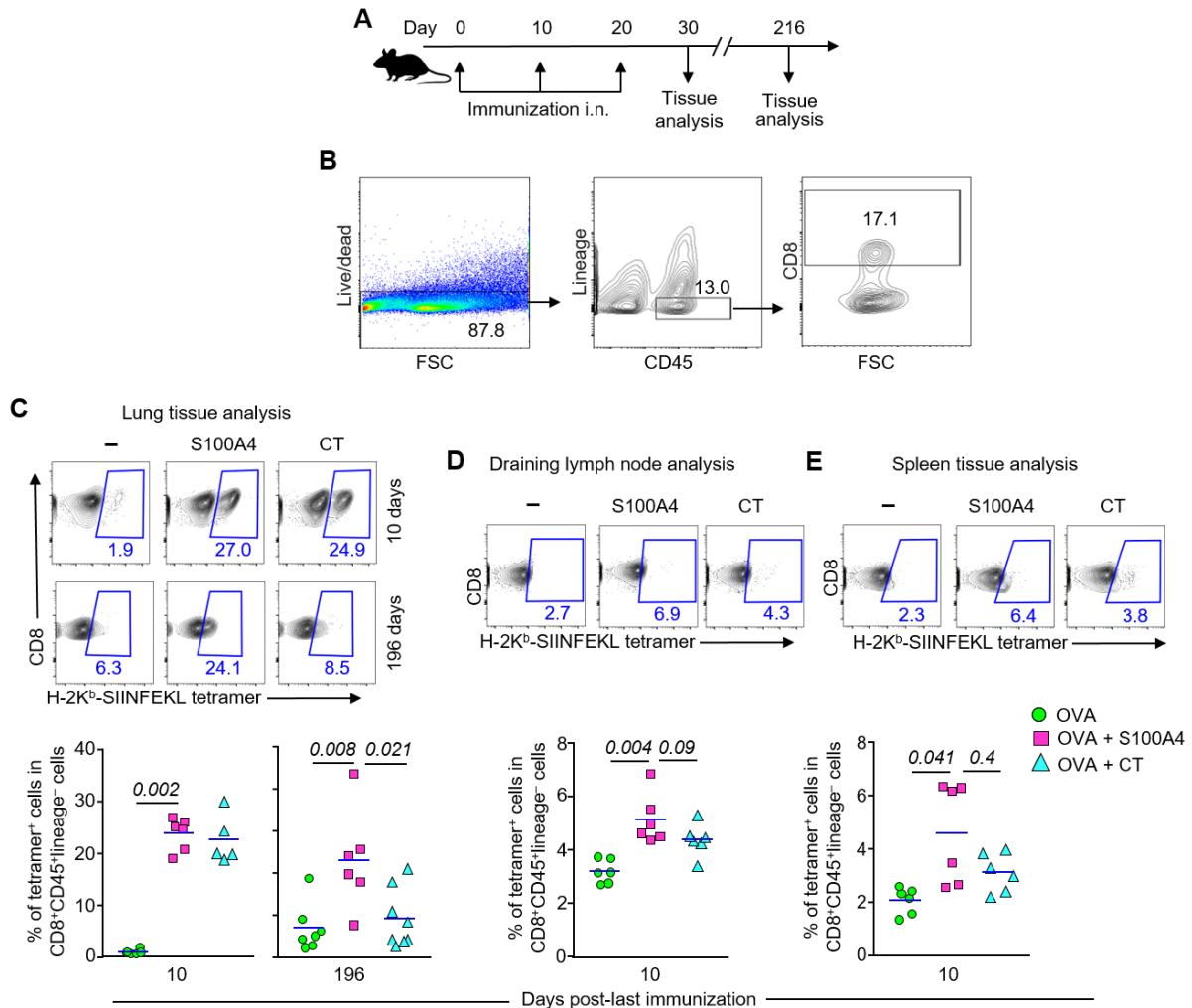


Figure 4.2. S100A4 expands antigen-specific cytotoxic T cell immune responses. Mice were immunized three times intranasally (i.n.) with ovalbumin (OVA; 10 μ g) alone or admixed to S100A4 (10 μ g) or cholera toxin (CT; 1 μ g) at an interval of 10 days. Various samples were harvested 10 days or 196 days after the last immunization (A). Gating strategies for identifying cytotoxic T cells are shown. To exclude cells from unwanted lineages, a set of antibodies (Ter-119, GR-1, CD11b, CD11c, and CD19) was used (B). Frequencies of cytotoxic T cells that recognized H-2K^b/OVA (SIINFEKL) tetramer in the lungs, lymph nodes, and spleen were measured using flow cytometry. Representative contour plots (upper panels) indicate measurements from a single mouse in each treatment and the lower panels show the pooled results (C to E). Numbers in or adjacent to outlined areas indicate percent cells in each gate. Each symbol represents measurement from a single mouse, and blue lines indicate the average values. The exact *P*-values (italic numbers) are determined by Mann-Whitney *U* test. (Adapted from reference No. 84).

harvesting the splenocytes for incubation with OVA (Fig. 4.3A and B). Following such antigen recall responses, OVA-specific cytotoxic T cell-associated expression of granzyme B was greatly increased in the spleen cell culture derived from S100A4-adjuvanted mice (Fig. 4.3C). Co-immunization with S100A4 induced granzyme B production by cytotoxic T cells more effectively than CT for comparison (Fig. 4.3C).

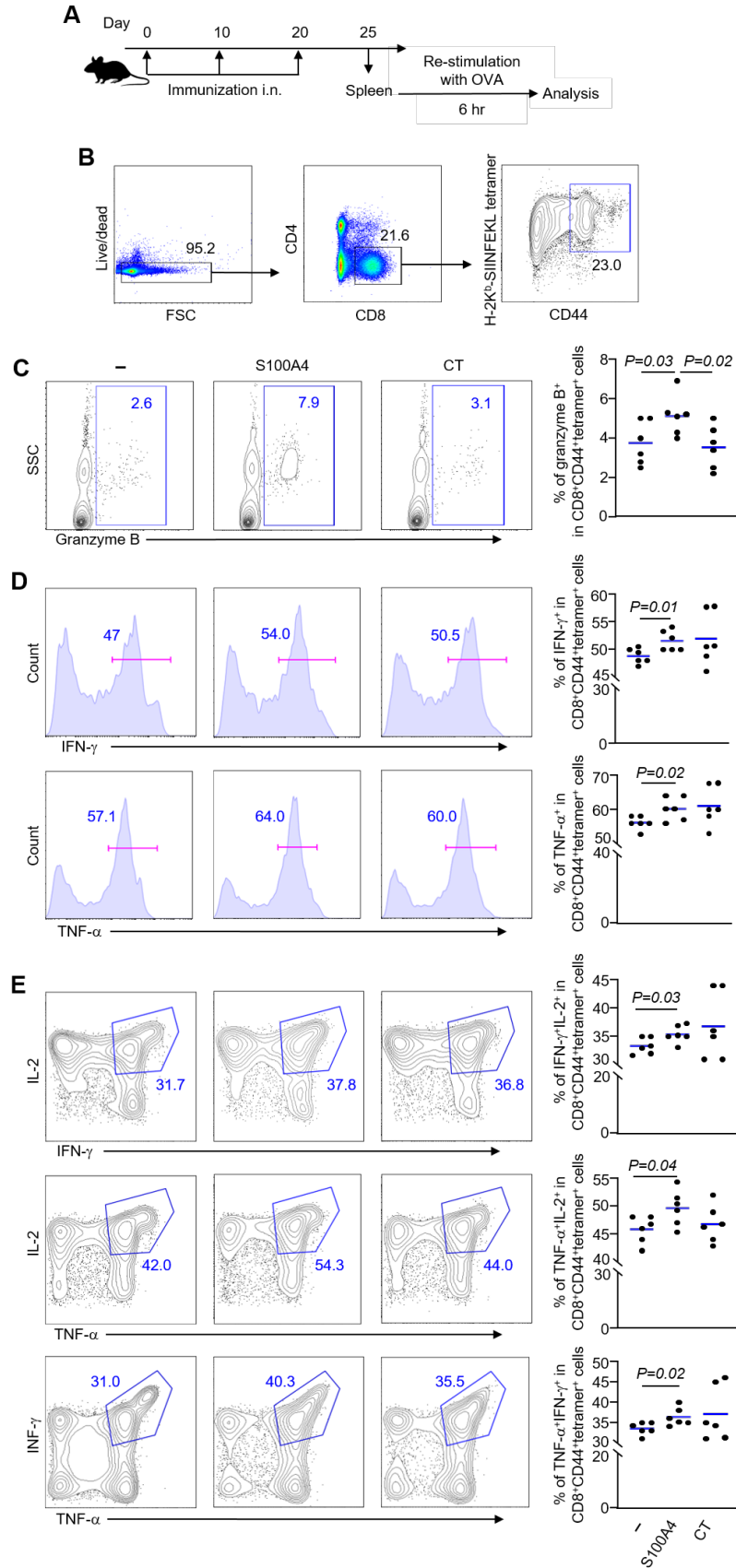


Figure 4.3. S100A4 induces H-2K^b/OVA-specific memory cytotoxic T cells that express granzyme B and pro-inflammatory cytokines upon re-stimulation with immunizing antigen. Mice were intranasally (i.n.) received ovalbumin (OVA; 10 µg) in the presence or absence of S100A4 (10 µg) or cholera toxin (CT; 10 µg) three times at an interval of 10 days. The mouse spleen was collected five days after the last immunization for analysis. Next, cells were treated with OVA (10 µg/ml) for 6 hr at 37°C in 5% CO₂ (A). Flow cytometric gating strategies for identifying H-2K^b/OVA (SIINFEKL)-specific memory cytotoxic T cells that expressed granzyme B and pro-inflammatory cytokines are shown (B). Frequencies of H-2K^b/OVA (SIINFEKL)-specific memory cytotoxic T cells that produced granzyme B and pro-inflammatory cytokines were analyzed. Representative contour plots or histograms indicate results from a single mouse in each treatment condition (left panels) and pooled results from all the mice (right panels) are indicated (C to E). Numbers in or adjacent to outlined areas indicate percent cells in each gate. Each dot represents measurement from a single mouse, and the blue lines indicate the average values. The exact *P*-values (*italic numbers*) are determined by Student's *t*-test.

Furthermore, immunization adjuvanted with S100A4 markedly increased the production of IFN- γ or TNF- α (Fig. 4.3D) as well as different combinations of pro-inflammatory cytokines (IFN- γ /TNF- α , IFN- γ /IL-2, or TNF- α /IL-2) by OVA-specific cytotoxic T cells (Fig. 4.3E).

4.3. S100A4 provokes greater mucosal and cellular immune responses than subcutaneous immunization adjuvanted with alum

Alum has been used as a clinically applicable adjuvant for more than a centennium. However, this adjuvant is not suitable for facilitating mucosal immunization (120). It was thus interesting to compare the mucosal adjuvant activity of S100A4 with alum. Thus, intranasal immunization with OVA admixed to S100A4 in parallel with subcutaneous immunization with OVA adsorbed to alum was evaluated (Fig. 4.4A). For serum anti-OVA total IgG antibody levels, nasal immunization adjuvanted with S100A4 was comparable to subcutaneous immunization adjuvanted with alum (Fig. 4.4B). However, for antibody responses at various mucosal sites, as measured in BALF (Fig. 4.4C), vaginal secretion (Fig. 4.4D), and feces (Fig. 4.4E), S100A4 outperformed alum. Alum failed to stimulate the production of pulmonary CD8⁺ T cells reactive with the OVA peptide, the immunizing antigen, in contrast to the robust effect potentiated by S100A4 in this regard (Fig. 4.4F). The observation on the failure of alum in stimulating effective mucosal immune defence and cytotoxic T cell responses is consistent with general expectations on the use of alum (121).

4.4. S100A4 migrates to the spleen and lung tissues following intranasal administration

Before assessing the adjuvanticity of S100A4 in transporting antigen, the biodistribution of this molecule in secondary lymphoid organs and mucosal tissues was evaluated. For this purpose, mice were intranasally administered with a recombinant His-tagged S100A4 (Fig. 4.5A). The

results depicted in Fig. 4.5 clearly confirmed the distribution of S100A4 in both spleen (Fig. 4.5B) and lung tissues (Fig. 4.5C) 24 hr after intranasal administration, supporting a long-distance function of the adjuvant (84).

4.5. S100A4 facilitates antigen transport to secondary lymphoid organs and mucosal tissues

Adaptive immune responses require efficient antigen transport, which is vital for effective antigen-specific immune responses (122). Together with my colleagues, we investigated whether the adjuvant activity of nasally co-administered S100A4 could promote antigen transport to secondary lymphoid organs. To this end, 6 hr following intranasal administration of fluorescent OVA as an antigen, nasal tissues, lungs, and cervical lymph nodes were collected for flow cytometric analysis. S100A4 greatly promoted the accumulation of antigen-loaded dendritic cells and macrophages in nasal tissues and cervical lymph nodes (Fig. 4.6), as well as lung tissues (Fig. 4.7). Importantly, 12 hr after the delivery of the fluorescent antigen, the accumulation of the antigen-loaded cells in lung tissues remained robust (Fig. 4.7C). Thus, it is likely that S100A4 is an effective mucosal adjuvant that can promote the migration of APC-associated antigen from the nasal mucosa (84). The efficient uptake and transport of antigens by APCs, a process that is facilitated by adjuvant, is crucial to the successful mobilization of adaptive immune responses (123).

To better elucidate the mechanisms underlying the adjuvant activity of S100A4 in supporting antigen transport, an adoptive transfer assay was carried out. For this purpose, BMDCs were incubated in the presence or absence of S100A4. Next, these dendritic cells were injected into the mouse footpad (Fig. 4.8A). S100A4 substantially enhanced the accumulation of S100A4-treated dendritic cells in the popliteal lymph nodes, which drain the injection site, compared with control dendritic cells (Fig. 4.8B) (84).

4.6. S100A4 does not induce olfactory bulb inflammation following intranasal delivery

In preclinical mucosal vaccine studies, as a gold standard mucosal adjuvant, CT is routinely used for enhancing immune responses toward the vaccine antigen. However, CT is not suitable for human use because of its strong neurotoxicity (124). To confirm the safety of S100A4, S100A4 or CT was intranasally administered and the olfactory bulb was collected for analysis 24 hr later (Fig. 4.9A).

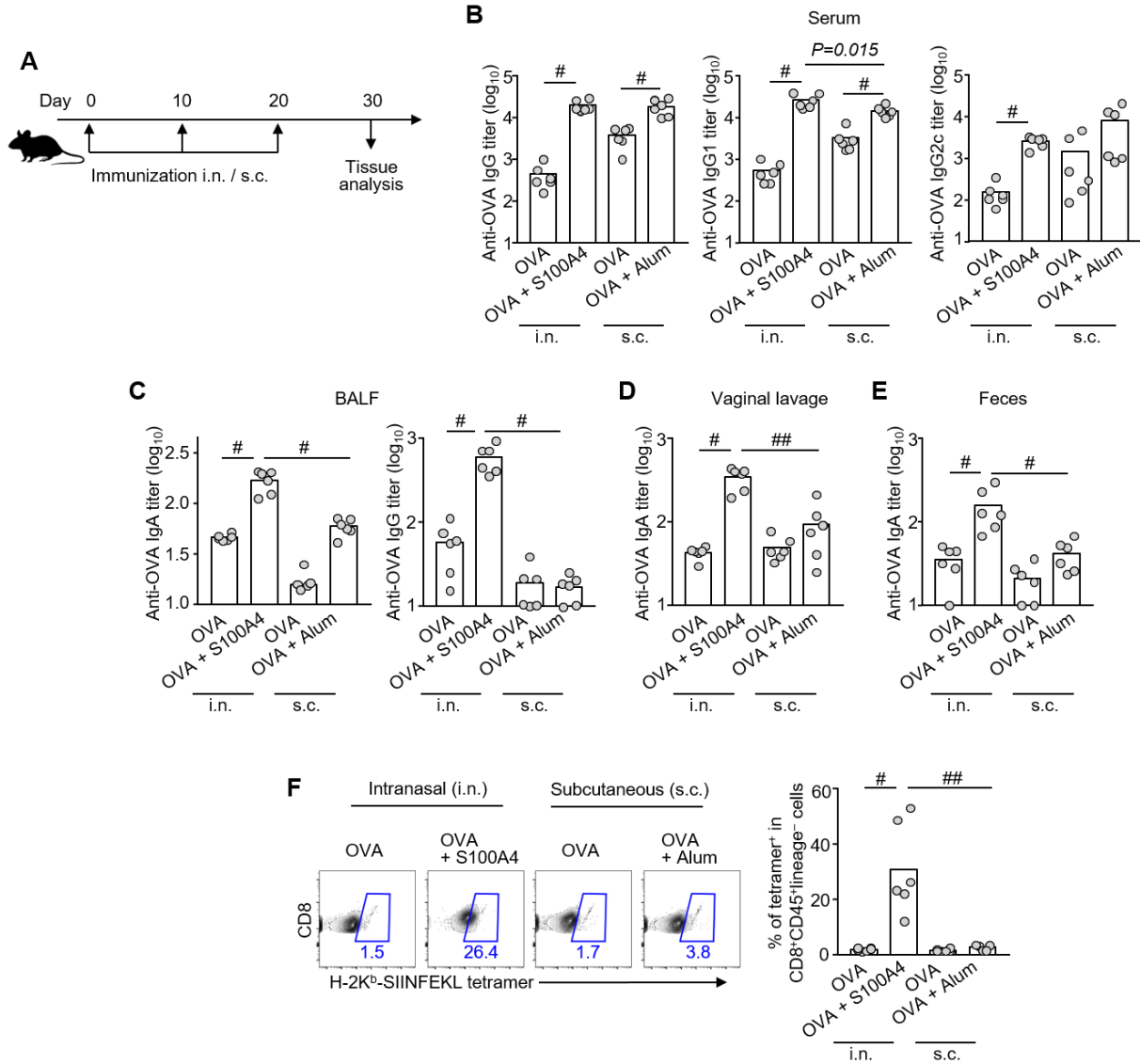


Figure 4.4. S100A4 provokes greater mucosal and cellular immune responses in intranasal immunization compared to subcutaneous immunization adjuvanted with alum. Mice were immunized three times at a 10-day interval intranasally (i.n.) with ovalbumin (OVA; 10 μ g) admixed to S100A4 (10 μ g) or vehicle control. The mouse lungs, lymph nodes and spleen were collected 10 days after the last immunization for analysis. Alternatively, mice were immunized subcutaneously (s.c.) with OVA (10 μ g) alone or adsorbed to 40 μ g alum. Relevant tissue samples were harvested 10 days after the last immunization (A). Levels of OVA-specific IgG, IgG1 and IgG2c in serum (B), OVA-specific IgA and total IgG in bronchoalveolar lavage fluid (BALF) (C), as well as OVA-specific IgA in vaginal washing (D) and pooled feces (E) were measured using ELISA. Single-cell suspensions were prepared from the lung tissues and percentages of CD8 T cells that recognized H-2K^b/OVA (SIINFEKL) tetramer were revealed by flow cytometry. Representative contour plots indicate results from a single mouse in each treatment condition (left panels) and pooled results from all the mice (right panel) are indicated (F). Numbers adjacent to outlined areas indicate percent cells in each gate. Each symbol indicates measurement from a single mouse, and the columns indicate the average values. # $P=0.0022$; ### $P=0.0043$ or the exact P -value (italic number) is determined by Mann-Whitney U test.

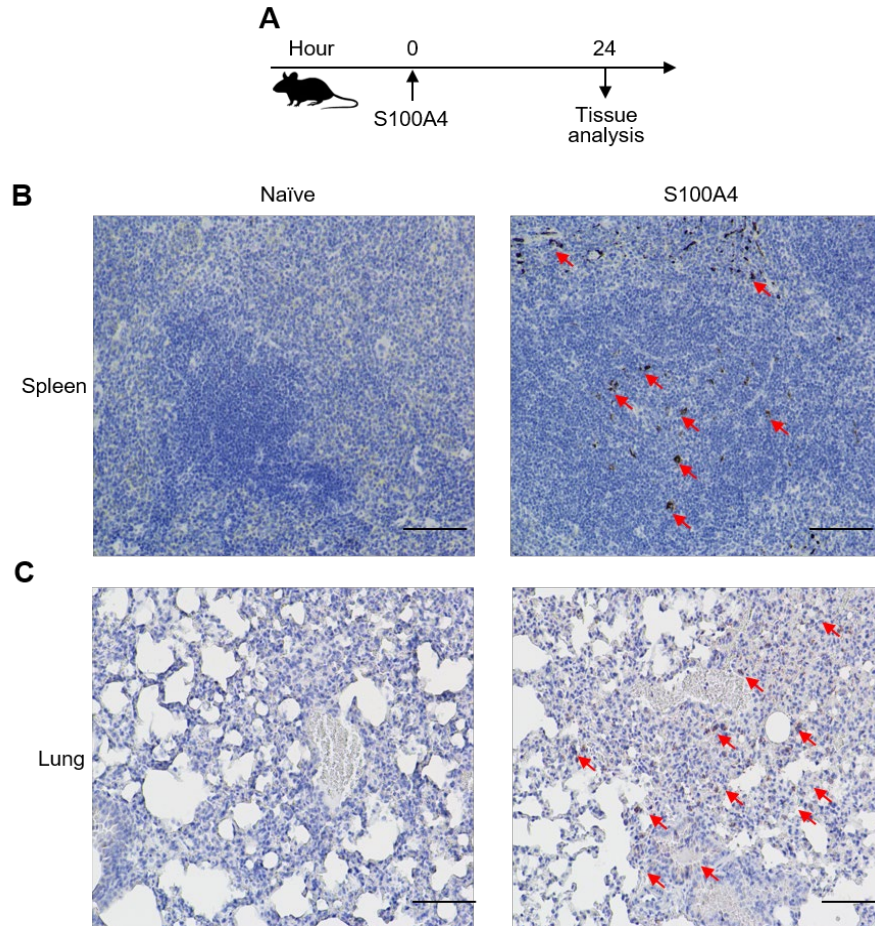


Figure 4.5. S100A4 migrates to the spleen and lung tissues following intranasal administration. Mice were intranasally (i.n.) administered with recombinant His-tagged S100A4 (20 μ g). Unmanipulated naive mice were included for background control (A). Spleen (B) and lungs (C) were collected 24 hr later, followed by sectioning and immunohistochemistry staining for the His-tag. Arrows indicate the His-tagged S100A4. Scale bar, 100 μ m. (Adapted from reference No. 84).

My data clearly showed leukocyte accumulation in the olfactory bulb of mice that received CT compared with the absence of leukocyte accumulation in mice that received S100A4 (Fig. 4.9B). Furthermore, the olfactory bulb was collected 10 days after the last immunization with ESAT-6 admixed to S100A4 (Fig. 4.9C). S100A4 did not promote the expression of pro-inflammatory cytokines, such as IL-6 and IL-12, in the olfactory bulb (Fig. 4.9D) (84).

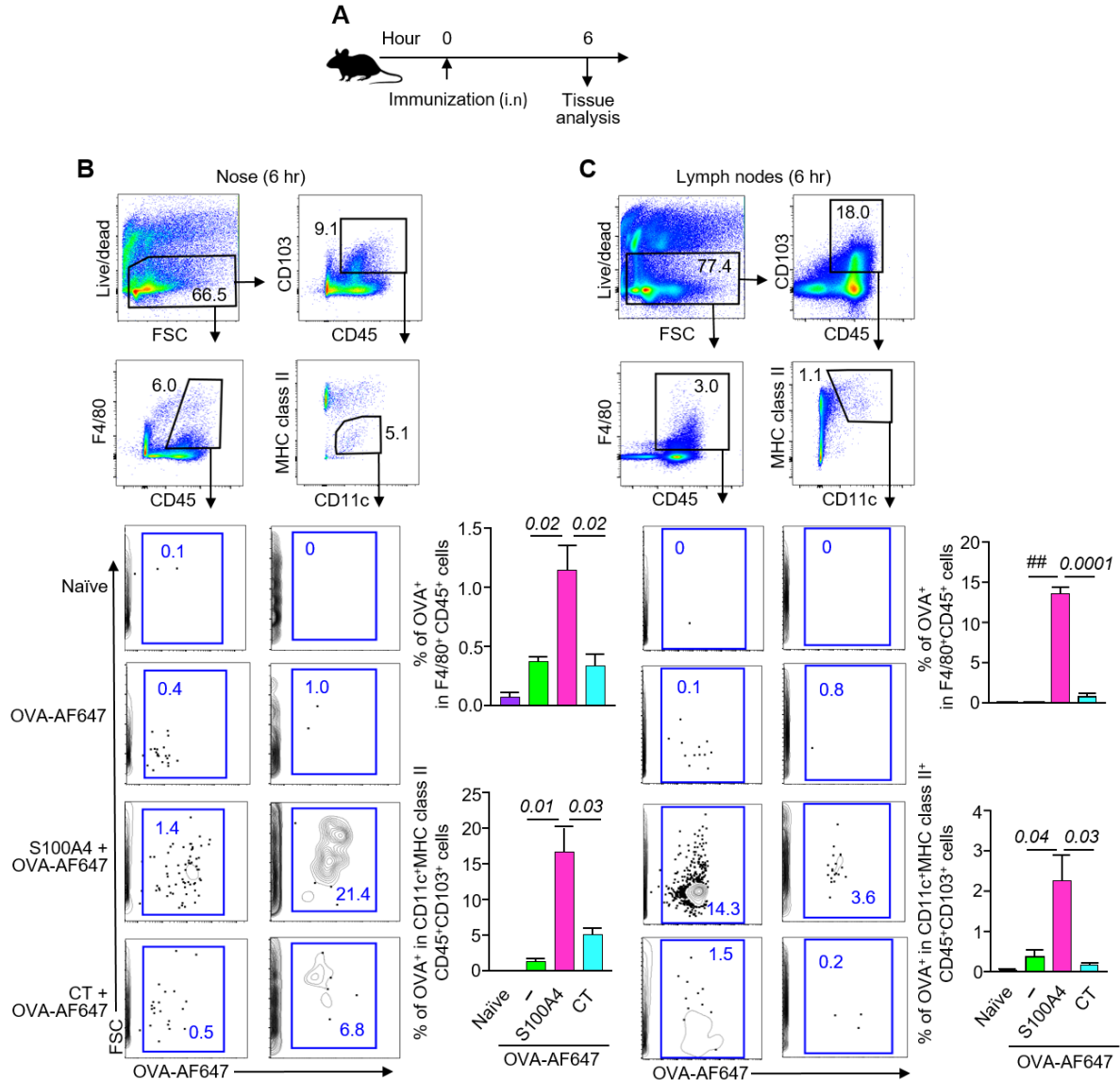


Figure 4.6. S100A4 facilitates antigen transport to nasal tissues and lymph nodes. Mice received a single intranasal (i.n.) delivery of Alexa Fluor 647-conjugated ovalbumin (OVA-AF647; 10 μ g) alone or admixed to S100A4 (20 μ g) or cholera toxin (CT; 1 μ g). For background control, naive mice were used (A). Nasal tissues and lymph nodes were collected 6 hr after antigen delivery for analysis. Gating strategies for identifying antigen-loaded dendritic cells (CD45⁺CD103⁺CD11c⁺MHC II⁺) and macrophages (CD45⁺F4/80⁺) in nasal tissues (B) and cervical lymph nodes (C) are shown. Representative contour plots indicate results from a single mouse in each treatment condition and columns show pooled results from all the mice (B and C). Numbers in or adjacent to outlined areas indicate percent cells in each gate. Results are presented as the mean + SEM of three biological replicates (B and C). ##*P* < 0.0001 or the exact *P*-values (italic numbers) are determined by Student's *t*-test. (Adapted from reference No. 84).

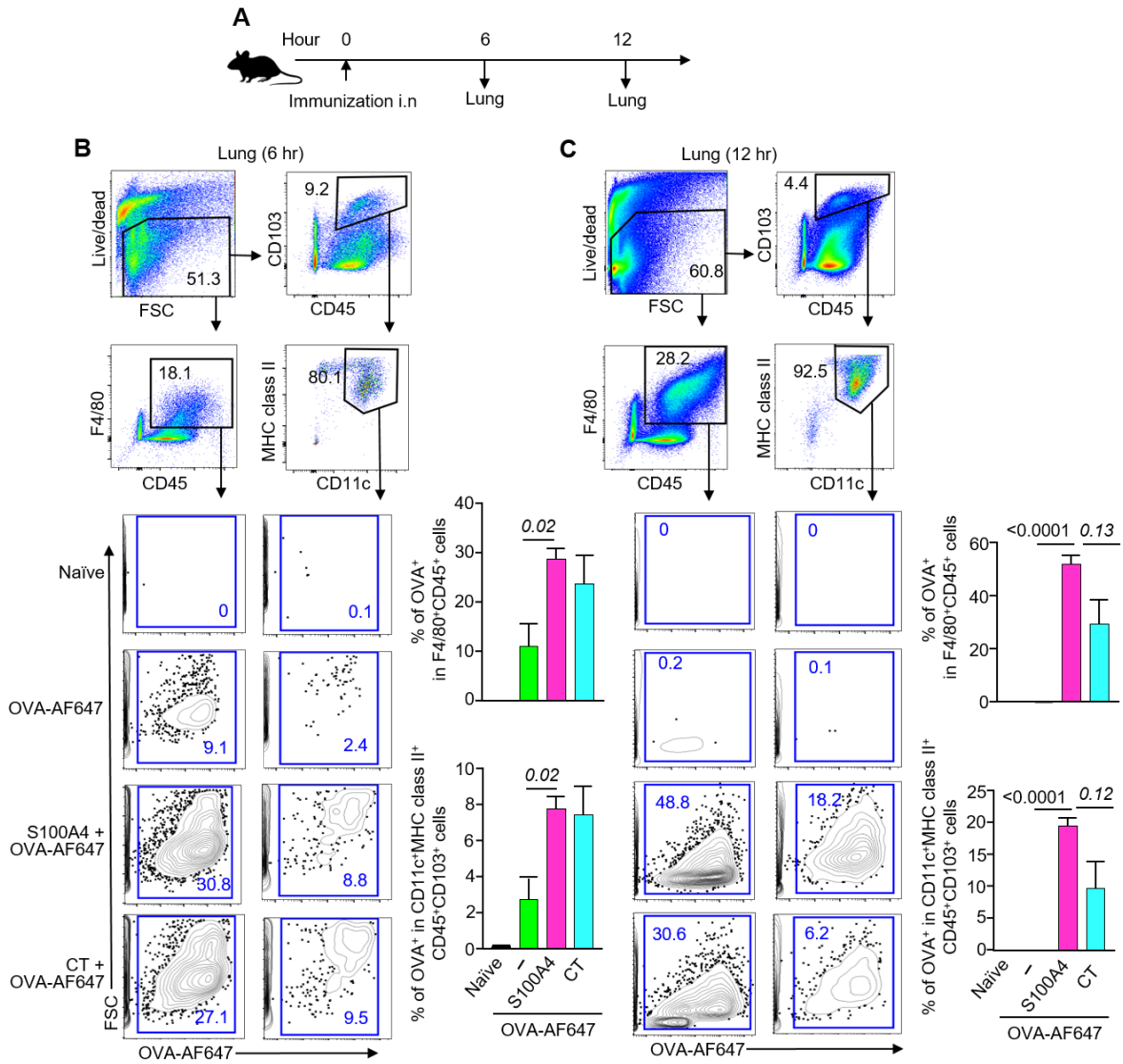


Figure 4.7. S100A4 facilitates antigen transport to lung tissues. Mice received a single intranasal (i.n.) delivery of Alexa Fluor 647-conjugated ovalbumin (OVA-AF647; 10 μ g) alone or admixed to S100A4 (20 μ g) or cholera toxin (CT; 1 μ g). For background control, naive mice were used (A). Lung tissues were collected 6 hr (B) or 12 hr (C) after antigen delivery for analysis. Gating strategies for identifying antigen-loaded dendritic cells (CD45⁺CD103⁺CD11c⁺MHC II⁺) and macrophages (CD45⁺F4/80⁺) in the lungs are shown (B and C). Representative contour plots indicate results from a single mouse in each treatment condition and columns show pooled results from all the mice (B and C). Numbers in or adjacent to outlined areas indicate percent cells in each gate. Results are presented as the mean + SEM of three biological replicates (B and C). The exact *P*-values (italic numbers) are determined by Student's *t*-test. (Adapted from reference No. 84).

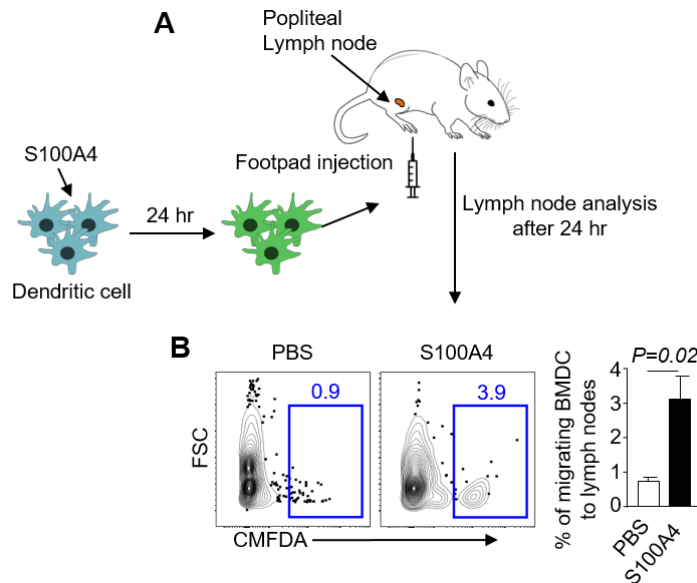


Figure 4.8. S100A4 promotes transport of antigen delivered at the footpad to draining lymph nodes. Mouse bone marrow cells were cultured to obtain bone marrow-derived dendritic cells (BMDCs) in the presence of Flt3-L. BMDCs were treated with or without S100A4 (1 $\mu\text{g/ml}$) overnight at 37°C in 5% CO_2 , and stained with CellTracker™ (CMFDA-green). Mice were then injected with 2×10^6 BMDCs into the footpad and popliteal lymph nodes were harvested 24 hr later for flow cytometric analysis (A). Representative contour plots based on one experiment (left panels) and pooled results from three biological replicates (right panel) are shown (B). Numbers adjacent to outlined areas indicate percent cells in each gate. Results are presented as mean + SEM of three biological replicates. The exact *P*-value (*italic number*) is determined by Student's *t*-test. (Adapted from reference No. 84).

4.7. S100A4 potentiates antigen-specific antibody production after intranasal immunization with the *Mycobacterium tuberculosis*-derived antigen ESAT-6

Although cell-mediated immune responses are believed critical in controlling infection by the intracellular pathogen such as *Mycobacterium tuberculosis* (125), the recent success of vaccination against many intracellular pathogens mediated by antibodies has prompted researchers to investigate the significance of humoral immunity in the development of TB vaccines (126). To investigate the potent adjuvant activity of S100A4 in enhancing antibody production, mice were immunized with ESAT-6, a candidate vaccine antigen derived from *Mycobacterium tuberculosis* alone or admixed to S100A4 or CT three times at an interval of 10 days. Various mucosal tissue secretions and serum were collected to determine the levels of antibody production (Fig. 4.10A). ESAT-6-specific total IgG, IgG1, and IgG2c antibody levels were robustly augmented in the blood circulation of mice that received S100A4 admixed to ESAT-6 (Fig. 4.10B).

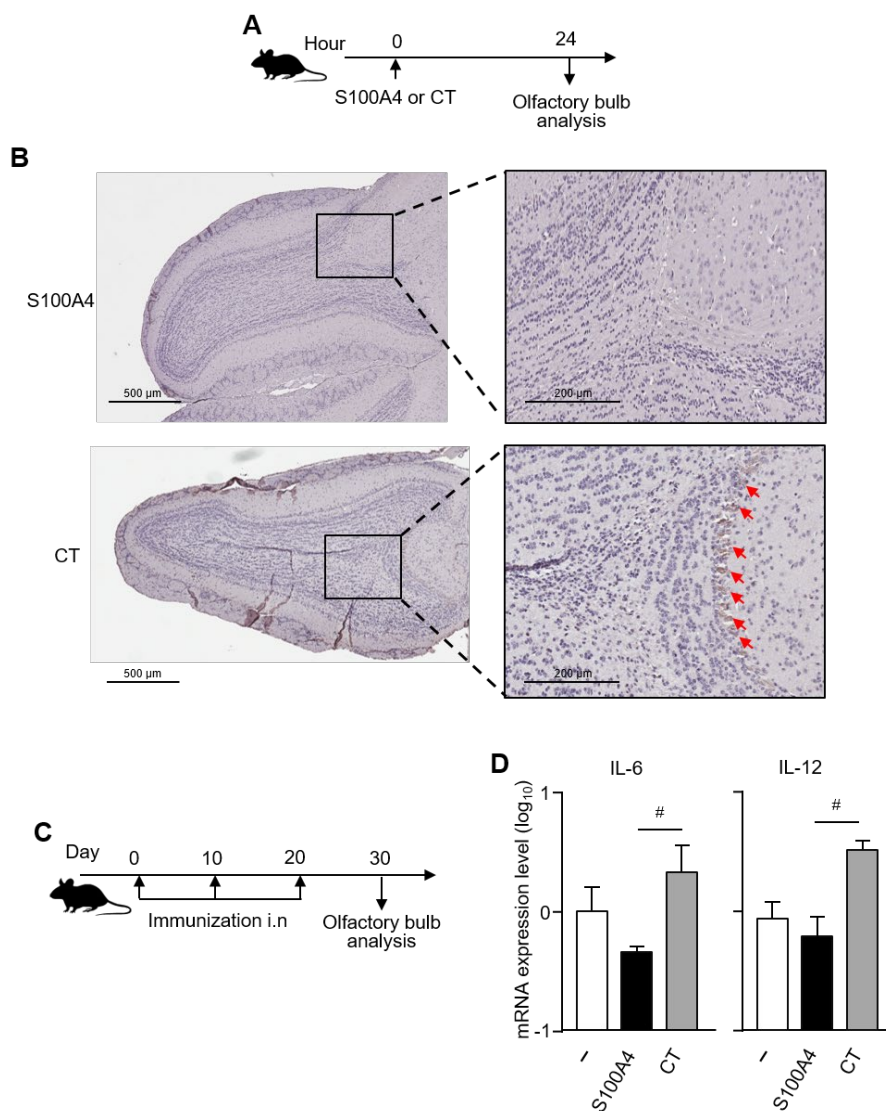


Figure 4.9. S100A4 does not induce olfactory bulb inflammation following intranasal administration. (A and B) Mice received a single intranasal (i.n.) delivery of S100A4 (20 μ g) or cholera toxin (CT; 1 μ g). Olfactory bulb was collected 24 hr later (A). The olfactory bulb tissue was sectioned for immunohistochemistry staining using an anti-CD45 antibody. Arrows indicate CD45⁺ leukocytes. The boxed areas are magnified for clearer views (B). (C and D) Mice were intranasally (i.n.) immunized with ESAT-6 (5 μ g) alone or admixed to S100A4 (10 μ g) or CT (1 μ g) three times at a 10-day interval. Olfactory bulb was collected 10 days after the last immunization (C). mRNA expression levels of cytokines as indicated were analyzed using RT-qPCR. Gene expression was normalized using glyceraldehyde 3-phosphate dehydrogenase (GAPDH) as a calibrator gene. Data are expressed as mean + SEM of three biological replicates, and the columns indicate the average values. # P = 0.0082 is determined by Mann-Whitney U test. (Adapted from reference No. 84)

Importantly, S100A4 enhanced the production of ESAT-6-specific IgA and total IgG antibody levels in the lung tissue exudate to a greater extent than the performance of CT for comparison as a benchmark adjuvant (Fig. 4.10C). Furthermore, intranasal administration of S100A4 substantially enhanced ESAT-6-specific IgA antibody production in BALF and nasal mucosa (Fig. 4.10D and E). Taken together, these findings demonstrate that ESAT-6-specific antibody production was profoundly elevated in both systemic and mucosal compartments, implying that S100A4 is a potent mucosal adjuvant with respect to antigen-specific humoral immune responses. The abundance of IgA at mucosal surfaces is critical not only in combating infectious pathogens that can cross the mucosal barrier, but also in neutralizing pathogens at their point of entry (33).

4.8. S100A4 expands antigen-specific CD4 T cell responses after intranasal immunization with the *Mycobacterium tuberculosis*-derived antigen ESAT-6

To determine whether S100A4 could enhance the accumulation of CD4 T cells that recognized the immunizing *Mycobacterium tuberculosis* antigen, a tetramer that is composed of ESAT-6 peptide (QQWNFAGIEAAASA) in association with the MHC class II molecule (I-A^b/ESAT-6 tetramer) was employed for the measurement of ESAT-6 peptide-specific CD4 T cells in the lungs and spleen after immunization (Fig. 4.11A-C). Administration of the immunizing antigen ESAT-6 admixed to S100A4 overwhelmingly enhanced the expansion of CD4 T cells that could recognize MHC class II-restricted ESAT-6 peptide in both lungs and spleen (Fig. 4.11D). The enhancement brought by S100A4 was greater than that by CT (Fig. 4.11D).

4.9. S100A4 upregulates cytokine secretion in the blood circulation in response to intranasal immunization with the *Mycobacterium tuberculosis*-derived antigen ESAT-6

To determine whether S100A4 could induce cytokine secretion in the blood circulation, mice were immunized with ESAT-6 alone or admixed to S100A4. Sera were collected for the measurement of cytokine production. Immunization adjuvanted with S100A4 consistently increased the levels of a panel of cytokines, including IFN- γ , IL-12, IL-1 β , IL-4, IL-5, and IL-6 (Fig. 4.12). These cytokines have various immune potentiating roles in adaptive immune responses.

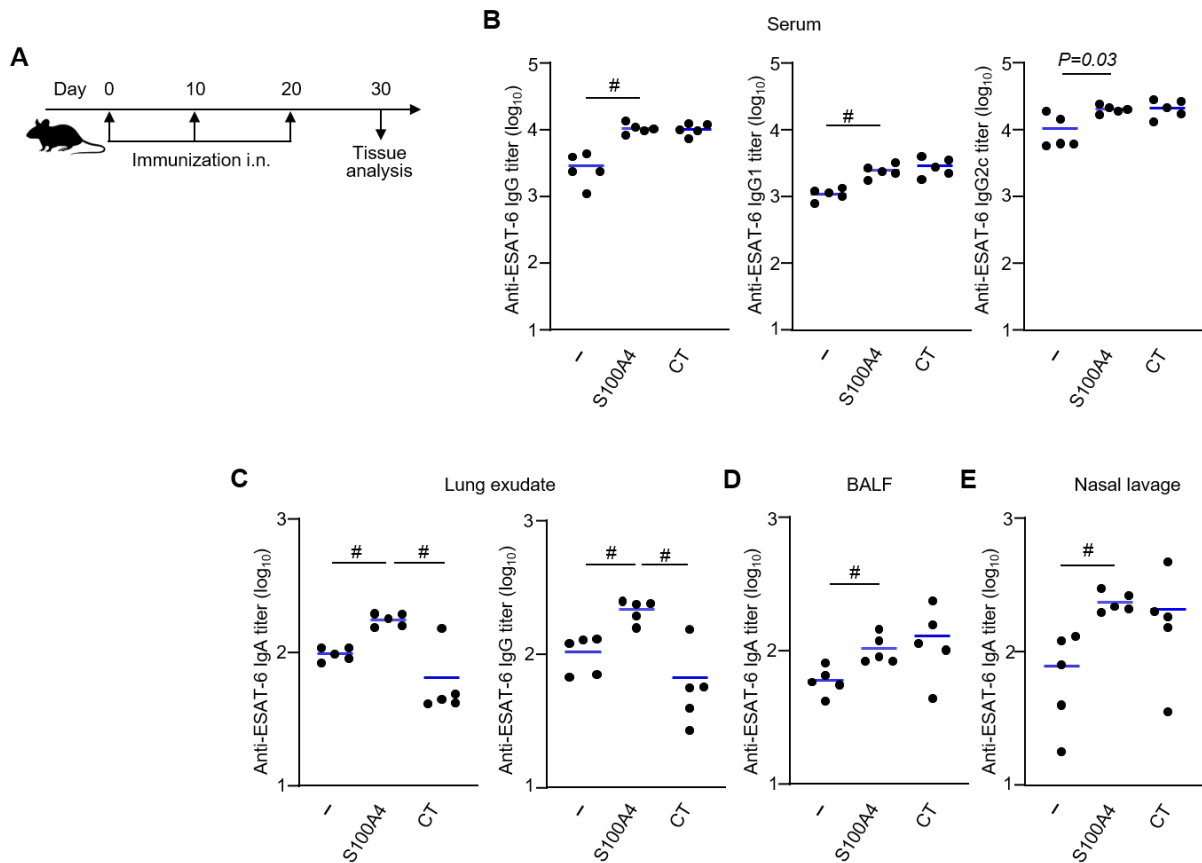


Figure 4.10. S100A4 potentiates antigen-specific antibody production after intranasal immunization with the *Mycobacterium tuberculosis*-derived antigen ESAT-6. Mice were intranasally (i.n.) immunized with ESAT-6 (5 μ g) alone or admixed to S100A4 (10 μ g) or cholera toxin (CT; 1 μ g) three times at an interval of 10 days. Various samples were harvested 10 days after the last immunization for analysis (A). Levels of ESAT-6-specific total IgG, IgG1 and IgG2c in serum (B), ESAT-6-specific IgA and total IgG in lung exudates (C), as well as ESAT-6-specific IgA in bronchoalveolar lavage fluid (BALF) (D), and nasal exudates (E) were measured using ELISA. Each dot represents measurement from a single mouse, and blue lines indicate the average values. # $P = 0.007$ or the exact P -value (italic number) is determined by Mann-Whitney U test.

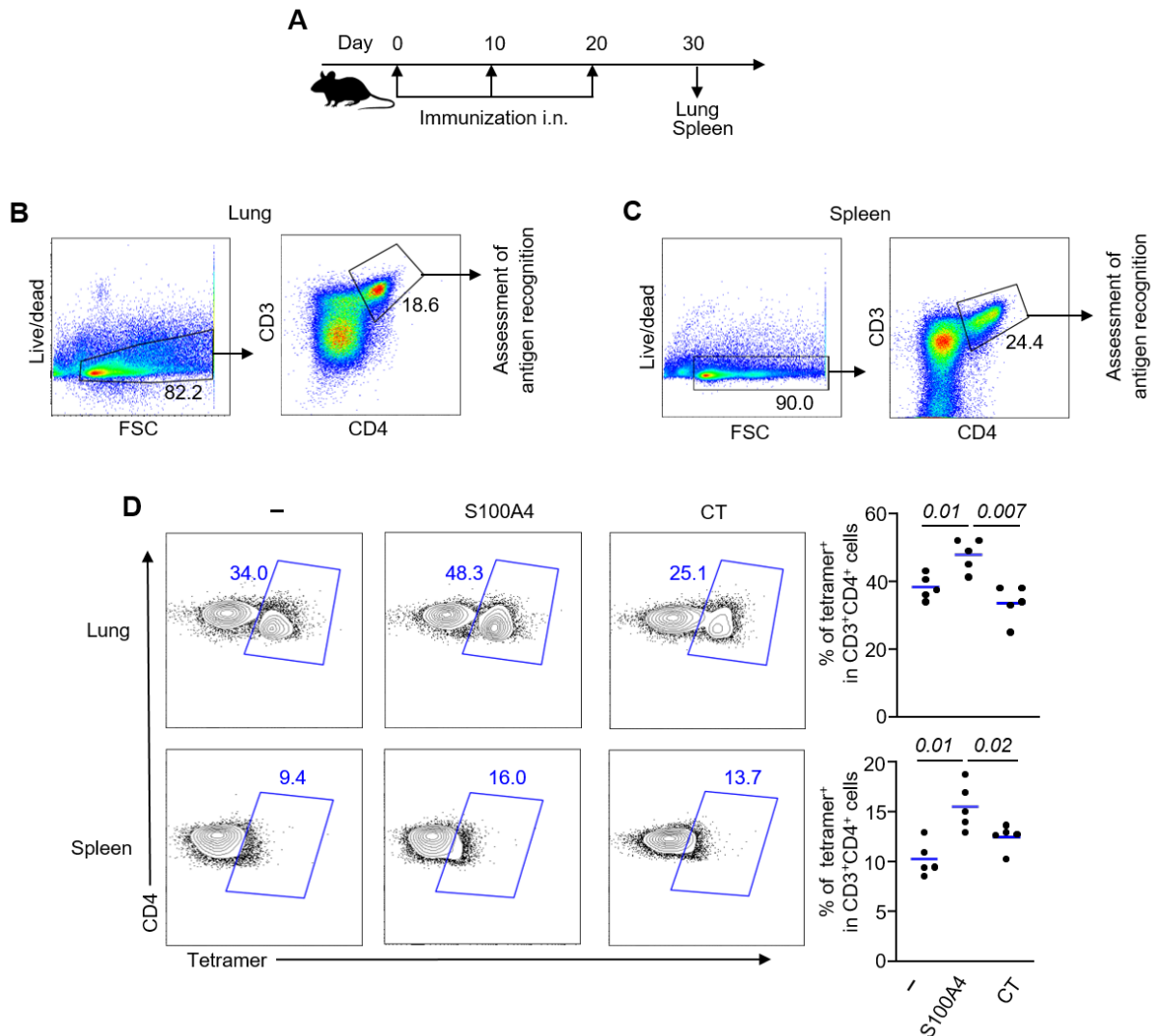


Figure 4.11. S100A4 expands antigen-specific CD4 T cell responses after intranasal immunization with the *Mycobacterium tuberculosis*-derived antigen ESAT-6. Mice were intranasally (i.n.) immunized with ESAT-6 (5 μ g) alone or admixed to S100A4 (10 μ g) or cholera toxin (CT; 1 μ g) three times at an interval of 10 days. The mouse lungs and spleen were harvested 10 days after the last immunization for analysis (A). Gating strategies for identifying I-A^b/ESAT-6 peptide-specific CD4⁺ T cells from the lungs (B) and spleen (C) tissue are indicated. Frequencies of I-A^b/ESAT-6-specific CD4⁺ T cells were examined using flow cytometry. Representative contour plots indicate results from a single mouse in each treatment condition (left panels) and pooled results from all the mice (right panels) are indicated (D). Numbers adjacent to outlined areas indicate percent cells in each gate. Each dot represents measurement from a single mouse, and the blue lines indicate the average values. The exact *P*-values (italic numbers) are determined by Mann-Whitney *U* test.

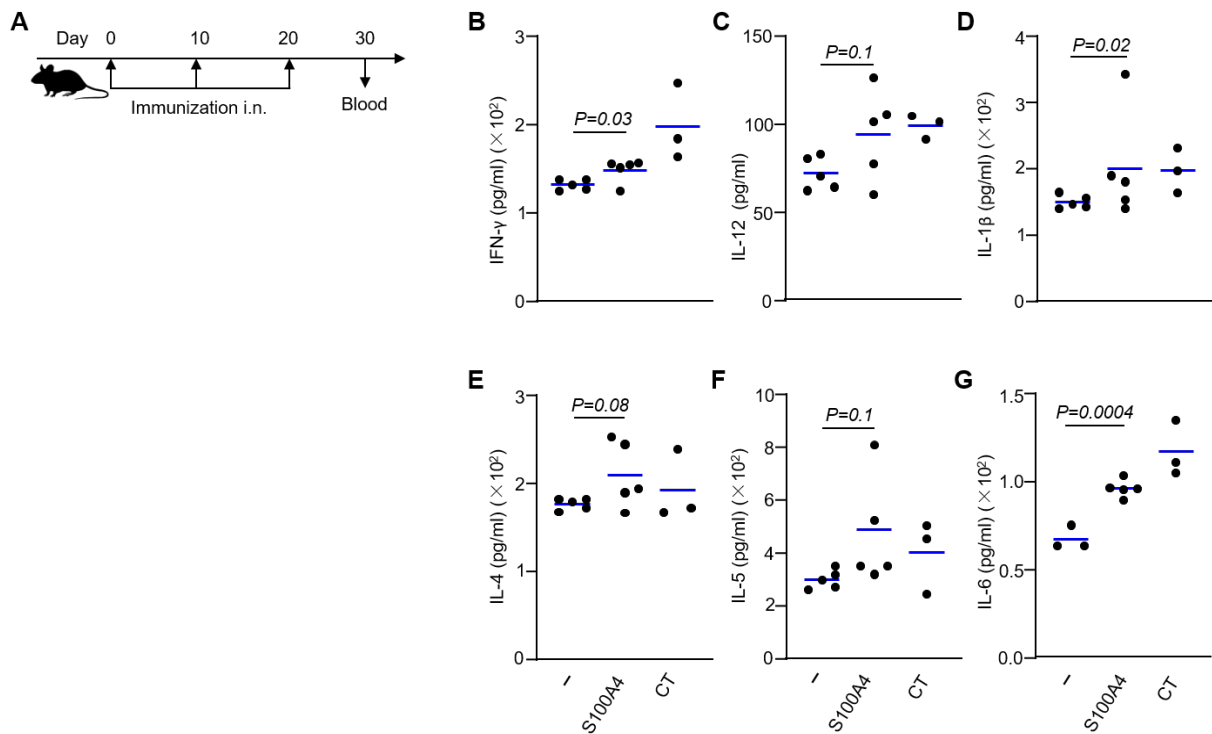


Figure 4.12. S100A4 upregulates cytokine secretion in the blood circulation in response to intranasal immunization with the *Mycobacterium tuberculosis*-derived antigen ESAT-6. Mice were intranasally (i.n.) immunized with ESAT-6 (5 μ g) alone or admixed to S100A4 (10 μ g) or cholera toxin (CT; 1 μ g) three times at an interval of 10 days. The mouse blood was collected 10 days after the last immunization for analysis (A). Concentrations of secreted cytokines as indicated in the serum were measured using the Bio-Plex multiplex assay (B to G). Data were analyzed using Bio-Plex Manager software. The average values are represented by the blue lines, and each dot indicates measurement from a single mouse. The exact *P*-values (italic numbers) are determined by *Student's t-test*.

4.10. S100A4 enhances immune memory-associated T cell activation and proliferation after re-stimulation ex vivo with the immunizing antigen ESAT-6 derived from *Mycobacterium tuberculosis*

The formation of memory T cells is a consequence of successful immunization, as the activation of memory T cells upon re-stimulation by the vaccine antigen is critical not only in sustaining T cell responses but also in supporting humoral immune responses. To analyze the effect of S100A4 in enhancing T cell memory responses, primed splenocytes, which contained both T cells and APCs, were harvested from mice that had been immunized as described in Fig. 4.13A. The splenocytes were re-stimulated ex vivo with the immunizing *Mycobacterium tuberculosis* antigen ESAT-6. Next,

T cell proliferative responses were analyzed using the gating strategies defined in Fig. 4.13B. ESAT-6-induced proliferation of spleen T cells was enhanced if the mice had received S100A4 as an adjuvant as evidenced by increased expression of the proliferation marker Ki-67 in both CD8⁺ (Fig. 4.13C) and CD4⁺ T cells (Fig. 4.13D). Furthermore, T cell activation was examined by the expression of cell activation markers CD69 and CD25 (Fig. 4.14 and Fig. 4.15). Splenic CD8⁺ cells from S100A4-adjuvanted mice increased the expression of CD69 (Fig. 4.14C) and CD25 (Fig. 4.15C) after treatment with the immunizing antigen. Similarly, the expression of CD69 (Fig. 4.14D) and CD25 (Fig. 4.15D) was markedly elevated in splenic CD4⁺ T cells if the mice had previously received immunizing *Mycobacterium tuberculosis* antigen admixed to S100A4. Next, cell activation and proliferation were simultaneously measured by gating on CD69 and Ki-67 double-positive cells (Fig. 4.16). S100A4-mediated increase of CD69⁺Ki-67⁺CD8⁺ cells and CD69⁺Ki-67⁺CD4⁺ cells after antigen re-stimulation was observed (Fig. 4.16C and D).

4.11. S100A4 enhances immune memory-associated B cell activation and proliferation after re-stimulation ex vivo with the immunizing antigen ESAT-6 derived from *Mycobacterium tuberculosis*

To assess the adjuvant activity of S100A4 in promoting clonal expansion of memory B cells, mice were immunized intranasally and splenocytes were re-stimulated ex vivo with the vaccine antigen ESAT-6 (Fig. 4.17A). The expression of the proliferation marker Ki-67⁺ on B cells was gated as shown in Fig. 4.17B. Splenic B cells from mice that were immunized with ESAT-6 together with S100A4 as an adjuvant demonstrated a higher expression of Ki-67, suggesting the enhanced proliferation of these cells, upon in vitro re-stimulation with ESAT-6 (Fig. 4.17C). The activation of the spleen B cells was confirmed by the expression of the cell activation marker CD69 (Fig. 4.17B). Immunization of the mice in the presence of S100A4 as adjuvant led to the generation of B cells that were activated to a greater extent upon re-encounter with the immunizing antigen ESAT-6 (Fig. 4.17D).

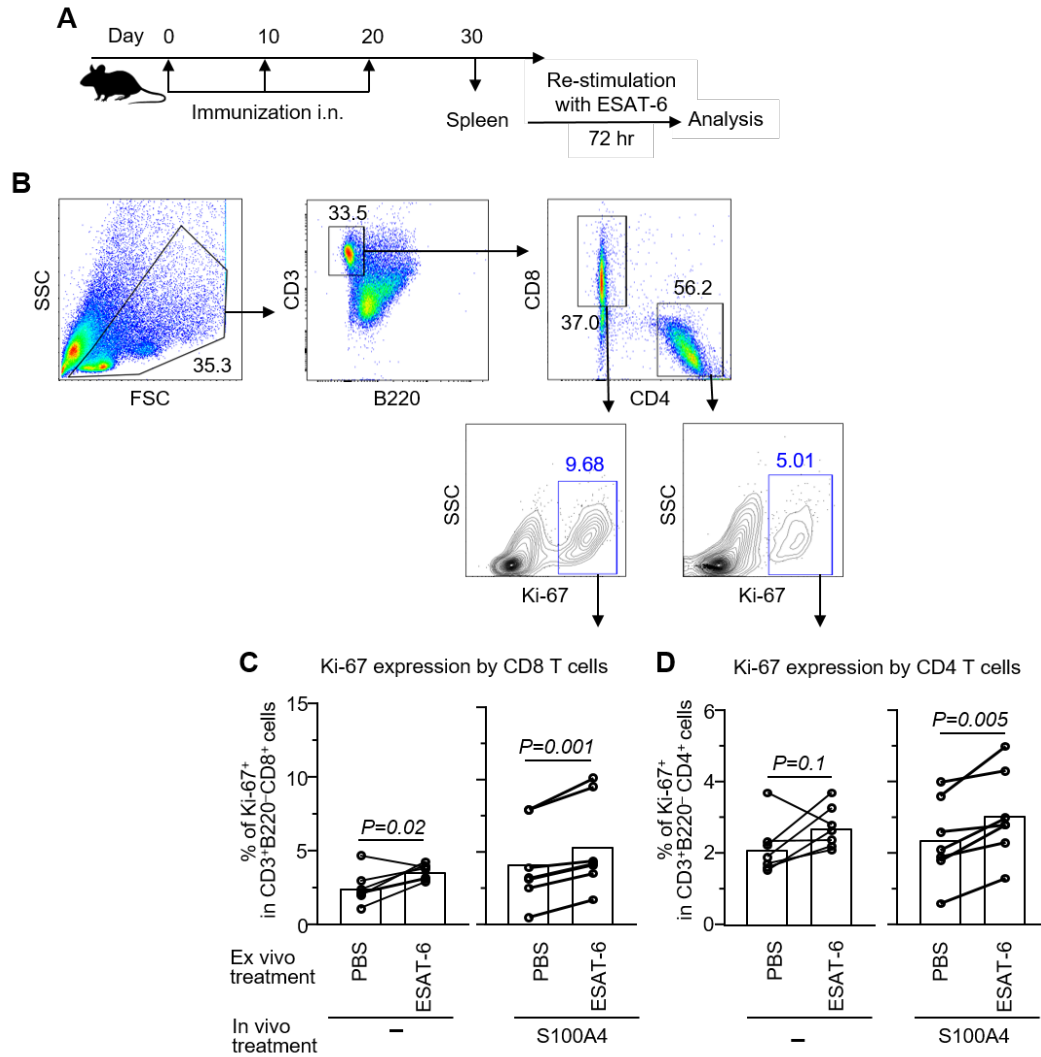


Figure 4.13. S100A4 enhances the proliferation of spleen T cells after re-stimulation ex vivo with the immunizing antigen ESAT-6 derived from *Mycobacterium tuberculosis* based on the cell proliferation marker Ki-67. Mice were intranasally (i.n.) administered with ESAT-6 (5 μ g) in the absence or presence of S100A4 (10 μ g) three times at an interval of 10 days. The mouse spleen was harvested for single-cell preparation. Cells were treated with or without ESAT-6 (2 μ g/ml) for 72 hr at 37°C in 5% CO₂ (A). CD4⁺ and CD8⁺ T cells were gated for assessing the subpopulation that highly expressed Ki-67, which is a cell proliferation marker, and representative flow cytometry plots indicate results from a single mouse in each treatment condition (B). Pooled results from all the mice (C and D) are indicated. Each line represents measurement from a single mouse, and the columns indicate the average values. Numbers adjacent to outlined areas indicate percent cells in each gate. The exact *P*-values (italic numbers) are determined by *Student's t-test*

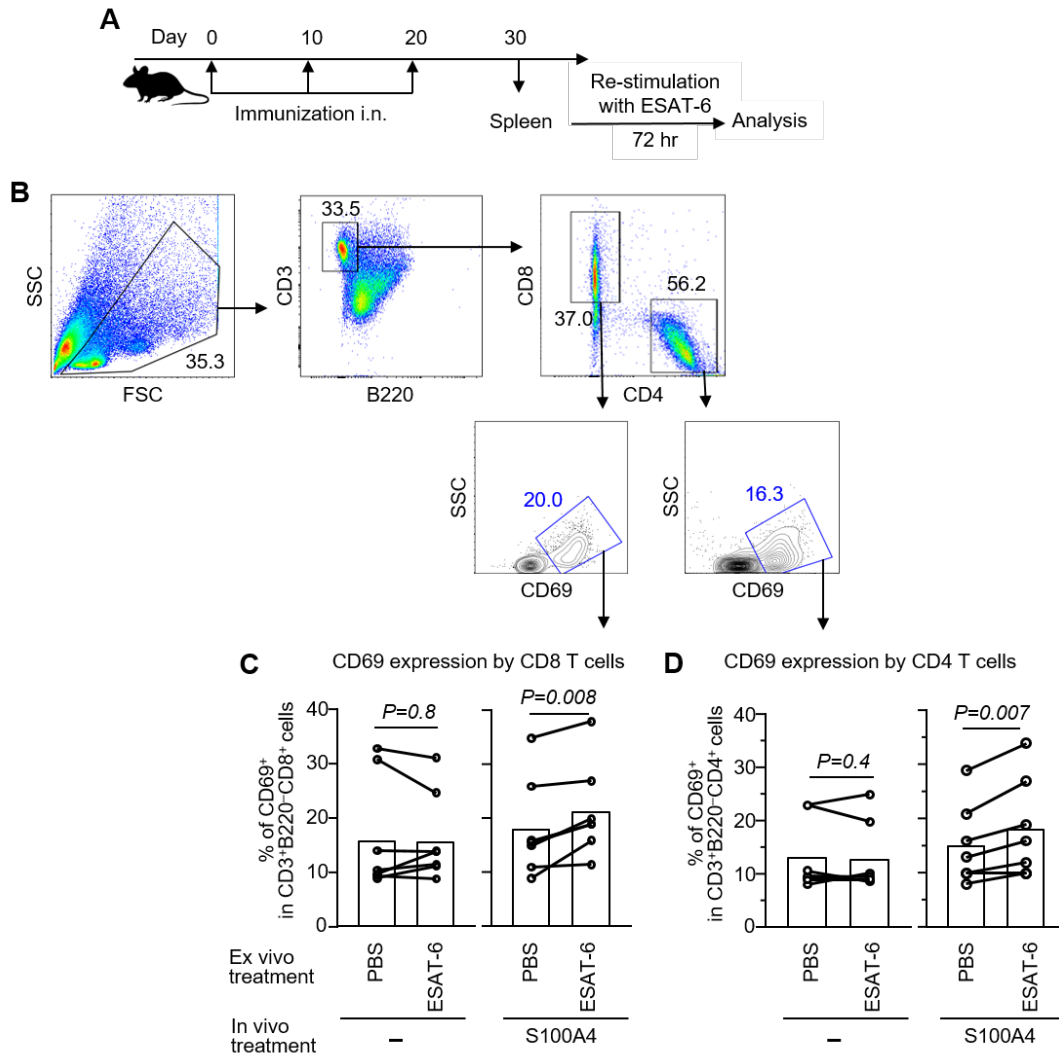


Figure 4.14. S100A4 enhances the activation of spleen T cells after re-stimulation ex vivo with the immunizing antigen ESAT-6 derived from *Mycobacterium tuberculosis* based on the cell activation marker CD69. Mice were intranasally (i.n.) administered with ESAT-6 (5 μ g) in the absence or presence of S100A4 (10 μ g) three times at an interval of 10 days. The mouse spleen was harvested for single-cell preparation. Cells were treated with or without ESAT-6 (2 μ g/ml) for 72 hr at 37°C in 5% CO₂ (A). CD4⁺ and CD8⁺ T cells were gated for assessing the subpopulation that highly expressed CD69, which is a cell activation marker, and representative flow cytometry plots indicate results from a single mouse in each treatment condition (B). Pooled results from all the mice (C and D) are indicated. Each line represents measurement from a single mouse, and the columns indicate the average values. Numbers adjacent to outlined areas indicate percent cells in each gate. The *P*-values are determined by Student *t*-test.

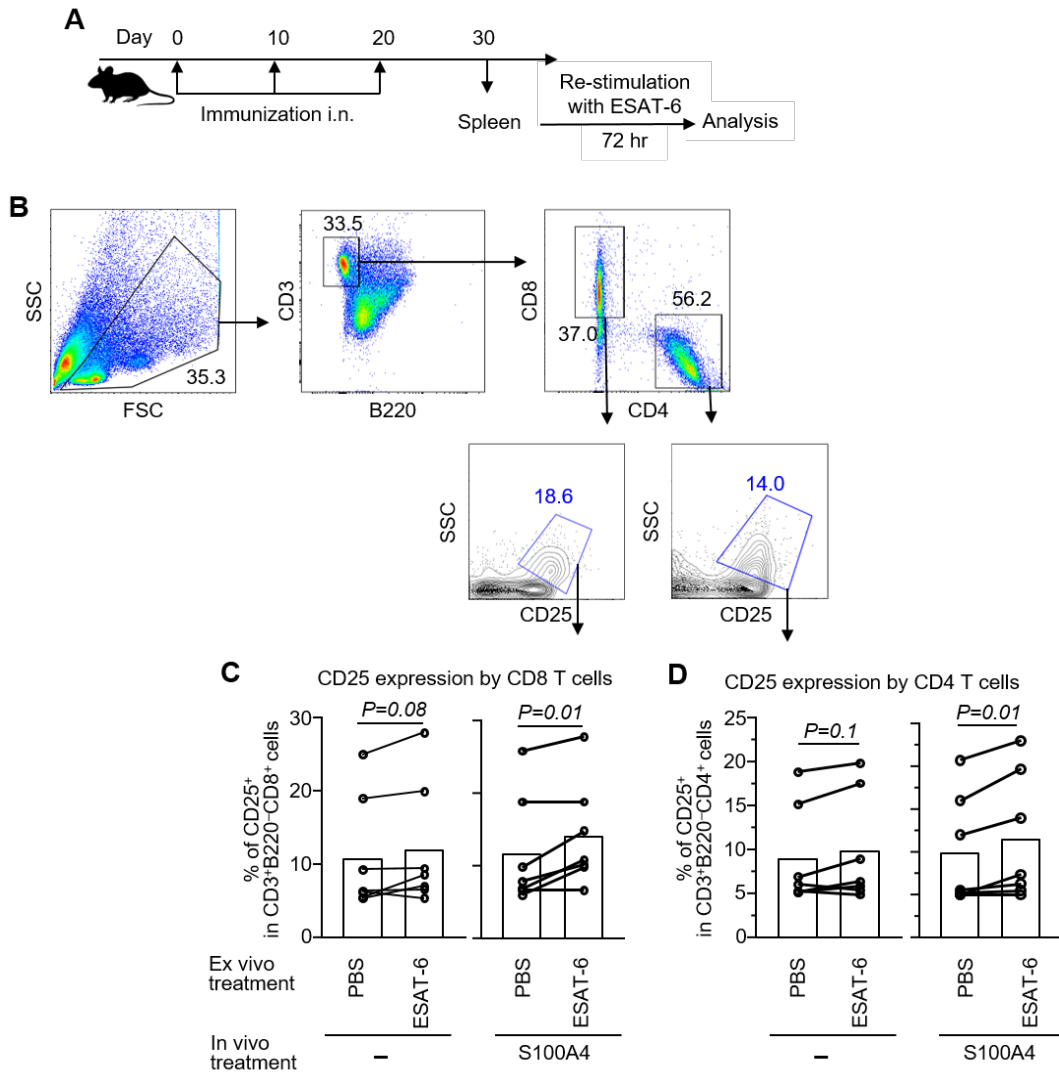


Figure 4.15. S100A4 enhances the activation of spleen T cells after re-stimulation ex vivo with the immunizing antigen ESAT-6 derived from *Mycobacterium tuberculosis* based on the cell activation marker CD25. Mice were intranasally (i.n.) administered with ESAT-6 (5 μ g) in the absence or presence of S100A4 (10 μ g) three times at a 10-day interval. The mouse spleen was harvested for single-cell preparation. Cells were treated with or without ESAT-6 (2 μ g/ml) for 72 hr at 37°C in 5% CO₂ (A). CD4⁺ and CD8⁺ T cells were gated for assessing the subpopulation that highly expressed CD25, which is a cell activation marker, and representative flow cytometry plots indicate results from a single mouse in each treatment condition (B). Pooled results from all the mice (C and D) are indicated. Each line represents measurement from a single mouse, and the columns indicate the average values. Numbers adjacent to outlined areas indicate percent cells in each gate. The exact *P*-values (italic numbers) are determined by Student's *t*-test.

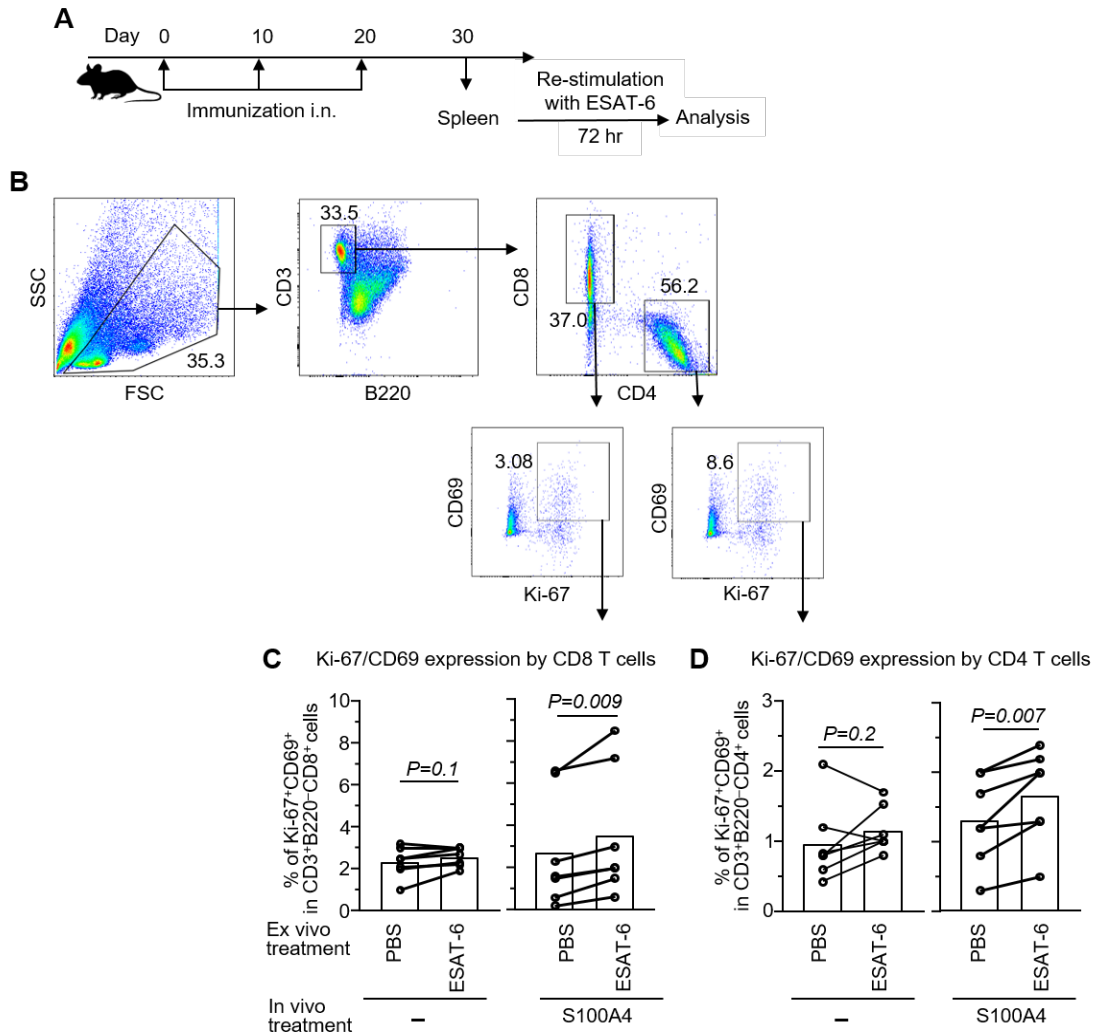


Figure 4.16. S100A4 enhances the proliferation/activation of spleen T cells after re-stimulation ex vivo with the immunizing antigen ESAT-6 derived from *Mycobacterium tuberculosis* based on both Ki-67 and CD69 expression. Mice were intranasally (i.n.) administered with ESAT-6 (5 μ g) in the absence or presence of S100A4 (10 μ g) three times at a 10-day interval. The mouse spleen was harvested for single-cell preparation. Cells were treated with or without ESAT-6 (2 μ g/ml) for 72 hr at 37°C in 5% CO₂ (A). CD4⁺ and CD8⁺ T cells were gated for assessing the subpopulation that highly expressed Ki-67 and CD69, which are the cell proliferation and activation markers, respectively, and representative flow cytometry plots indicate results from a single mouse in each treatment condition (B). Pooled results from all the mice (C and D) are indicated. Each line represents measurement from a single mouse, and the columns indicate the average values. Numbers adjacent to outlined areas indicate percent cells in each gate. The exact *P*-values (italic numbers) are determined by Student's *t*-test.

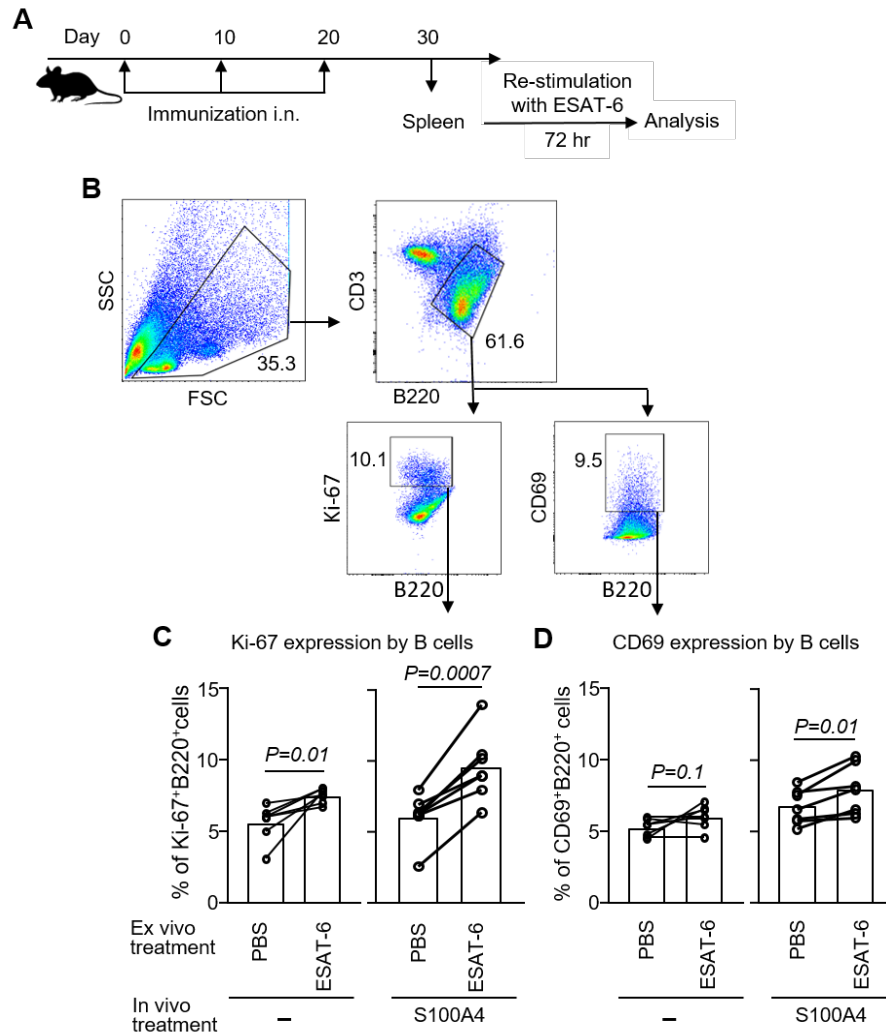


Figure 4.17. S100A4 enhances the proliferation/activation of spleen B cells after re-stimulation ex vivo with the immunizing antigen ESAT-6 derived from *Mycobacterium tuberculosis* based on both Ki-67 and CD69 expression. Mice were intranasally (i.n.) administered with ESAT-6 (5 μ g) in the absence or presence of S100A4 (10 μ g) three times at a 10-day interval. The mouse spleen was harvested for single-cell preparation. Cells were treated with or without ESAT-6 (2 μ g/ml) for 72 hr at 37°C in 5% CO₂ (A). B cells were gated for assessing the subpopulation that highly expressed Ki-67 and CD69, which are the cell proliferation and activation markers, respectively, and representative flow cytometry plots indicate results from a single mouse in each treatment condition (B). Pooled results from all the mice (C and D) are indicated. Each line represents measurement from a single mouse, and the columns indicate the average values. Numbers adjacent to outlined areas indicate percent cells in each gate. The exact *P*-values (italic numbers) are determined by Student's *t*-test.

4.12. S100A4 enhances activation of antigen-specific Th1 memory cells after re-stimulation *ex vivo* with the immunizing antigen ESAT-6 derived from *Mycobacterium tuberculosis*

The differentiation of helper T cells into effector Th1 cells, which is dependent on the expression of the transcription factor T-bet (127), is critical to the clearance of intracellular pathogens. To investigate whether S100A4 promotes T-bet expression, thus facilitating the polarization of T cell development to the Th1 cell lineage, I stimulated splenocytes and lung cells isolated from immunized mice with the *Mycobacterium tuberculosis* antigen as described in Fig. 4.18A. Antigen-specific CD4⁺ Th1 cell-associated T-bet expression was determined by flow cytometry using the gating strategy defined in Fig. 4.18B and C. The frequencies of ESAT-6-specific T-bet-expressing CD4⁺ Th1 cells were profoundly increased in both the splenocytes and the lung cells derived from S100A4-adjuvanted immunized mice (Fig. 4.18D). Furthermore, co-immunization with CT failed to promote the expression of T-bet by CD4⁺ T cells in lung cells, despite similar levels of Th1 cell differentiation with S100A4 or CT as an adjuvant in the spleen (Fig. 4.18).

4.13. S100A4 induces antigen-specific memory CD4 helper T cells and CD8 cytotoxic T cells that express pro-inflammatory cytokines upon re-stimulation with the immunizing antigen ESAT-6 derived from *Mycobacterium tuberculosis*

The importance of cytokines and chemokines in TB protection has been well established. They are critical in the activation, coordination, and migration of immune cells in order to contain the disease. When activated T cells recognize cognate antigenic peptides presented by APCs, cytokines are rapidly released, enhancing the effector functions of immune responses against the target pathogen (128). For measuring the intracellular cytokine expression, including TNF- α , IL-17, and IFN- γ , upon antigen recall responses, both lung and spleen cells derived from mice immunized with ESAT-6 in the presence or absence of S100A4 were cultured together with ESAT-6 (Fig. 4.19A). CD4⁺CD44⁺ memory cells were gated for analysis (Fig. 4.19B and C). Antigen-specific memory CD4 T cell-associated production of IFN- γ , TNF- α or IL-17 was markedly enhanced in lung cells derived from mice that received ESAT-6 admixed to S100A4 (Fig. 4.19D). Again, CT as an adjuvant failed in promoting the activation of both lung and spleen CD4 memory T cells for cytokine production (Fig. 4.19).

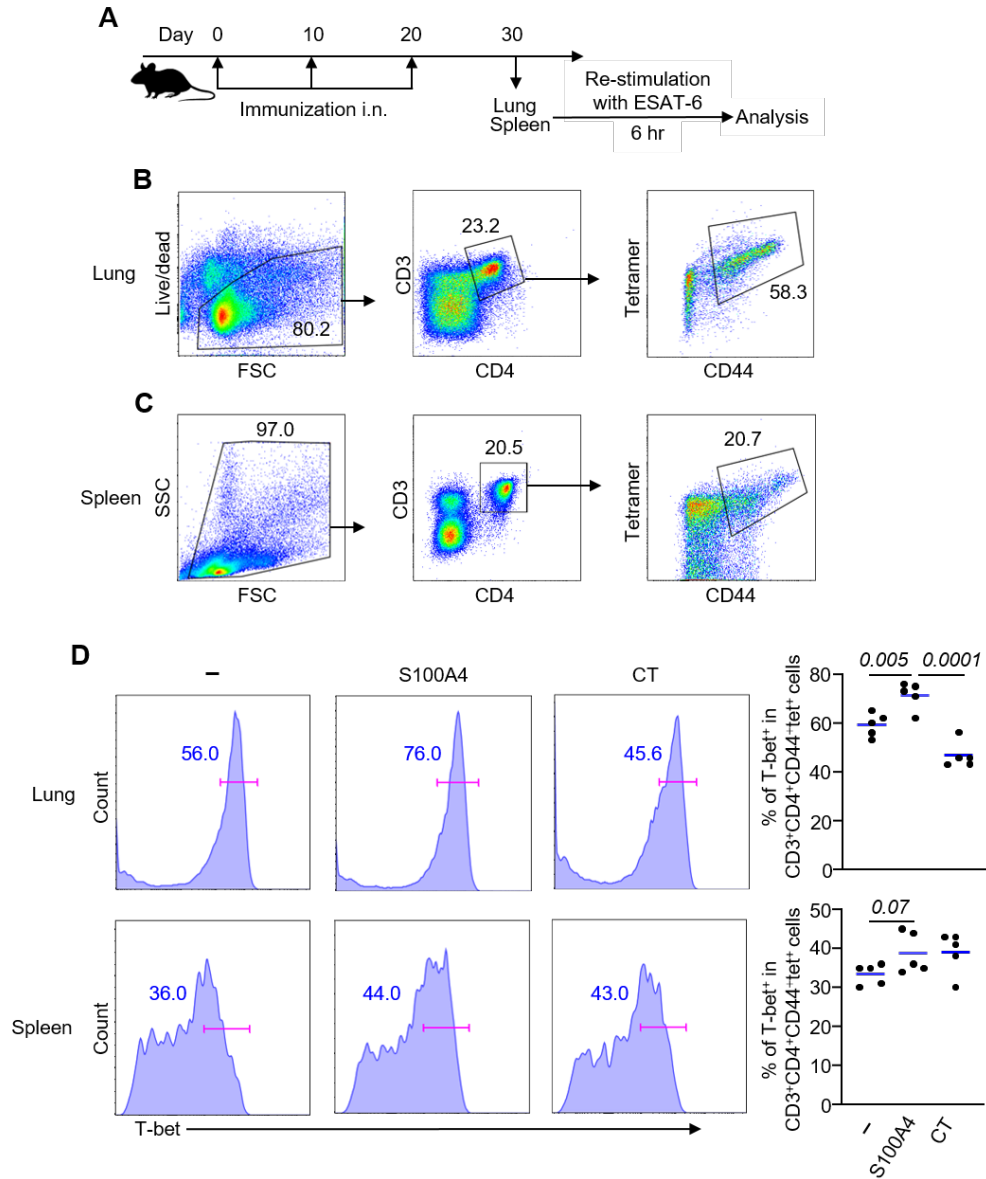


Figure 4.18. S100A4 enhances activation of antigen-specific Th1 memory cells after re-stimulation ex vivo with the immunizing antigen ESAT-6 derived from *Mycobacterium tuberculosis*. Mice were intranasally (i.n.) immunized with ESAT-6 (5 μ g) alone or admixed to S100A4 (10 μ g) or cholera toxin (CT; 1 μ g) three times at an interval of 10 days. The mouse lungs and spleen were harvested 10 days after the last immunization for single-cell preparation. Cells were treated with ESAT-6 (2 μ g/ml) for 6 hr at 37°C in 5% CO₂ (A). T cell recognition of the ESAT-6 peptide (QQWNFAGIEAAASA) was determined by using an I-A^b/ESAT-6 peptide tetramer. Frequencies of I-A^b/ESAT-6 peptide-specific memory CD4⁺ T cells that expressed T-bet (Th1 cell transcription factor) from the lung (B) and spleen (C) cultures were measured using flow cytometry. Representative histogram plots indicate results from a single mouse in each treatment condition (left panels) and pooled results from all the mice (right panels) are indicated (D). Numbers in or adjacent to outlined areas indicate percent cells in each gate. Each symbol represents measurement from a single mouse, and the blue lines indicate the average values. The exact *P*-values (italic numbers) are determined by Student's *t*-test.

Furthermore, I also assessed the expression of different combinations of pro-inflammatory cytokines by antigen-specific memory CD4 T cells. The frequencies of ESAT-6-specific memory CD4 T cell-associated expression of IFN- γ /TNF- α , IFN- γ /IL-17 or TNF- α /IL-17 was significantly increased in the lung cells and spleen cells derived from mice that received ESAT-6 admixed to S100A4 (Fig. 4.20). Taken together, these findings suggest that S100A4 is a robust mucosal adjuvant that promotes both Th1 (IFN- γ and TNF- α) and Th17 (IL-17) cell development, which is fundamentally important in controlling *Mycobacterium tuberculosis* infection.

Next, I assessed antigen-specific cytotoxic T cell-associated expression of pro-inflammatory cytokines. ESAT-6-specific memory cytotoxic T cell-associated production of IL-17, IFN- γ , or TNF- α was robustly increased in lung cells derived from mice immunized with ESAT-6 in the presence of S100A4 (Fig. 4.21). Immunization with S100A4 significantly displayed higher frequencies of antigen-specific memory cytotoxic T cells that were double positive for IFN- γ /TNF- α or TNF- α /IL-17 (Fig. 4.22).

4.14. S100A4 promotes production of granzyme B in cytotoxic T cells after re-stimulation ex vivo with the immunizing antigen ESAT-6 derived from *Mycobacterium tuberculosis*

Controlling the intracellular pathogen is mediated by cytotoxic effector T cells that release granzyme B, a toxic substance that is effective in killing target cells (119). Granzyme B expression is a surrogate marker for cytotoxic T cell differentiation (129). To examine if the adjuvant effect of S100A4 also included promotion of granzyme B production by cytotoxic T cells, splenocytes and lung cells were stimulated with the immunizing *Mycobacterium tuberculosis*-associated antigen ESAT-6, followed by analysis using flow cytometry as shown in Fig. 4.23A-C. S100A4 markedly induced the expression of granzyme B by memory cytotoxic T cells in both lung cells and spleen cells (Fig. 4.23D).

4.15. S100A4 augments cytokine and chemokine secretion by splenocytes after re-stimulation ex vivo with the immunizing antigen ESAT-6 derived from *Mycobacterium tuberculosis*

Using flow cytometric analysis, I have already demonstrated the T cell-associated intracellular production of cytokines in the memory response following mouse immunization adjuvanted with S100A4 (Fig. 4.19-Fig. 4.22).

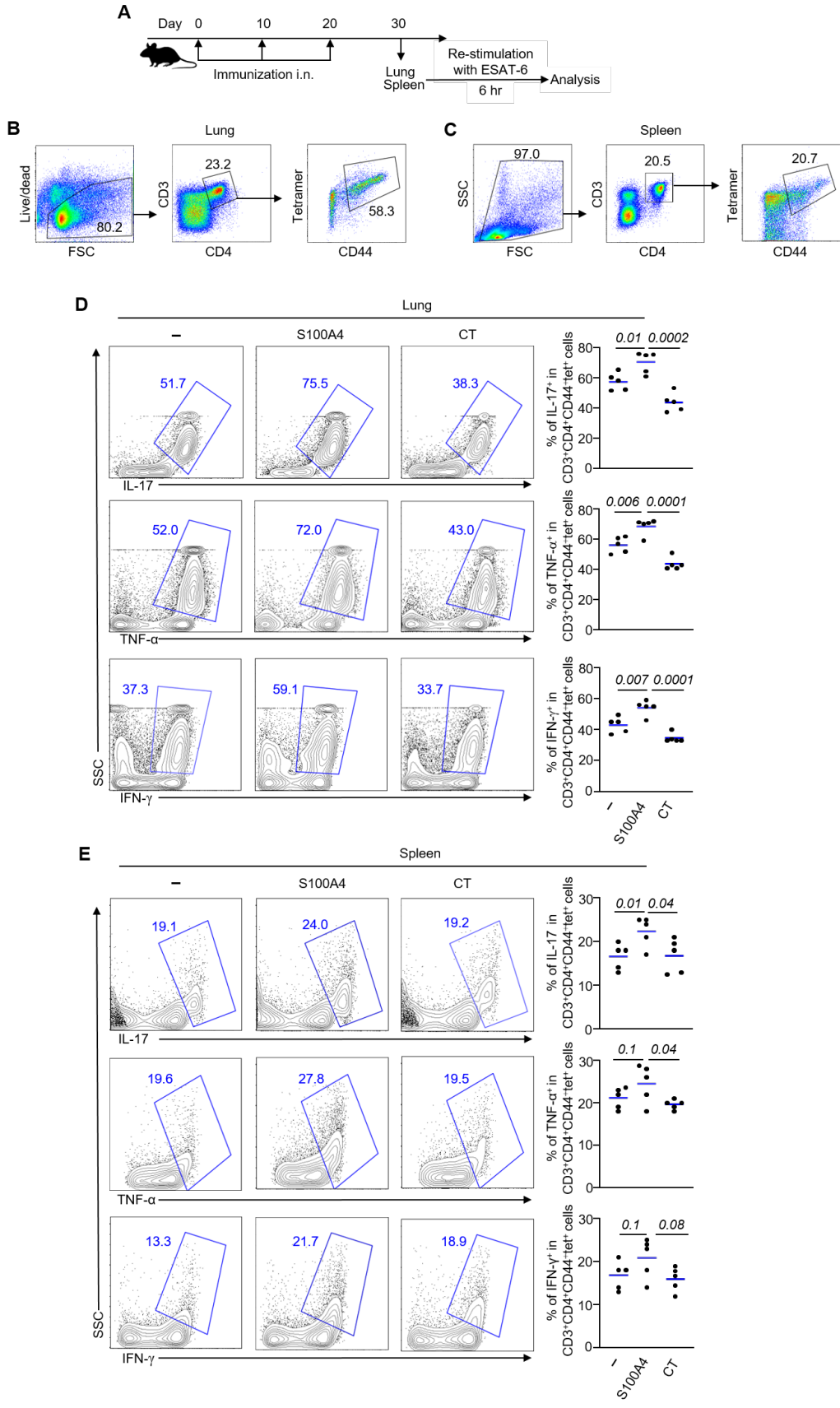


Figure 4.19. S100A4 induces antigen-specific memory CD4 helper T cells that express pro-inflammatory cytokines upon re-stimulation with the immunizing antigen ESAT-6 derived from *Mycobacterium tuberculosis*. Mice were intranasally (i.n.) immunized with ESAT-6 (5 µg) alone or admixed to S100A4 (10 µg) or cholera toxin (CT; 1 µg) three times at an interval of 10 days. The mouse lungs and spleen were harvested 10 days after the last immunization for single-cell preparation. Cells were treated with ESAT-6 (2 µg/ml) for 6 hr at 37°C in 5% CO₂ (A). T cell recognition of the ESAT-6 peptide (QQWNFAGIEAAASA) was determined by using an I-A^b/ESAT-6 peptide tetramer. Frequencies of I-A^b/ESAT-6 peptide-specific memory CD4⁺ T cells that produced IL-17, TNF-α, or IFN-γ from the lung (B) and spleen (C) cultures were measured using flow cytometry. Representative contour plots indicate results from a single mouse in each treatment condition (left panels) and pooled results from all the mice (right panels) are indicated (D and E). Numbers in or adjacent to outlined areas indicate percent cells in each gate. Each symbol represents measurement from a single mouse, and the blue lines indicate the average values. The exact *P*-values (italic numbers) are determined by Student's *t*-test.

Next, I tried to confirm these findings by measuring the release of cytokines into the supernatants using a multiplex assay which can measure more than a dozen cytokines simultaneously (Fig. 4.24A). Antigen re-encounter-mediated production of Th1-associated cytokines, including TNF-α (Fig. 4.24B) and IFN-γ (Fig. 4.24C) was increased if the mice had previously been immunized with ESAT-6 admixed to S100A4, compared with the cytokine production in cells from control mice. Production of IFN-γ and TNF-α in T cell memory responses is a strong predictor of effective T cell-mediated protection against intracellular pathogens including *Mycobacterium tuberculosis*. Furthermore, IFN-γ promotes the differentiation of cytotoxic T cells and induces antibody class switching of B cells (130,131).

Similar to Th1-associated cytokines, Th2-associated cytokine levels were also increased in the culture supernatants. Co-immunization with S100A4 elicited consistently increased production of Th2-associated cytokines, including IL-4, IL-5, IL-10, IL-13, and IL-6 (Fig. 4.24D to H). All of these cytokines are essential for enhancing Th2 effector functions, including B cell activation and antibody responses (132). Furthermore, co-immunization with S100A4 substantially enhanced antigen-recall induced production of IL-9 (Fig. 4.24I). IL-1β production was also observed to be enhanced in antigen recall responses if mice were immunized with S100A4 admixed to ESAT-6 (Fig. 4.24J). IL-1β is a prominent pro-inflammatory cytokine required for the full-blown adaptive immune responses (133). Moreover, antigen recall-induced production of GM-CSF, a critical cytokines for maintaining granuloma integrity in *Mycobacterium tuberculosis* infection (134), by splenocytes in S100A4-adjuvanted immunization was markedly increased (Fig. 4.24K).

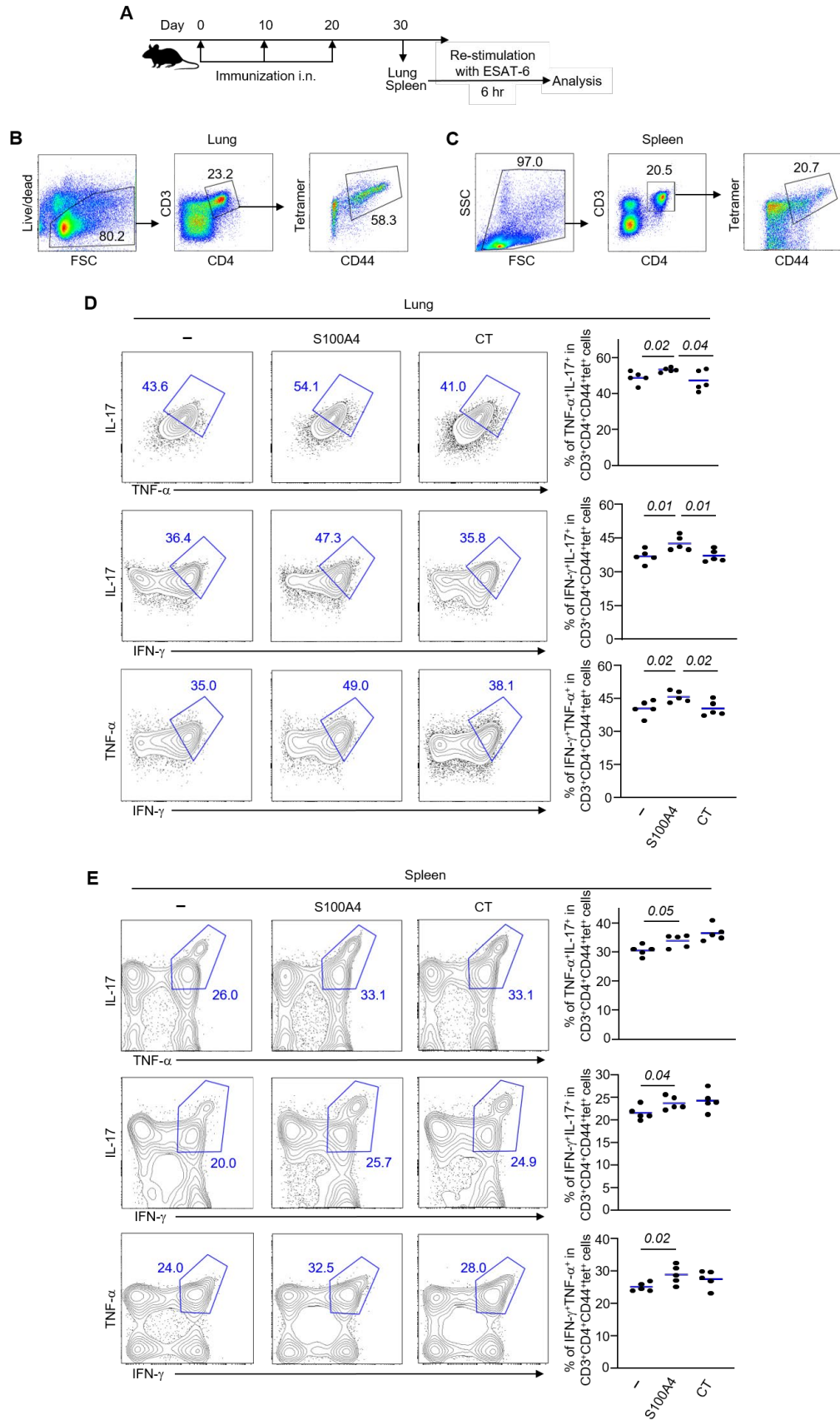


Figure 4.20. S100A4 induces antigen-specific memory CD4 T cells that express a combination of different pro-inflammatory cytokines upon re-stimulation with the immunizing antigen ESAT-6 derived from *Mycobacterium tuberculosis*. Mice were intranasally (i.n.) immunized with ESAT-6 (5 µg) alone or admixed to S100A4 (10 µg) or cholera toxin (CT; 1 µg) three times at an interval of 10 days. Mouse lungs and spleen were harvested 10 days after the last immunization for analysis. Cells were treated with ESAT-6 (2 µg/ml) for 6 hr at 37°C in 5% CO₂ (A). T cell recognition of the ESAT-6 peptide (QQWNFAGIEAAASA) was determined by using an I-A^b/ESAT-6 peptide tetramer. Frequencies of I-A^b/ESAT-6 peptide-specific memory CD4⁺ T cells that produced IL-17/TNF-α, IFN-γ/IL-17, or IFN-γ/TNF-α from the lung (B) and spleen (C) cultures were measured using flow cytometry. Representative contour plots indicate results from a single mouse in each treatment condition (left panels) and pooled results from all the mice (right panels) are indicated (D and E). Numbers in or adjacent to outlined areas indicate percent cells in each gate. Each symbol represents data from a single mouse, and the blue lines indicate the average values. The exact *P*-values (italic numbers) are determined by Student's *t*-test.

Although there was a trend of antigen recall-mediated augmentation of G-CSF (Fig. 4.24L) and IL-17 (Fig. 4.24M), these have not reached statistically significant levels. S100A4 also modestly augmented the production of a number of chemokines in the antigen recall response, including MIP-1β (Fig. 4.24N), MIP-1α (Fig. 4.24O), RANTES (Fig. 4.24P), and MCP-1 (Fig. 4.24Q). Chemokines are crucial molecules in orchestrating the localization of T lymphocytes at the infection site following infection with *Mycobacterium tuberculosis* (128). Chemokines are also required for controlling granuloma formation during *Mycobacterium tuberculosis* infection through regulating the activity of various innate and adaptive immune cells.

4.16. S100A4 induces the expression of cytokines in the lung tissues after immunization with the *Mycobacterium tuberculosis*-derived antigen ESAT-6

Promotion and maintenance of adaptive T-cell immune responses that mediate the killing of intracellular pathogens are controlled by cytokines at tissue sites (135). To assess the upregulation of cytokines that are critical for adaptive immune responses in the lung tissue, mice were vaccinated as described in Fig. 4.25 and the lung tissues were collected and processed for mRNA expression of various cytokines 10 days after the last immunization. The expression of TNF-α, a critical cytokine for inflammatory responses, was remarkably enhanced in mice that received the vaccine antigen ESAT-6 together with S100A4 (Fig. 4.25). Moreover, there was a strong trend of augmented expression of IFN-γ, IL-4, and IL-23 in the lung tissue of mice that received S100A4 (Fig. 4.25). IFN-γ is a critical cytokine for promoting Th1 responses and macrophage activation. IFN-γ is a critical cytokine for promoting Th1 responses and macrophage activation in the lung tissues (136). IL-4 is important for humoral immune responses that are responsible for antibody production (137). IL-23 plays a pivotal role in Th17 responses (138).

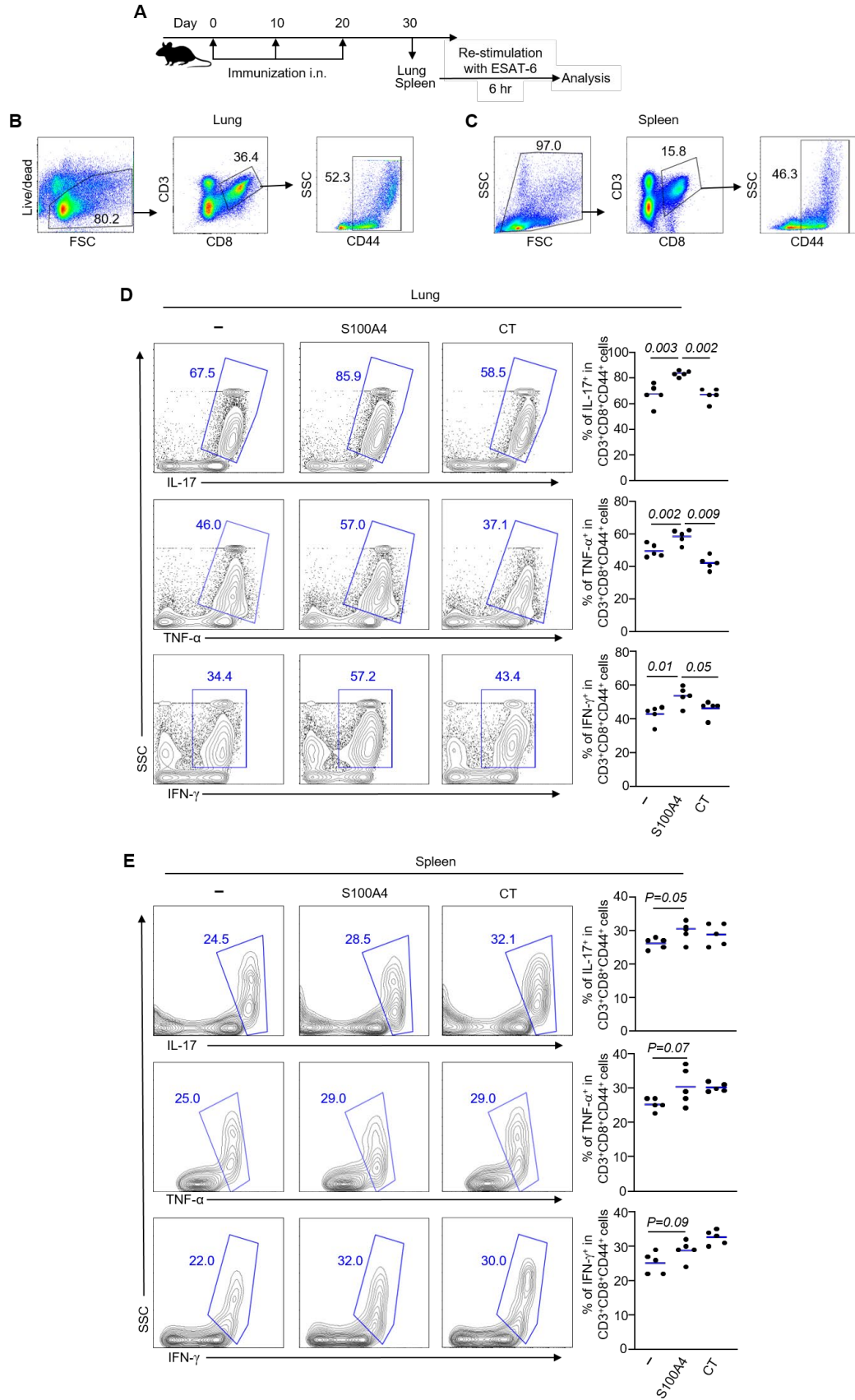


Figure 4.21. S100A4 induces antigen-specific memory CD8 cytotoxic T cells that express pro-inflammatory cytokines upon re-stimulation with the immunizing antigen ESAT-6 derived from *Mycobacterium tuberculosis*. Mice were intranasally (i.n.) administered with ESAT-6 (5 µg) alone or admixed to S100A4 (10 µg) or cholera toxin (CT; 1 µg) three times at a 10-day interval. The mouse lungs and spleen were harvested 10 days after the last immunization for analysis. Cells were treated with ESAT-6 (2 µg/ml) for 6 hr at 37°C in 5% CO₂ (A). Gating strategies for identifying memory cytotoxic T cells from the lung (B) and spleen (C) cultures are indicated. Percentages of ESAT-6-specific memory cytotoxic T cells that produced IL-17, TNF-α, and IFN-γ were measured using flow cytometry. Representative contour plots indicate results from a single mouse in each treatment condition (left panels) and pooled results from all the mice (right panels) are indicated (D and E). Numbers in or adjacent to outlined areas indicate percent cells in each gate. Each symbol represents measurement from a single mouse, and the blue lines indicate the average values. The exact *P*-values (*italic numbers*) are determined by Student's *t*-test.

4.17. S100A4 enhances the expression of MHC class II and costimulatory molecules by dendritic cells in vitro

The cross-talk between antigen-specific T cells and APCs is critical to the successful induction of adaptive immunity (139). Previously, together with my colleagues, we already demonstrated the potential of S100A4 in activating dendritic cells, the most important APC type, in a model system without the presence of any pathogen-derived molecules (84). The currently proposed vaccination model uses a pathogen-derived vaccine antigen (i.e., ESAT-6) to target *Mycobacterium tuberculosis*. As ESAT-6, which is capable of interacting with TLR2 and TLR4, might itself activate dendritic cells to some extent, I would like to investigate whether S100A4 could further activate dendritic cells in the presence of ESAT-6. For this purpose, BMDCs were cultured and their purity was assessed by the surface expression of CD11c (Fig. 4.26A). Next, BMDCs were incubated overnight with ESAT-6 alone or in the presence of S100A4. While ESAT-6 modestly enhanced the expression of MHC class II and costimulatory molecules, including CD86, CD80, and CD40, the addition of S100A4 substantially augmented the expression of these molecules (Fig. 4.26B to E). Moreover, the expression of costimulatory molecules, such as CD40 and CD80, was also substantially enhanced at the transcript level after treatment with S100A4 (Fig. 4.26F). There was a trend of enhancement in CD86 expression, although it has not reached statistical significance (Fig. 4.26F). Taken together, these data confirm that S100A4 was potent in activating dendritic cells for augmenting costimulatory molecule expression in a vaccination setting using a pathogen-derived vaccine antigen.

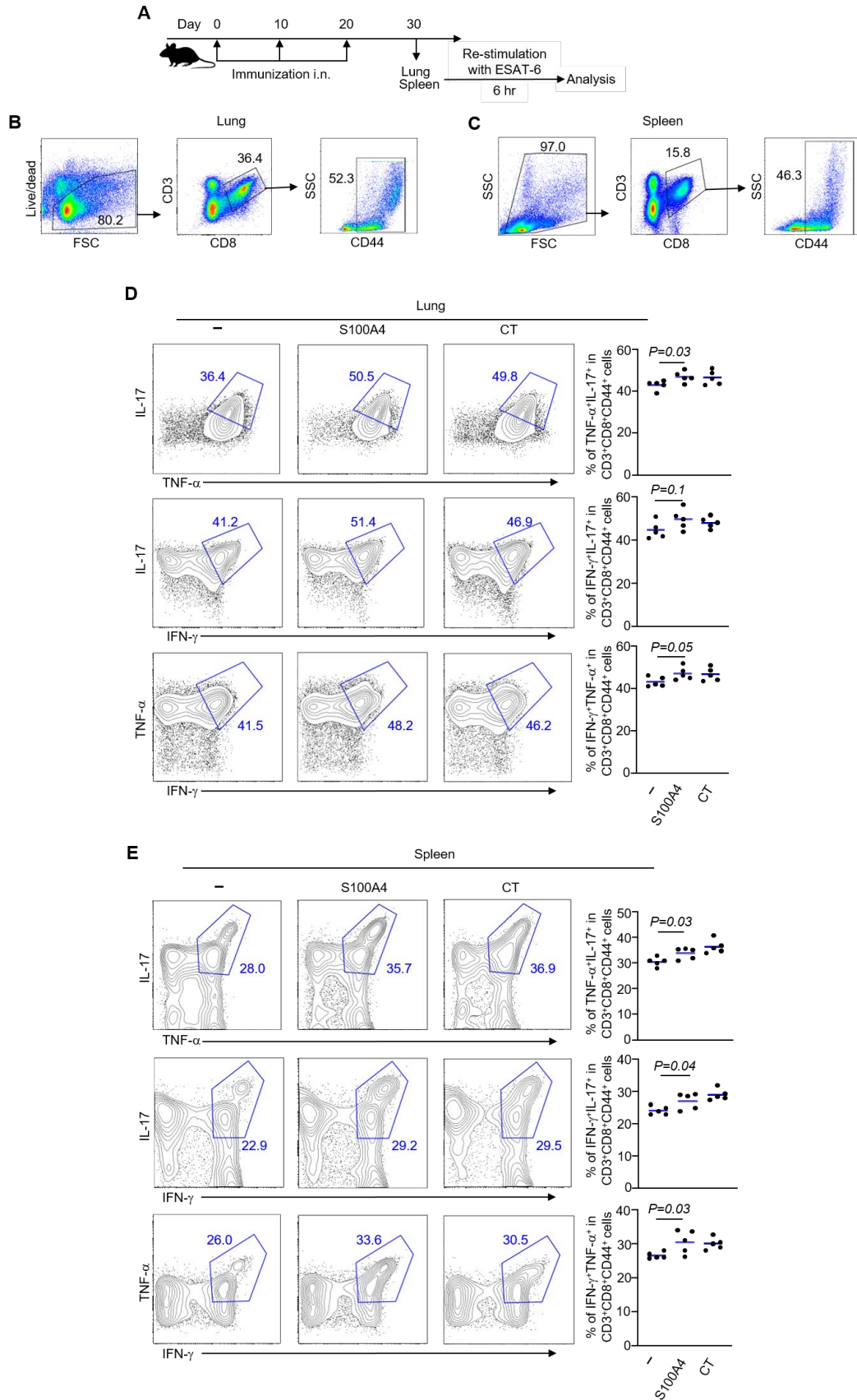


Figure 4.22. S100A4 induces antigen-specific memory CD8 cytotoxic T cells that express a combination of different pro-inflammatory cytokines upon re-stimulation with the immunizing antigen ESAT-6 derived from *Mycobacterium tuberculosis*. Mice were intranasally (i.n.) administered with ESAT-6 (5 μ g) alone or admixed to S100A4 (10 μ g) or cholera toxin (CT; 1 μ g) three times at a 10-day interval. The mouse lungs and spleen were harvested 10 days after the last immunization for analysis. Cells were treated with ESAT-6 (2 μ g/ml) for 6 hr at 37°C in 5% CO₂ (A). Gating strategies for identifying memory cytotoxic T cells from the lung (B) and spleen (C) cultures are indicated. Frequencies of memory cytotoxic T cells that produced IL-17/TNF- α , IFN- γ /IL-17, or IFN- γ /TNF- α were measured using flow cytometry. Representative contour plots indicate results from a single mouse in each treatment condition (left panels) and pooled results from all the mice (right panels) are indicated (D and E). Numbers in or adjacent to outlined areas indicate percent cells in each gate. Each symbol represents data from a single mouse, and the blue lines indicate the average values. The exact *P*-values (italic numbers) are determined by Student's *t*-test.

4.18. S100A4 promotes secretion of pro-inflammatory cytokines by dendritic cells in vitro

The secretion of pro-inflammatory cytokines by dendritic cells is critical in the activation and differentiation of T lymphocytes (140). Again, the BMDCs were cultured (Fig. 4.27A). Importantly, the protein expression of IL-1 β , a cytokine critical for the pro-inflammatory response, was remarkably augmented in S100A4-treated dendritic cells (Fig. 4.27B). S100A4 also enhanced the secretion of IL-6 (Fig. 4.27C), a cytokine that is important for adaptive immune responses. Furthermore, the expression of a group of pro-inflammatory cytokines, including IL-6, IL-12, IL-1 β and TNF- α , was significantly upregulated at the mRNA level following incubation with S100A4 (Fig. 4.27D).

4.19. S100A4 enhances the expression of TLR2 on dendritic cells in vitro

APCs can be activated by antigen-mediated stimulation via the TLR family molecules. TLR2 and TLR4, the two receptors for interacting with various proteins derived from *Mycobacterium tuberculosis*, including ESAT-6, are important in potentiating immune responses (72). BMDCs were cultured to examine the expression of TLR2 and TLR4 (Fig. 4.28A). While TLR2 protein upregulation was modestly increased in ESAT-6-treated dendritic cells, the addition of S100A4 significantly augmented its expression (Fig. 4.28B). There was also a trend of S100A4-mediated increase of TLR4, although it did not reach statistical significance (Fig. 4.28C). For the mRNA transcript expression, I could consistently show that S100A4 augmented TLR2 expression, while the transcript expression of TLR4 did not seem to be regulated by S100A4 (Fig. 4.28D).

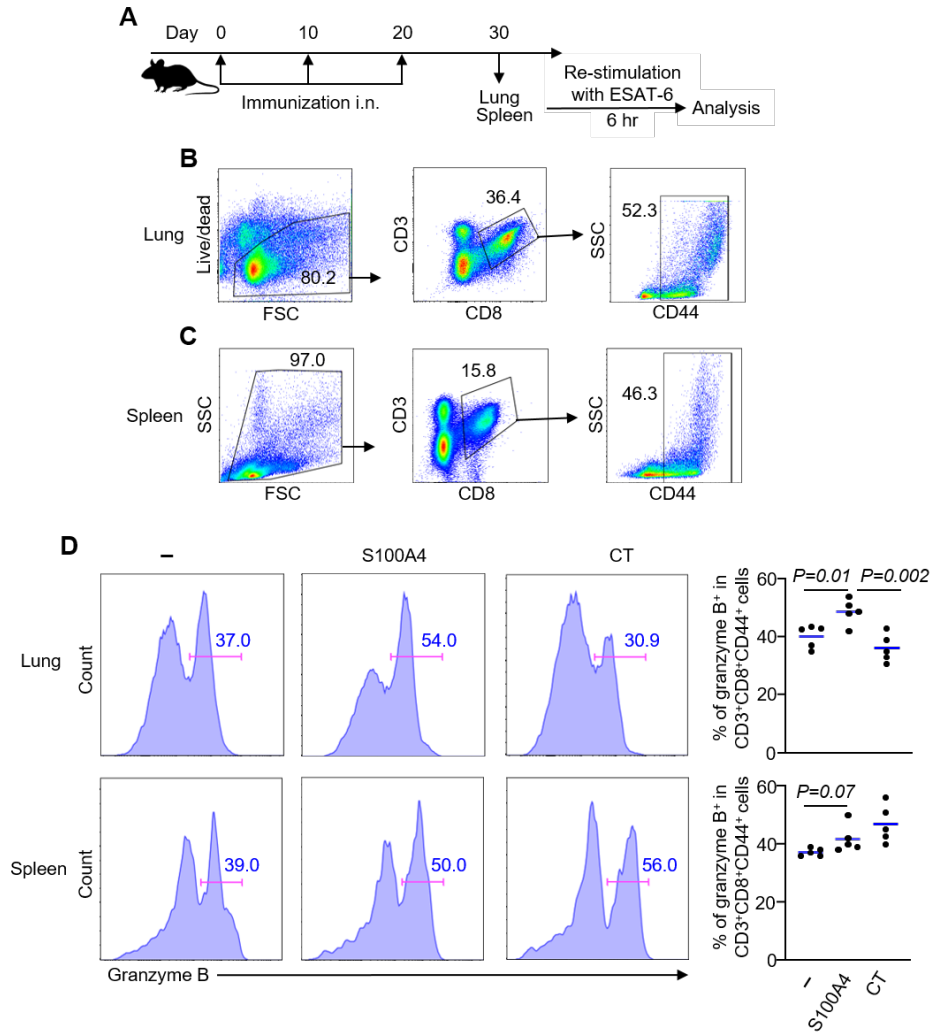


Figure 4.23. S100A4 promotes production of granzyme B in cytotoxic T cells after re-stimulation ex vivo with the immunizing antigen ESAT-6 derived from *Mycobacterium tuberculosis*. Mice were intranasally (i.n.) administered with ESAT-6 (5 μ g) alone or admixed to S100A4 (10 μ g) or cholera toxin (CT; 1 μ g) three times at a 10-day interval. Mouse lungs and spleen were harvested 10 days after the last immunization for analysis. Cells were treated with ESAT-6 (2 μ g/ml) for 6 hr at 37°C in 5% CO₂ (A). Gating strategies for identifying memory cytotoxic T cells from the lung and spleen (B and C) cultures are indicated. Frequencies of memory cytotoxic T cells that produced granzyme B were analyzed using flow cytometry. Representative histogram plots indicate results from a single mouse in each treatment condition (left panels) and pooled results from all the mice (right panels) are indicated (D). Numbers in or adjacent to outlined areas indicate percent cells in each gate. Each symbol represents measurement from a single mouse, and the blue lines indicate the average values. The exact *P*-values (italic numbers) are determined by Student's *t*-test.

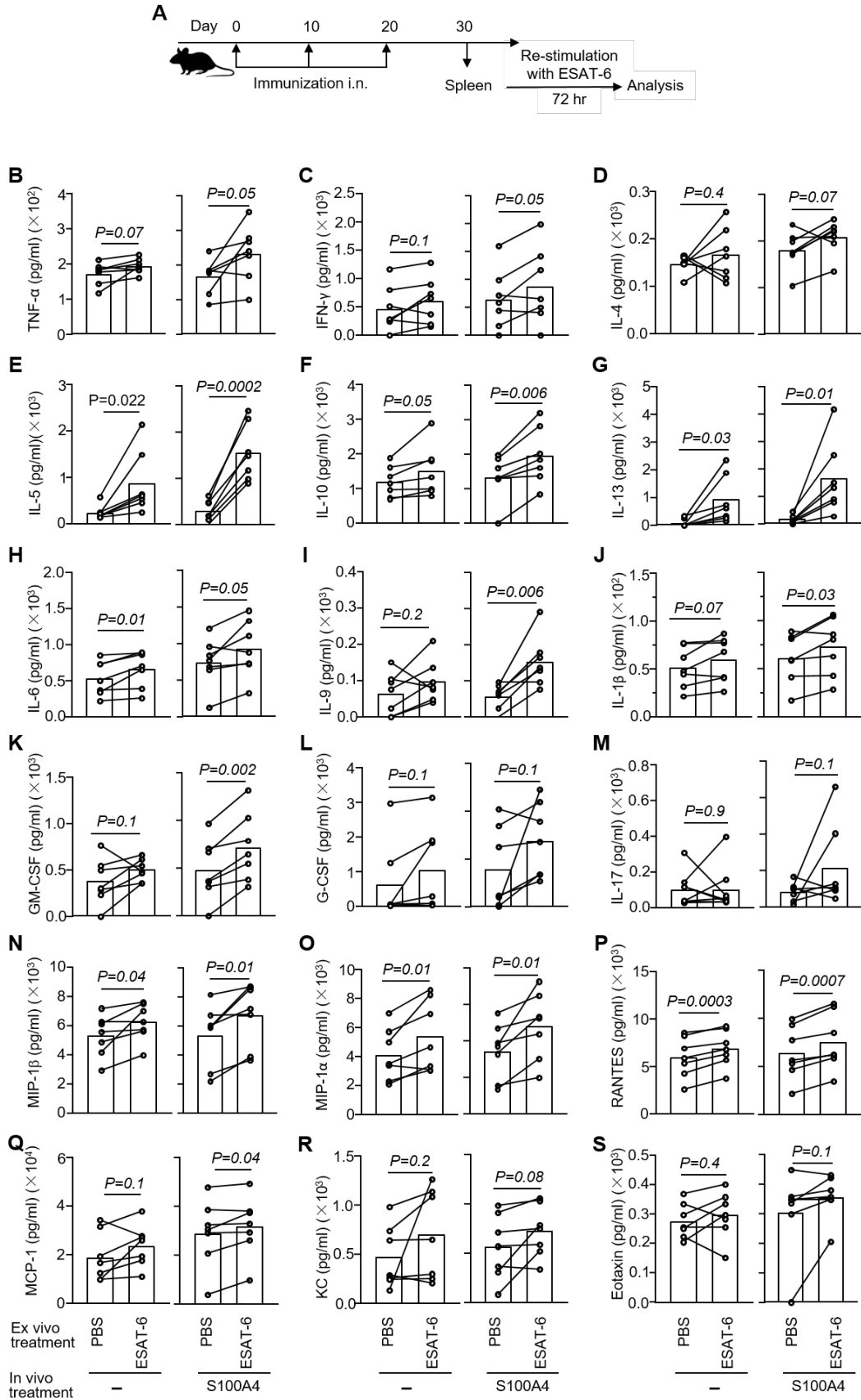


Figure 4.24. S100A4 augments cytokine and chemokine secretion by splenocytes after re-stimulation ex vivo with the immunizing antigen ESAT-6 derived from *Mycobacterium tuberculosis*. Mice were intranasally (i.n.) immunized with ESAT-6 (5 µg) alone or admixed to S100A4 (10 µg) three times at an interval of 10 days. The mouse spleen was harvested 10 days after the last immunization for analysis. Splenocytes were treated with or without ESAT-6 (2 µg/ml) for 72 hr at 37°C in 5% CO₂ (A). Concentrations of secreted cytokines and chemokines as indicated in the splenocyte culture supernatants were measured using the Bio-Plex multiplex assay (B to S). Each line represents data from a single mouse, and each column indicates the average values. The exact *P*-values (italic numbers) are determined by Student's *t*-test.

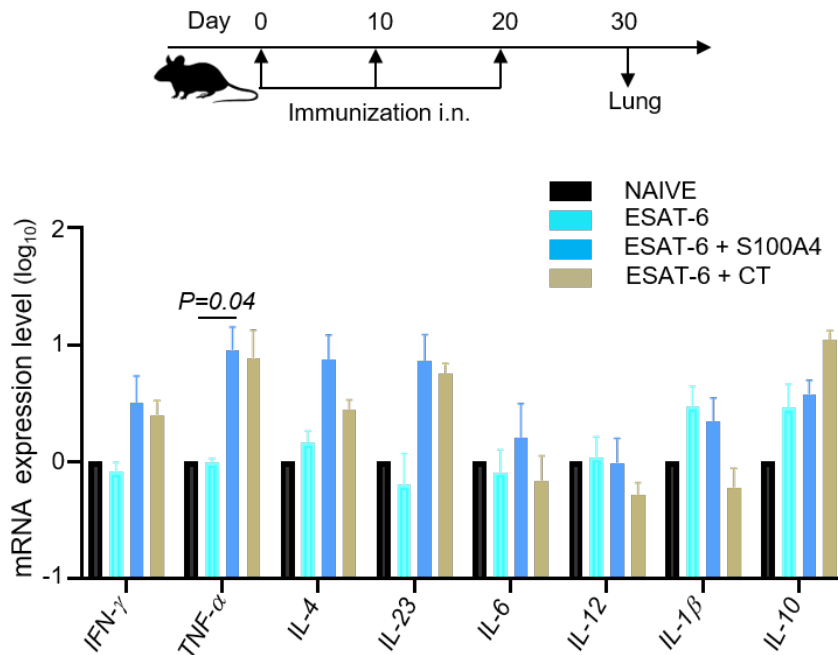


Figure 4.25. S100A4 induces the expression of cytokines in the lung tissues after immunization with a *Mycobacterium tuberculosis*-derived antigen ESAT-6. Mice were intranasally (i.n.) immunized with ESAT-6 (5 µg) alone or admixed to S100A4 (10 µg) or cholera toxin (CT; 1 µg) three times at an interval of 10 days. The mouse lung tissues were harvested and processed for the measurement of mRNA expression of relevant cytokines. Glyceraldehyde 3-phosphate dehydrogenase (GAPDH) was used as the calibrator gene to normalize gene expression. Data are expressed as mean + SEM. The exact *P*-value (italic number) is determined by ANOVA with a multiple comparison test.

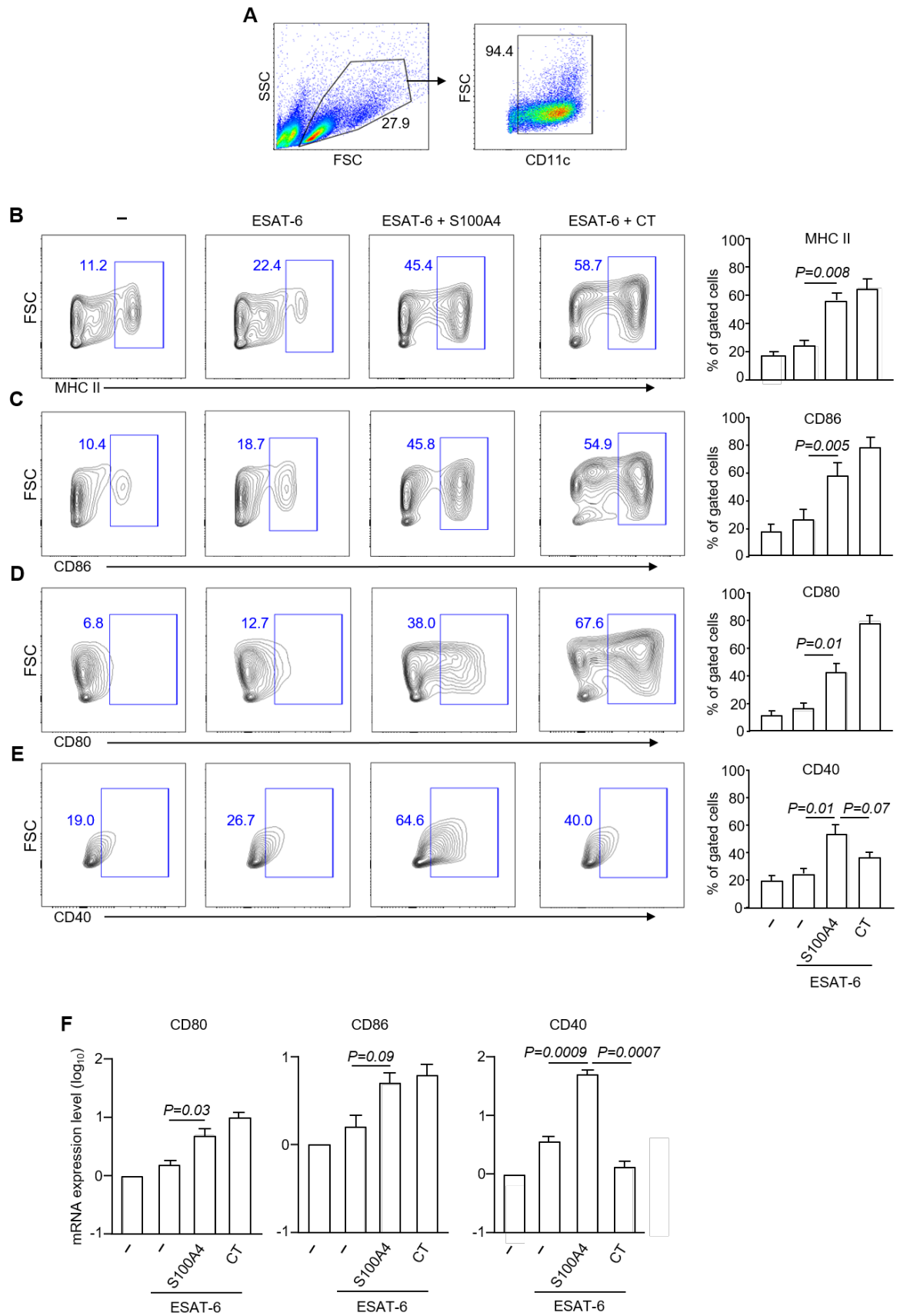


Figure 4.26. S100A4 enhances the expression of MHC class II and costimulatory molecules by dendritic cells *in vitro*. Mouse bone marrow cells were cultured in the presence of Flt3-L for nine days to obtain bone marrow-derived dendritic cells (BMDCs) confirmed by CD11c expression using flow cytometry (A). BMDCs were treated overnight with or without ESAT-6 (1 $\mu\text{g}/\text{ml}$), or with ESAT-6 together with S100A4 (1 $\mu\text{g}/\text{ml}$) or cholera toxin (CT; 1 $\mu\text{g}/\text{ml}$) (B to E). Dendritic cell activation was determined by measuring the expression of MHC class II (B) and costimulatory molecules, including CD80 (C), CD86 (D) and CD40 (E) using flow cytometry. Representative contour plots based on one experiment (left panels) and pooled results from three biological replicates (right panels) are shown (B to E). Numbers adjacent to outlined areas indicate percent cells in each gate. (F) BMDCs were treated for 3 hr with ESAT-6 (1 $\mu\text{g}/\text{ml}$) alone or together with S100A4 (1 $\mu\text{g}/\text{ml}$) or CT (1 $\mu\text{g}/\text{ml}$). Costimulatory molecules as indicated were measured using RT-qPCR. Glyceraldehyde 3-phosphate dehydrogenase (GAPDH) was used as the calibrator gene to normalize gene expression. Data are presented as mean + SEM of three biological replicates. The exact *P*-values (*italic numbers*) are determined by Student's *t*-test.

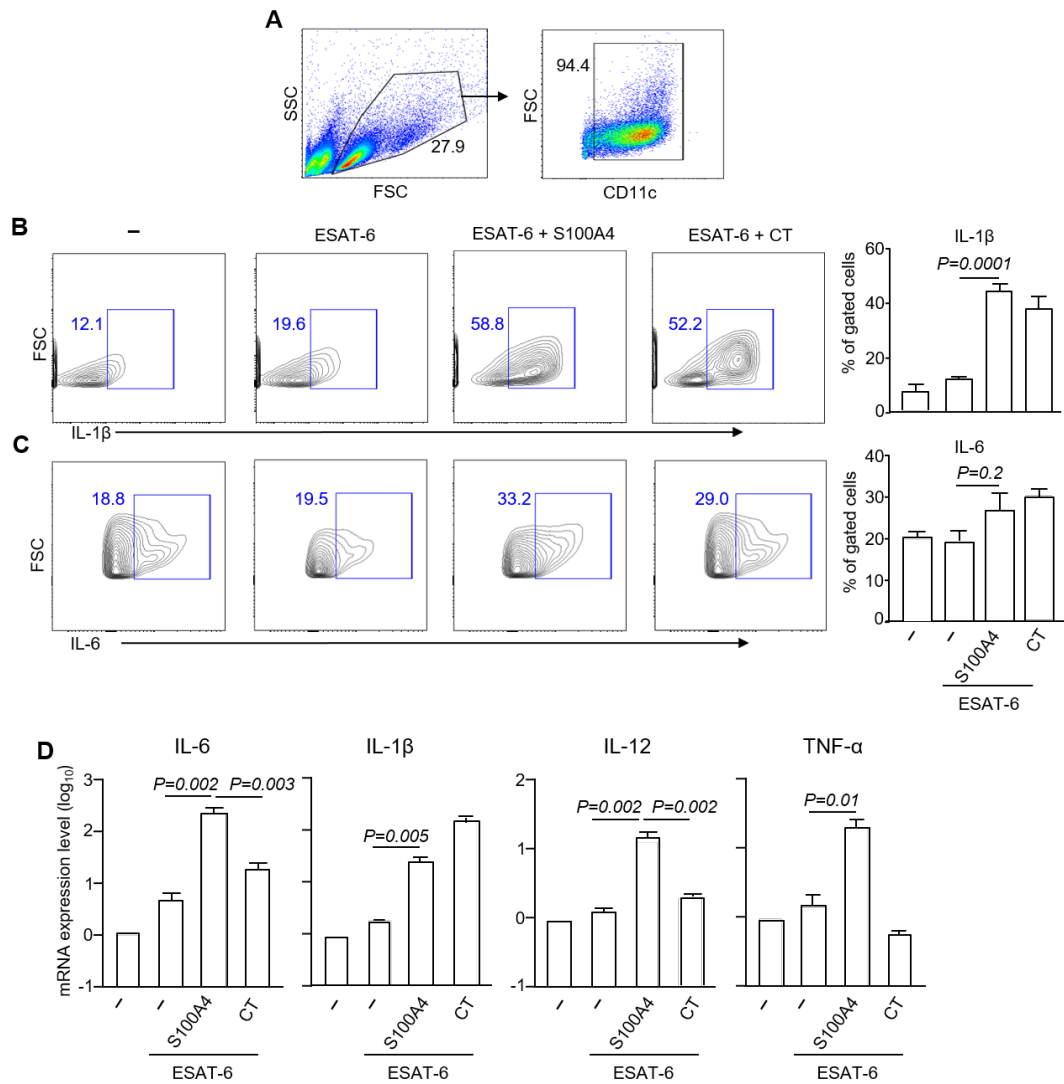


Figure 4.27. S100A4 promotes secretion of pro-inflammatory cytokines by dendritic cells in vitro. Mouse bone marrow cells were cultured in the presence of Flt3-L for nine days to obtain bone marrow-derived dendritic cells (BMDCs). (A to C) BMDCs were treated overnight with or without ESAT-6 (1 $\mu\text{g/ml}$), or with ESAT-6 together with S100A4 (1 $\mu\text{g/ml}$) or cholera toxin (CT; 1 $\mu\text{g/ml}$). The gating strategy for identifying BMDC using flow cytometry is shown (A). Intracellular expression of IL-6 (B) and IL-1 β (C) was measured using flow cytometry. Representative contour plots based on one experiment (left panels) and pooled results from three biological replicates (right panels) are shown (B and C). Numbers adjacent to outlined areas indicate percent cells in each gate. (D) BMDCs were treated for 3 hr with ESAT-6 (1 $\mu\text{g/ml}$) alone or together with S100A4 (1 $\mu\text{g/ml}$) or CT (1 $\mu\text{g/ml}$). Pro-inflammatory cytokines as indicated were measured using RT-qPCR. Glyceraldehyde 3-phosphate dehydrogenase (GAPDH) was used as the calibrator gene to normalize gene expression. Data are presented as mean + SEM of three biological replicates. The exact *P*-values (italic numbers) are determined by Student's *t*-test.

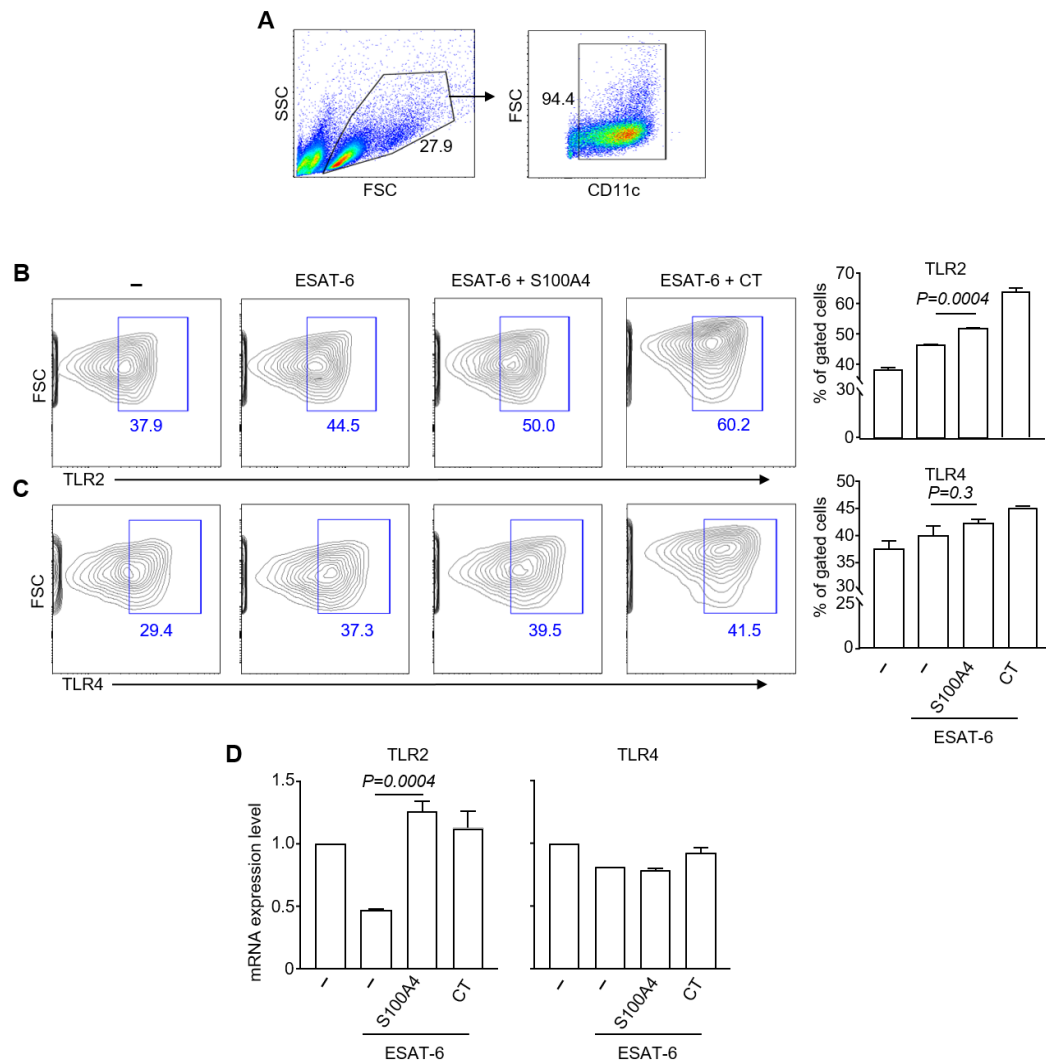


Figure 4.28. S100A4 enhances the expression of TLR2 on dendritic cells in vitro. Mouse bone marrow cells were cultured in the presence of Flt3-L for nine days to obtain bone marrow-derived dendritic cells (BMDCs). (A to C) BMDCs were treated overnight with or without ESAT-6 (1 $\mu\text{g}/\text{ml}$), or with ESAT together with S100A4 (1 $\mu\text{g}/\text{ml}$) or cholera toxin (CT; 1 $\mu\text{g}/\text{ml}$). The gating strategy for identifying BMDC using flow cytometry is shown (A). The expression of TLR2 and TLR4 by dendritic cells was analyzed. Representative contour plots based on one experiment (left panels) and pooled results from three biological replicates (right panels) are shown (B and C). Numbers adjacent to outlined areas indicate percent cells in each gate. (D) BMDCs were treated for 3 hr with ESAT-6 (1 $\mu\text{g}/\text{ml}$) alone or together with S100A4 (1 $\mu\text{g}/\text{ml}$) or CT (1 $\mu\text{g}/\text{ml}$). Total RNA was extracted to measure the mRNA expression of TLR2 and TLR4 using RT-qPCR. Glyceraldehyde 3-phosphate dehydrogenase (GAPDH) was used as a calibrator gene to normalize gene expression. Data are presented as mean + SEM of three biological replicates. The exact *P*-values (*italic numbers*) are determined by Student's *t*-test.

5. DISCUSSION

Prior to my thesis work, together with my colleagues, we had published our initial observation demonstrating the robust mucosal adjuvant activity of S100A4 (84). In the current study, I have sufficiently advanced our understanding of S100A4 as a potential mucosal adjuvant with compelling experimental data. My work not only confirmed the remarkable adjuvanticity of S100A4 previously revealed but also provided further insights into the relevance and mechanism supporting the translational value of this molecule as a clinically applicable mucosal adjuvant. Essentially, my data show that S100A4 effectively augmented antigen-specific immune responses to both a model vaccine antigen (i.e., OVA) and a clinically relevant vaccine antigen derived from *Mycobacterium tuberculosis* (i.e., ESAT-6) after intranasal immunization. S100A4 clearly augmented both humoral immune responses and T cell responses at late memory time points. Importantly, exogenous delivery of S100A4 through the nasal cavity did not engender any signs of toxicity or tumorigenicity. Taken together, my data support S100A4 as a potential mucosal adjuvant candidate for formulating a clinically applicable nasal-spray vaccine against TB.

The search for novel vaccine formulations with reliable protective efficacy to replace the currently licensed BCG vaccine for tackling TB remains one of the major challenges for the vaccinology community. In fact, the extrapulmonary form of TB can largely be controlled when children are widely vaccinated with the BCG vaccine which is available worldwide (92). However, despite the widespread use of the BCG vaccine, TB still remains one of the dreadful infectious diseases (141). This is assumed to be due to the ineffectiveness of BCG in protecting adults, especially against pulmonary infection. Over the last two decades, numerous vaccine candidates have been vigorously evaluated using various vaccine development platforms. Unfortunately, the results of recent clinical trials of several TB vaccine candidates are discouraging (115).

Mycobacterium tuberculosis-derived antigen selection is crucial in the development of protective subunit vaccines against TB (142). Various subunit vaccines against TB have been explored (143). ESAT-6 is a major virulence factor that plays a critical role in inducing the lysis of host cell phagosomes to facilitate mycobacterial survival (102). It is an abundantly secreted

protein and is maintained throughout the infection (100). Importantly, ESAT-6 is an immunodominant antigen that induces both humoral and cell-mediated immune responses (144). It is therefore expected that immune responses launched against ESAT-6 will generate protective immunity against infection caused by *Mycobacterium tuberculosis*. Compared with an inert protein such as OVA, ESAT-6 alone could induce higher levels of antigen-specific antibody production and T-cell responses, probably because ESAT-6 is a pathogen-derived peptide that can interact with TLR2 (72). However, I assume that the immune responses generated by ESAT-6 are not sufficiently high from a vaccination efficacy point of view. Only a few adjuvants have been tested for use in developing TB vaccines, including those using ESAT-6 as an antigen (98). I first tested the adjuvant activity of S100A4 in augmenting immune responses against ESAT-6. Indeed, when admixed to S100A4, ESAT-6 potentiated a much stronger humoral and cellular adaptive immune response.

For achieving long-lasting immune memory and effective protection against intracellular pathogens such as *Mycobacterium tuberculosis*, adjuvants that can modulate the host response toward Th1 cell-dependent immunity are demanded (145). Therefore, many of the adjuvants currently under exploitation for augmenting anti-*Mycobacterium tuberculosis* vaccines, including AS01E (a liposome-based vaccine adjuvant system), IC31 [combination of antibacterial peptide (KLKL(5)KLLK and synthetic oligodeoxynucleotides], GLA-SE (glucopyranosyl lipid adjuvant-stable emulsion), and CAF01 (cationic adjuvant formulation 01) are being tested for their capacity in potentiating Th1-polarized effector cytokine responses (115). The vaccine formulation M72/AS01E, comprising *Mycobacterium tuberculosis*-derived Mtb39a and Mtb32a proteins as antigen and AS01E as adjuvant, is essential for dendritic cell stimulation and adaptive immune response activation. Another formulation, H56/IC31, which contains *Mycobacterium tuberculosis* antigens Ag85B, ESAT-6, and Rv2660c together with the adjuvant IC31, induces Th1-mediated immune responses with the Th1-associated effector cytokines. Furthermore, H1/CAF01, which contains Ag85B and ESAT-6 as antigen with the CAF01 adjuvant, is known to induce multifunctional T cells with Th1/Th17 profiles (115,116). On the other hand, alum, which is a classical adjuvant, and squalene-based adjuvants like AS03 and MF59, although approved for human use, are known to be poor inducers of Th1 immunity (146,147). Therefore, my data, which revealed the strong Th1-associated activity of S100A4,

further support the relevance of S100A4 as a mucosal adjuvant in the vaccine formulation that is effective in protecting against *Mycobacterium tuberculosis* infection.

Although the primary immunologic axis in developing TB vaccines points to cell-mediated immune responses, mounting evidence suggests that antibody responses also play a critical role in controlling the infection (131,148). An experimental study using a mouse vaccination model supports that the *Mycobacterium tuberculosis* antigen-specific antibodies are critical in reducing bacterial loads (131), and inducing microbicidal activity (149). Furthermore, a number of studies have recently reported evidence of the protective potential of *Mycobacterium tuberculosis*-specific IgG antibodies (150–152). A variety of mechanisms underlying antibody-mediated protection against *Mycobacterium tuberculosis* have been described, which include antibody-dependent cell-mediated cytotoxicity (ADCC), enhancement of phagocytosis, neutralization, and inflammasome activation (150,153). Antigen-specific antibody can also promote a rapid uptake, processing and presentation of pathogen-derived antigen by APCs through Fc receptors (FcR) (31). Indeed, M72/AS01E, a subunit vaccine formulation under phase IIb clinical trial, induced protective anti-M72-specific antibody responses in the blood circulation (154). Increased antigen-specific serum IgG antibody production is observed following intranasal immunization of ESAT-6 admixed to c-di-AMP as adjuvant (155). Thus, *Mycobacterium tuberculosis*-specific antibody responses also deserve consideration for the development of effective TB vaccines (153). In this thesis work, I showed that S100A4-adjuvanted mice displayed robust production of ESAT-6-specific total IgG, IgG1 and IgG2c antibody in the blood circulation as well as ESAT-6-specific IgA and total IgG antibody in mucosal tissues. These findings confirming the role of S100A4 in augmenting robust humoral immune responses also support the relevance of an S100A4-containing TB vaccine formulation. Stimulation of antigen-specific humoral immune responses following S100A4-adjuvanted immunization led to the production of antigen-specific Th1-dependent IgG2c and Th2-dependent IgG1 antibody, indicating effective activation of both Th1 and Th2 arms of immunity.

In addition to IgG, increases in antigen-specific IgA antibody production in various mucosal tissues were observed after nasal administration of S100A4 with ESAT-6. A previous study has

shown that mucosal immunization with MTBVAC and BCG elicited strong *Mycobacterium tuberculosis*-specific antibodies in mucosal tissues, which improved phagocytosis (150). Similarly, mucosal immunization with heat-killed MTBVAC in BCG-primed mice induced high levels of IgA in mucosal tissues, providing enhanced protection against *Mycobacterium tuberculosis* infection (156). Importantly, in vitro experiments have shown that *Mycobacterium tuberculosis*-specific IgA from TB patients successfully inhibits the growth of *Mycobacterium tuberculosis* in a lung epithelial cell line (157). Furthermore, a number of adjuvanted subunit vaccine formulations augmented antibody production in mucosal tissues (151,155). The enhanced *Mycobacterium tuberculosis*-specific antibody production in respiratory mucosal tissues consistent with the current study suggests that vaccine-induced mucosal IgA antibody response is crucial in eliminating the pathogens that cross the mucosal barrier (56). It has been demonstrated that Th17 cells in the mucosal compartments, particularly the lung, play a crucial role in enhancing IgA antibody production (158). Consistently, I have observed S100A4-mediated enhancement of Th17 cell responses and antigen-specific IgA production.

T cells play a crucial role in protecting against intracellular pathogens that cause pulmonary diseases. Immunization with M72/AS01E significantly increases antigen-specific polyfunctional CD4 T cell responses, improving protection efficacy against TB in clinical trials (154). Mucosal immunization with H56/CAF01 induces polyfunctional CD4 T cells that localize to the lung parenchyma and provides long-term protection against virulent *Mycobacterium tuberculosis* infection (159). Several previous studies using adjuvanted subunit vaccine formulations have demonstrated that strong antigen-specific Th1 immune responses can confer protection against *Mycobacterium tuberculosis* infection (116). Therefore, vaccines that effectively potentiate the activation of antigen-specific Th1 cells are predicted to be relevant for combating intracellular pathogens such as *Mycobacterium tuberculosis*. In the current study, my data demonstrate that S100A4-adjuvanted intranasal immunization induced robust antigen-specific Th1 immune responses.

Multiple effector pro-inflammatory cytokines expressed by antigen-specific memory T cells have been shown to confer long-term protection against *Mycobacterium tuberculosis* infection (115). Hence, T cells expressing multiple effector pro-inflammatory cytokines are functionally

superior to their single cytokine-producing counterparts (115). Th1-associated effector cytokines, specifically IFN- γ and TNF- α , are critical in priming phagocytic cells to combat *Mycobacterium tuberculosis* infection (160). *Mycobacterium tuberculosis* and other intracellular pathogens have been shown to be effectively controlled by IFN- γ . It activates macrophages, through the production of inducible nitric oxide synthase (iNOS) for their effector function against intracellular pathogens (161). Co-expression of TNF- α and IFN- γ can more effectively eliminate intracellular pathogens (162). Therefore, the fact that S100A4 could stimulate the production of antigen-specific memory T cells that were capable of simultaneously producing multiple effector cytokines suggests that this molecule is a good mucosal adjuvant candidate that elicits plausible protective T cell-mediated immune responses.

In addition to Th1, my work has also revealed that S100A4 promoted Th17 cell responses, with increased levels of IL-17 expression in both systemic and respiratory mucosal compartments. Th17 cells have emerged as key players in protecting against mycobacterial infection by recruiting activated phagocytic cells (163). Furthermore, Th17 cells play a critical role in vaccine-mediated immunity by promoting early recruitment of IFN- γ -producing T cells to the lungs, resulting in early control of *Mycobacterium tuberculosis* replication (163). Importantly, the increased production of antimicrobial peptides and lymphocyte chemoattractants by Th1/Th17 cells is critical for effective immune responses against TB (164). It has been shown that various adjuvanted subunit vaccine formulations containing relevant *Mycobacterium tuberculosis* antigens, such as HSP90-E6 and H1/CAF01, promote strong Th1/Th17 immune responses, conferring protection against *Mycobacterium tuberculosis* infection (164,165). Notably, mucosal immunization with H56/CAF01 remarkably increased antigen-specific Th1 and Th17 responses to inhibit the replication of *Mycobacterium tuberculosis* (159). Mounting evidence suggests that the synergistic immune responses of IFN- γ and IL-17 effectively inhibit *Mycobacterium tuberculosis* growth by promoting phagolysosomal fusion and maturation (164). IL-17 is an inflammatory cytokine that acts as a double-edged sword of immunity, mediating protective immune responses to pathogens as well as triggering inflammatory responses (163). However, antigen-specific Th1/Th17 immune responses are assumed to provide balanced protection and inflammation, ensuring *Mycobacterium tuberculosis* control without causing pathological damage (164). Taken together, S100A4-promoted expression of IFN- γ , IL-17 and

IL-10 observed in the current study suggests that S100A4 is a strong mucosal adjuvant in inducing a mixed Th1/Th17/Treg immune responses, which might orchestrate balanced protective immune responses against TB.

Cytotoxic T cells are major effector cells in directly fighting intracellular pathogens. Activated cytotoxic T cells released a variety of effector molecules, including perforin and granzymes. Granzyme B is a toxic molecule that is essential for the potent killing of target cells by cytotoxic T cells (119). Proinflammatory cytokines, particularly IFN- γ and TNF- α are also highly expressed when cytotoxic T cells are activated (119). The production of IFN- γ by cytotoxic T cells is critical in inhibiting the growth of intracellular pathogens and this cytokine plays a key role in inducing the expression of MHC class I molecules (119). Hence, in the current scenario, the fact that S100A4 could enhance antigen-specific cytotoxic T cell-associated expression of granzyme B and pro-inflammatory cytokines supports the capacity of S100A4 in driving the cytotoxic T cell-mediated clearance of intracellular pathogens such as *Mycobacterium tuberculosis*.

Mycobacterium tuberculosis is capable of subverting the host immune system during natural infection by limiting antigen presentation, the first step in kicking off the adaptive immune response (166). Thus, a vaccine adjuvant that can facilitate antigen presentation is desirable. The *Mycobacterium tuberculosis*-derived antigen ESAT-6 is taken up by APCs via TLR2 or TLR4 (167,168). Interestingly, S100A4-treated dendritic cells promoted the expression of TLR2, a central receptor for ESAT-6. When dendritic cells were treated with ESAT-6 admixed to S100A4, costimulatory molecules including CD86, CD80, and CD40 were substantially increased.

Despite the fact that the current thesis has provided overwhelming experimental evidence supporting a potential role of S100A4 in augmenting mucosal immunization using a *Mycobacterium tuberculosis*-relevant vaccine antigen, a fundamentally important experiment that is still lacking is the live-bacteria challenge assay. However, *Mycobacterium tuberculosis* is a human pathogen that has to be handled under biosafety level 3 containment (169). Unfortunately, I did not have access to such a facility at the Hong Kong Polytechnic University. Therefore, animal challenge

experiments using live bacteria are warranted to assess the real protective capacity of S100A4-driven vaccination efficacy in the future.

In conclusion, my thesis work demonstrates that S100A4 is an effective mucosal adjuvant that augments robust antigen-specific humoral and cellular immune responses with remarkable durability. As a mechanistic explanation, S100A4 can remarkably enhance dendritic cell activation and migration. This is also the first study that implicates the suitability of inclusion of S100A4 in a clinically applicable vaccine formulation, which is exemplified by robust S100A4-mediated adaptive immune responses against TB both systemically and in mucosal tissues. Importantly, S100A4 presents a good safety profile as a mucosal adjuvant for intranasal immunization. This study has shed light on the future development of S100A4 as a clinically applicable mucosal adjuvant suitable for being formulated into a nasal-spray TB vaccine.

6. REFERENCES

1. World Health Organization. Global Tuberculosis Report 2022. (WHO, Geneva, 2022).
2. World Health Organization. Global Tuberculosis Report 2020. (WHO, Geneva, 2020).
3. Peloquin CA, Davies GR. The Treatment of Tuberculosis. *Clin Pharmacol Ther.* 2021 Dec;110(6):1455–66.
4. Pietersen E, Ignatius E, Streicher EM, Mastrapa B, Padanilam X, Pooran A, et al. Long-term outcomes of patients with extensively drug-resistant tuberculosis in South Africa: a cohort study. *Lancet.* 2014;383(9924):1230–9.
5. Mirzayev F, Viney K, Linh NN, Gonzalez-Angulo L, Gegia M, Jaramillo E, et al. World Health Organization recommendations on the treatment of drug-resistant tuberculosis, 2020 update. *Eur Respir J.* 2021;57(6).
6. Shah NS, Auld SC, Brust JCM, Mathema B, Ismail N, Moodley P, et al. Transmission of extensively drug-resistant tuberculosis in South Africa. *N Engl J Med.* 2017;376(3):243–53.
7. WHO End TB Strategy: global strategy and targets for tuberculosis prevention, care and control after 2015. Geneva: World Health Organization; 2015.
8. Houben RMGJ, Dodd PJ. The Global Burden of Latent Tuberculosis Infection: A Re-estimation Using Mathematical Modelling. *PLoS Med.* 2016;13(10):1–13.
9. World Health Organization. Global Tuberculosis Report 2019. (WHO, Geneva, 2019).
10. Daffé M. The cell envelope of tubercle bacilli. *Tuberculosis (Edinb).* 2015;95 Suppl 1:S155-8.
11. Daffé M, Marrakchi H. Unraveling the structure of the mycobacterial envelope. *Microbiol Spectr.* 2019;7(4).
12. Gabriel AP, Mercado CP. Evaluation of task shifting in community-based DOTS program as an effective control strategy for tuberculosis. *ScientificWorldJournal.* 2011;11:2178–86.
13. Gustin KM, Katz JM, Tumpey TM, Maines TR. Comparison of the levels of infectious virus in respirable aerosols exhaled by ferrets infected with influenza viruses exhibiting diverse transmissibility phenotypes. *J Virol.* 2013;87(14):7864–73.
14. Sia JK, Rengarajan J. Immunology of *Mycobacterium tuberculosis* infections. *Microbiol Spectr.* 2019;7(4).
15. Zhai W, Wu F, Zhang Y, Fu Y, Liu Z. The Immune escape mechanisms of *Mycobacterium tuberculosis*. *Int J Mol Sci.* 2019;20(2).
16. Cronan MR. In the thick of it: formation of the tuberculous granuloma and its effects on host and therapeutic responses. *Front Immunol.* 2022;13:820134.
17. Kaufmann SHE. Future vaccination strategies against tuberculosis: thinking outside the box. *Immunity.* 2010;33(4):567–77.
18. Scriba TJ, Coussens AK, Fletcher HA. Human immunology of tuberculosis. 2017;1–24.
19. Pattanaik KP, Sengupta S, Jit BP, Kotak R, Sonawane A. Host-mycobacteria conflict: immune responses of the host vs. the mycobacteria TLR2 and TLR4 ligands and concomitant host-directed therapy. *Microbiol Res.* 2022;264:127153.
20. Jang A-R, Kim G, Hong JJ, Kang SM, Shin SJ, Park J-H. *Mycobacterium tuberculosis* ESAT-6 drives the activation and maturation of bone marrow-derived dendritic cells via TLR4-mediated signaling. *Immune Netw.* 2019;19(2).
21. Khan N, Vidyarthi A, Pahari S, Agrewala JN. Distinct strategies employed by dendritic cells and macrophages in restricting *Mycobacterium tuberculosis* infection: different

- philosophies but same desire. *Int Rev Immunol*. 2016;35(5):386–98.
22. Guirado E, Schlesinger LS, Kaplan G. Macrophages in tuberculosis: friend or foe. *Semin Immunopathol*. 2013;35(5):563–83.
 23. Sia JK, Georgieva M, Rengarajan J. Innate immune defenses in human tuberculosis: an overview of the interactions between *Mycobacterium tuberculosis* and innate immune cells. *J Immunol Res*. 2015;2015.
 24. Wolf AJ, Linas B, Trevejo-Nuñez GJ, Kincaid E, Tamura T, Takatsu K, et al. *Mycobacterium tuberculosis* infects dendritic cells with high frequency and impairs their function in vivo . *J Immunol*. 2007;179(4):2509–19.
 25. Henrickson SE, Mempel TR, Mazo IB, Liu B, Artyomov MN, Zheng H, et al. T cell sensing of antigen dose governs interactive behavior with dendritic cells and sets a threshold for T cell activation. *Nat Immunol*. 2008;9(3):282–91.
 26. Mellman I. Dendritic cells: master regulators of the immune response. *Cancer Immunol Res*. 2013;1(3):145–9.
 27. Lutz MB. Induction of CD4⁺ regulatory and polarized effector/helper T cells by dendritic cells. *Immune Netw*. 2016;16(1):13–25.
 28. Kim B, Kim TH. Fundamental role of dendritic cells in inducing Th2 responses. *Korean J Intern Med*. 2018;33(3):483–9.
 29. Korn T, Bettelli E, Oukka M, Kuchroo VK. IL-17 and Th17 Cells. *Annu Rev Immunol*. 2009;27:485–517.
 30. Mayer-Barber KD, Barber DL. Innate and adaptive cellular immune responses to *Mycobacterium tuberculosis* infection. *Cold Spring Harb Perspect Med*. 2015;5(12).
 31. Li H, Javid B. Antibodies and tuberculosis: finally coming of age? *Nat Rev Immunol*. 2018;18(9):591–6.
 32. Achkar JM, Prados-Rosales R. Updates on antibody functions in *Mycobacterium tuberculosis* infection and their relevance for developing a vaccine against tuberculosis. *Curr Opin Immunol*. 2018;53:30–7.
 33. Bemark M, Angeletti D. Know your enemy or find your friend?-Induction of IgA at mucosal surfaces. *Immunol Rev*. 2021;303(1):83–102.
 34. Basile JI, Liu R, Mou W, Gao Y, Carow B, Rottenberg ME. Mycobacteria-specific T cells are generated in the lung during mucosal BCG immunization or infection with *Mycobacterium tuberculosis*. *Front Immunol*. 2020;11:566319.
 35. Zeng G, Zhang G, Chen X. Th1 cytokines, true functional signatures for protective immunity against TB? *Cell Mol Immunol*. 2018;15(3):206–15.
 36. Morgan J, Muskat K, Tippalagama R, Sette A, Burel J, Lindestam Arlehamn CS. Classical CD4 T cells as the cornerstone of antimycobacterial immunity. *Immunol Rev*. 2021;301(1):10–29.
 37. Umemura M, Yahagi A, Hamada S, Begum MD, Watanabe H, Kawakami K, et al. IL-17-mediated regulation of innate and acquired immune response against pulmonary *Mycobacterium bovis* bacille Calmette-Guerin infection. *J Immunol*. 2007;178(6):3786–96.
 38. Enriquez AB, Izzo A, Miller SM, Stewart EL, Mahon RN, Frank DJ, et al. Advancing adjuvants for *Mycobacterium tuberculosis* therapeutics. *Front Immunol*. 2021;12:740117.
 39. Prezzemolo T, Guggino G, La Manna MP, Di Liberto D, Dieli F, Caccamo N. Functional signatures of human CD4 and CD8 T cell responses to *Mycobacterium tuberculosis*. *Front Immunol*. 2014;5:180.

40. Bhat P, Leggatt G, Waterhouse N, Frazer IH. Interferon- γ derived from cytotoxic lymphocytes directly enhances their motility and cytotoxicity. *Cell Death Dis.* 2017;8(6):e2836.
41. Russell MW, Ogra PL. Chapter 1 - Historical perspectives on mucosal vaccines. In: Kiyono H, Pascual DWBT-MV (Second E, editors. Academic Press; 2020. p. 3–17.
42. Greenwood B. The contribution of vaccination to global health: past, present and future. *Philos Trans R Soc Lond B Biol Sci.* 2014;369(1645):20130433.
43. Klugman KP, Black S. Impact of existing vaccines in reducing antibiotic resistance: Primary and secondary effects. *Proc Natl Acad Sci U S A.* 2018;115(51):12896–901.
44. Lavelle EC, Ward RW. Mucosal vaccines — fortifying the frontiers. *Nat Rev Immunol.* 2022;22(4):236–50.
45. Pollard AJ, Bijker EM. A guide to vaccinology: from basic principles to new developments. *Nat Rev Immunol.* 2021;21(2):83–100.
46. Johansen P, Kündig TM. Parenteral Vaccine Administration: Tried and True BT - subunit vaccine delivery. In: Foged C, Rades T, Perrie Y, Hook S, editors. New York, NY: Springer New York; 2015. p. 261–86.
47. Jonker EFF, Visser LG, Roukens AH. Advances and controversies in yellow fever vaccination. *Ther Adv Vaccines.* 2013;1(4):144–52.
48. Lindblad EB. Aluminum adjuvants: basic concepts and progress in understanding BT - subunit vaccine delivery. In: Foged C, Rades T, Perrie Y, Hook S, editors. New York, NY: Springer New York; 2015. p. 33–57.
49. SABIN AB. Present status of attenuated live-virus poliomyelitis vaccine. *J Am Med Assoc.* 1956;162(18):1589–96.
50. Takaki H, Ichimiya S, Matsumoto M, Seya T. Mucosal immune response in nasal-associated lymphoid tissue upon intranasal administration by adjuvants. *J Innate Immun.* 2018;10(5–6):515–21.
51. Mutsch M, Zhou W, Rhodes P, Bopp M, Chen RT, Linder T, et al. Use of the inactivated intranasal influenza vaccine and the risk of Bell's palsy in Switzerland. *N Engl J Med.* 2004;350(9):896–903.
52. Kim S-H, Jang Y-S. The development of mucosal vaccines for both mucosal and systemic immune induction and the roles played by adjuvants. *Clin Exp Vaccine Res.* 2017;6(1):15–21.
53. Bernasconi V, Norling K, Bally M, Höök F, Lycke NY. Mucosal vaccine development based on liposome technology. *J Immunol Res.* 2016;2016:5482087.
54. Mantis NJ, Forbes SJ. Secretory IgA: arresting microbial pathogens at epithelial borders. *Immunol Invest.* 2010;39(4–5):383–406.
55. Criscuolo E, Caputo V, Diotti RA, Sautto GA, Kirchenbaum GA, Clementi N. Alternative methods of vaccine delivery: an overview of edible and intradermal vaccines. *J Immunol Res.* 2019;2019:8303648.
56. Mangla B, Javed S, Sultan MH, Ahsan W, Aggarwal G, Kohli K. Nanocarriers-assisted needle-free vaccine delivery through oral and intranasal transmucosal routes: A novel therapeutic conduit. *Front Pharmacol.* 2021;12:757761.
57. Marasini N, Skwarczynski M, Toth I. Oral delivery of nanoparticle-based vaccines. *Expert Rev Vaccines.* 2014;13(11):1361–76.
58. Jin Z, Gao S, Cui X, Sun D, Zhao K. Adjuvants and delivery systems based on polymeric nanoparticles for mucosal vaccines. *Int J Pharm.* 2019;572:118731.

59. Feng F, Wen Z, Chen J, Yuan Y, Wang C, Sun C. Strategies to develop a mucosa-targeting vaccine against emerging infectious diseases. *Viruses*. 2022;14(3).
60. Goodnow CC, Vinuesa CG, Randall KL, Mackay F, Brink R. Control systems and decision making for antibody production. *Nat Immunol*. 2010;11(8):681–8.
61. Holmgren J, Czerkinsky C. Mucosal immunity and vaccines. *Nat Med*. 2005;11(4S):S45.
62. Raker VK, Domogalla MP, Steinbrink K. Tolerogenic dendritic cells for regulatory T cell induction in man. *Front Immunol*. 2015;6:569.
63. Awate S, Babiuk LA, Mutwiri G. Mechanisms of action of adjuvants. *Front Immunol*. 2013;4:114.
64. Reed SG, Orr MT, Fox CB. Key roles of adjuvants in modern vaccines. *Nat Med*. 2013;19(12):1597–608.
65. Correa VA, Portilho AI, De Gaspari E. Vaccines, adjuvants and key factors for mucosal immune response. *Immunology*. 2022;167(2):124–38.
66. Savelkoul HFJ, Ferro VA, Strioga MM, Schijns VEJC. Choice and design of adjuvants for parenteral and mucosal vaccines. *Vaccines*. 2015;3(1):148–71.
67. Sarkar I, Garg R, van Drunen Littel-van den Hurk S. Selection of adjuvants for vaccines targeting specific pathogens. *Expert Rev Vaccines*. 2019;18(5):505–21.
68. Manicassamy, S. & Pulendran B. Modulation of adaptive immunity with toll-like receptors. *Semin Immunol*. 2009;21:185–193.
69. Galli G, Hancock K, Hoschler K, DeVos J, Praus M, Bardelli M, et al. Fast rise of broadly cross-reactive antibodies after boosting long-lived human memory B cells primed by an MF59 adjuvanted prepandemic vaccine. *Proc Natl Acad Sci U S A*. 2009;106(19):7962–7.
70. Djuricic S, Jakobsen JC, Petersen SB, Kenfelt M, Klingenberg SL, Gluud C. Aluminium adjuvants used in vaccines. Vol. 2018, *The Cochrane Database of Systematic Reviews*. 2018.
71. Yang J-X, Tseng J-C, Yu G-Y, Luo Y, Huang C-YF, Hong Y-R, et al. Recent advances in the development of toll-like receptor agonist-based vaccine adjuvants for infectious diseases. *Pharmaceutics*. 2022;14(2).
72. Kim J-S, Kim Y-R, Yang C-S. Latest comprehensive knowledge of the crosstalk between TLR signaling and mycobacteria and the antigens driving the process. *J Microbiol Biotechnol*. 2019;29(10):1506–21.
73. Duan Q, Xia P, Nandre R, Zhang W, Zhu G. Review of newly identified functions associated with the heat-labile toxin of enterotoxigenic *Escherichia coli*. *Front Cell Infect Microbiol*. 2019;9:292.
74. Stratmann T. Cholera Toxin Subunit B as Adjuvant--An accelerator in protective immunity and a break in autoimmunity. *Vaccines*. 2015;3(3):579–96.
75. Lyeke N. Is the choice of vaccine adjuvant critical for long-term memory development? Vol. 9, *Expert review of vaccines*. England; 2010. p. 1357–61.
76. Schussek S, Bernasconi V, Mattsson J, Wenzel UA, Strömberg A, Gribonika I, et al. The CTA1-DD adjuvant strongly potentiates follicular dendritic cell function and germinal center formation, which results in improved neonatal immunization. *Mucosal Immunol*. 2020;13(3):545–57.
77. Anders H-J, Schaefer L. Beyond tissue injury-damage-associated molecular patterns, toll-like receptors, and inflammasomes also drive regeneration and fibrosis. *J Am Soc Nephrol*. 2014;25(7):1387–400.

78. Fleshner M, Crane CR. Exosomes, DAMPs and miRNA: Features of stress physiology and immune homeostasis. *Trends Immunol.* 2017;38(10):768–76.
79. Srivastava A, Gowda DV, Madhunapantula S V, Shinde CG, Iyer M. Mucosal vaccines: a paradigm shift in the development of mucosal adjuvants and delivery vehicles. *APMIS.* 2015;123(4):275–88.
80. Bianchi ME. DAMPs, PAMPs and alarmins: all we need to know about danger. *J Leukoc Biol.* 2007;81(1):1–5.
81. Fei F, Qu J, Li C, Wang X, Li Y, Zhang S. Role of metastasis-induced protein S100A4 in human non-tumor pathophysiologies. *Cell Biosci.* 2017;7:64.
82. Ambartsumian N, Klingelhöfer J, Grigorian M. The multifaceted S100A4 protein in cancer and inflammation. *Methods Mol Biol.* 2019;1929:339–65.
83. Nefla M, Holzinger D, Berenbaum F, Jacques C. The danger from within: alarmins in arthritis. *Nat Rev Rheumatol.* 2016;12(11):669–83.
84. Sen Chaudhuri A, Yeh Y-W, Zewdie O, Li NS, Sun J-B, Jin T, et al. S100A4 exerts robust mucosal adjuvant activity for co-administered antigens in mice. *Mucosal Immunol.* 2022;15(5):1028–39.
85. Park W-Y, Gray JM, Holewinski RJ, Andresson T, So JY, Carmona-Rivera C, et al. Apoptosis-induced nuclear expulsion in tumor cells drives S100A4-mediated metastatic outgrowth through the RAGE pathway. *Nat cancer.* 2023;4(3):419–35.
86. Cerezo LA, Remáková M, Tomčík M, Gay S, Neidhart M, Lukanidin E, et al. The metastasis-associated protein S100A4 promotes the inflammatory response of mononuclear cells via the TLR4 signalling pathway in rheumatoid arthritis. *Rheumatology (Oxford).* 2014;53(8):1520–6.
87. Bruhn S, Fang Y, Barrenäs F, Gustafsson M, Zhang H, Konstantinell A, et al. A generally applicable translational strategy identifies S100A4 as a candidate gene in allergy. *Sci Transl Med.* 2014;6(218):218ra4.
88. Wu T, Ma L, Jin X, He J, Chen K, Zhang D, et al. S100A4 is critical for a mouse model of allergic asthma by impacting mast cell activation. *Front Immunol.* 2021;12:692733.
89. Sun J-B, Holmgren J, Larena M, Terrinoni M, Fang Y, Bresnick AR, et al. Deficiency in calcium-binding protein S100A4 impairs the adjuvant action of cholera toxin. *Front Immunol.* 2017;8:1119.
90. Kunimura K, Sakata D, Tun X, Uruno T, Ushijima M, Katakai T, et al. S100A4 protein is essential for the development of mature microfold cells in Peyer’s Patches. *Cell Rep.* 2019;29(9):2823–2834.e7.
91. Mishra SK, Siddique HR, Saleem M. S100A4 calcium-binding protein is key player in tumor progression and metastasis: preclinical and clinical evidence. *Cancer Metastasis Rev.* 2012;31(1–2):163–72.
92. Mangtani P, Abubakar I, Ariti C, Beynon R, Pimpin L, Fine PEM, et al. Protection by BCG vaccine against tuberculosis: a systematic review of randomized controlled trials. *Clin Infect Dis an off publ infect Dis Soc Am.* 2014;58(4):470–80.
93. Abubakar I, Pimpin L, Ariti C, Beynon R, Mangtani P, Sterne JAC, et al. Systematic review and meta-analysis of the current evidence on the duration of protection by bacillus Calmette-Guérin vaccination against tuberculosis. *Health Technol Assess.* 2013;17(37):1–vi.
94. Nandakumar S, Kannanganat S, Posey JE, Amara RR, Sable SB. Attrition of T cell functions and simultaneous upregulation of inhibitory markers correspond with the

- waning of BCG-induced protection against tuberculosis in mice. PLoS One. 2014;9(11):e113951–e113951.
95. Gröschel MI, Sayes F, Simeone R, Majlessi L, Brosch R. ESX secretion systems: mycobacterial evolution to counter host immunity. Nat Rev Microbiol. 2016;14(11):677–91.
 96. Schrager LK, Izzo A, Velmurugan K. Immunopathogenesis of tuberculosis and novel mechanisms of vaccine activity. Tuberculosis (Edinb). 2016;99 Suppl 1:S3–7.
 97. Fletcher HA, Schrager L. TB vaccine development and the End TB Strategy: importance and current status. Trans R Soc Trop Med Hyg. 2016;110(4):212–8.
 98. Kaufmann SHE, Weiner J, von Reyn CF. Novel approaches to tuberculosis vaccine development. Int J Infect Dis. 2017;56:263–7.
 99. Augenstreich J, Briken V. Host cell targets of released lipid and secreted protein effectors of *Mycobacterium tuberculosis*. Front Cell Infect Microbiol. 2020;10:595029.
 100. Mogueche AO, Musvosvi M, Penn-Nicholson A, Plumlee CR, Mearns H, Geldenhuys H, et al. Antigen availability shapes T cell differentiation and function during tuberculosis. Cell Host Microbe. 2017;21(6):695-706.e5.
 101. Shah S, Briken V. Modular organization of the ESX-5 secretion system in *Mycobacterium tuberculosis*. 2016;6:1–7.
 102. Wong K-W. The Role of ESX-1 in *Mycobacterium tuberculosis* pathogenesis. Microbiol Spectr. 2017;5(3).
 103. Tiwari S, Casey R, Goulding CW, Hingley-Wilson S, Jacobs WRJ. Infect and inject: how *Mycobacterium tuberculosis* exploits its major virulence-associated type VII secretion system, ESX-1. Microbiol Spectr. 2019;7(3).
 104. Chirakos AE, Balaram A, Conrad W, Champion PA. Modeling tubercular ESX-1 secretion using *Mycobacterium marinum*. Microbiol Mol Biol Rev. 2020;84(4).
 105. Kwon B-E, Ahn J-H, Min S, Kim H, Seo J, Yeo S-G, et al. Development of new preventive and therapeutic vaccines for tuberculosis. Immune Netw. 2018;18(2):e17.
 106. Salvatore PP, Zhang Y. Tuberculosis: Molecular basis of pathogenesis. In: Reference Module in Biomedical Sciences. Elsevier; 2017.
 107. Hatherill M, White RG, Hawn TR. Clinical development of new TB vaccines: recent advances and next steps. Front Microbiol. 2020;10:1–12.
 108. Ellis RD, Hatherill M, Tait D, Snowden M, Churchyard G, Hanekom W, et al. Innovative clinical trial designs to rationalize TB vaccine development. Tuberculosis (Edinb). 2015;95(3):352–7.
 109. Nemes E, Geldenhuys H, Rozot V, Rutkowski KT, Ratangee F, Bilek N, et al. Prevention of *Mycobacterium tuberculosis* infection with H4:IC31 vaccine or BCG revaccination. N Engl J Med. 2018;379(2):138–49.
 110. Scriba TJ, Kaufmann SHE, Henri Lambert P, Sanicas M, Martin C, Neyrolles O. Vaccination against tuberculosis with whole-cell mycobacterial vaccines. J Infect Dis. 2016;214(5):659–64.
 111. Andrews JR, Noubary F, Walensky RP, Cerda R, Losina E, Horsburgh CR. Risk of progression to active tuberculosis following reinfection with *Mycobacterium tuberculosis*. Clin Infect Dis. 2012;54(6):784–91.
 112. Bonam SR, Partidos CD, Halmuthur SKM, Muller S. An overview of novel adjuvants designed for improving vaccine efficacy. Trends Pharmacol Sci. 2017;38(9):771–93.
 113. Stewart E, Triccas JA, Petrovsky N. Adjuvant strategies for more effective tuberculosis

- vaccine immunity. *Microorganisms*. 2019;7(8):1–16.
114. Kashangura R, Jullien S, Garner P, Johnson S. MVA85A vaccine to enhance BCG for preventing tuberculosis. *Cochrane database Syst Rev*. 2019;4(4):CD012915.
 115. Sable SB, Posey JE, Scriba TJ. Tuberculosis vaccine development: progress in clinical evaluation. *Clin Microbiol Rev*. 2019;33(1).
 116. Larsen SE, Williams BD, Rais M, Coler RN, Baldwin SL. It takes a village: the multifaceted immune response to *Mycobacterium tuberculosis* infection and vaccine-induced immunity. *Front Immunol*. 2022;13:840225.
 117. Mutlu GM, Green D, Bellmeyer A, Baker CM, Burgess Z, Rajamannan N, et al. Ambient particulate matter accelerates coagulation via an IL-6-dependent pathway. *J Clin Invest*. 2007;117(10):2952–61.
 118. Tian L, Zhou W, Wu X, Hu Z, Qiu L, Zhang H, et al. CTLs: Killers of intracellular bacteria. *Front Cell Infect Microbiol*. 2022;12:967679.
 119. Janeway CA Jr, Travers P, Walport M et al. *The immune system in health and disease*. 5th editio. 2001.
 120. Danielsson R, Eriksson H. Aluminium adjuvants in vaccines - A way to modulate the immune response. *Semin Cell Dev Biol*. 2021;115:3–9.
 121. Rapaka RR, Cross AS, McArthur MA. Using adjuvants to drive T cell responses for next-generation infectious disease vaccines. *Vaccines*. 2021;9(8).
 122. Irvine DJ, Aung A, Silva M. Controlling timing and location in vaccines. *Adv Drug Deliv Rev*. 2020;158:91–115.
 123. Liang F, Lindgren G, Sandgren KJ, Thompson EA, Francica JR, Seubert A, et al. Vaccine priming is restricted to draining lymph nodes and controlled by adjuvant-mediated antigen uptake. *Sci Transl Med*. 2017;9(393).
 124. Fujihashi K, Koga T, van Ginkel FW, Hagiwara Y, McGhee JR. A dilemma for mucosal vaccination: efficacy versus toxicity using enterotoxin-based adjuvants. *Vaccine*. 2002;20(19–20):2431–8.
 125. Ivanyi J. Tuberculosis vaccination needs to avoid “decoy” immune reactions. *Tuberculosis (Edinb)*. 2021;126:102021.
 126. Casadevall A. Antibody-based vaccine strategies against intracellular pathogens. *Curr Opin Immunol*. 2018;53:74–80.
 127. Grant NL, Kelly K, Maiello P, Abbott H, O’Connor S, Lin PL, et al. *Mycobacterium tuberculosis*-specific CD4 T cells expressing transcription factors T-Bet or ROR γ T associate with bacterial control in granulomas. *MBio*. 2023;14(3):e0047723.
 128. Domingo-Gonzalez R, Prince O, Cooper A, Khader SA. Cytokines and chemokines in *Mycobacterium tuberculosis* infection. *Microbiol Spectr*. 2016;4(5).
 129. Marinaik CB, Kingstad-Bakke B, Lee W, Hatta M, Sonsalla M, Larsen A, et al. Programming multifaceted pulmonary T cell immunity by combination adjuvants. *Cell Reports Med*. 2020;1(6):100095.
 130. Kisuya J, Chemtai A, Raballah E, Keter A, Ouma C. The diagnostic accuracy of Th1 (IFN- γ , TNF- α , and IL-2) and Th2 (IL-4, IL-6 and IL-10) cytokines response in AFB microscopy smear negative PTB- HIV co-infected patients. *Sci Rep*. 2019;9(1):2966.
 131. Jacobs AJ, Mongkolsapaya J, Sreaton GR, McShane H, Wilkinson RJ. Antibodies and tuberculosis. *Tuberculosis*. 2016;101:102–13.
 132. Amelio P, Portevin D, Reither K, Mhimbira F, Mpina M, Tumbo A, et al. Mixed Th1 and Th2 *Mycobacterium tuberculosis*-specific CD4 T cell responses in patients with

- active pulmonary tuberculosis from Tanzania. *PLoS Negl Trop Dis*. 2017;11(7):e0005817.
133. Ciraci C, Janczy JR, Sutterwala FS, Cassel SL. Control of innate and adaptive immunity by the inflammasome. *Microbes Infect*. 2012;14(14):1263–70.
 134. Rothchild AC, Stowell B, Goyal G, Nunes-Alves C, Yang Q, Papavinasasundaram K, et al. Role of granulocyte-macrophage colony-stimulating factor production by T cells during *Mycobacterium tuberculosis* infection. *MBio*. 2017;8(5).
 135. Shaw DM, Merien F, Braakhuis A, Dulson D. T-cells and their cytokine production: The anti-inflammatory and immunosuppressive effects of strenuous exercise. *Cytokine*. 2018;104:136–42.
 136. Kak G, Raza M, Tiwari BK. Interferon-gamma (IFN- γ): Exploring its implications in infectious diseases. *Biomol Concepts*. 2018;9(1):64–79.
 137. Mathers AR, Cuff CF. Role of interleukin-4 (IL-4) and IL-10 in serum immunoglobulin G antibody responses following mucosal or systemic reovirus infection. *J Virol*. 2004;78(7):3352–60.
 138. Dong C. Targeting Th17 cells in immune diseases. *Cell Res*. 2014;24(8):901–3.
 139. Gaudino SJ, Kumar P. Cross-talk between antigen presenting cells and T cells impacts intestinal homeostasis, bacterial infections, and tumorigenesis. *Front Immunol*. 2019;10:360.
 140. Hilligan KL, Ronchese F. Antigen presentation by dendritic cells and their instruction of CD4⁺ T helper cell responses. *Cell Mol Immunol*. 2020;17(6):587–99.
 141. Fatima S, Kumari A, Das G, Dwivedi VP. Tuberculosis vaccine: A journey from BCG to present. *Life Sci*. 2020;252:117594.
 142. Abdallah AM, Gey van Pittius NC, DiGiuseppe Champion PA, Cox J, Luirink J, Vandembroucke-Grauls CMJE, et al. Type VII secretion—mycobacteria show the way. *Nat Rev Microbiol*. 2007;5(11):883–91.
 143. Russo G, Pappalardo F, Juarez MA, Pennisi M, Cardona PJ, Coler R, et al. Evaluation of the efficacy of RUTI and ID93/GLA-SE vaccines in tuberculosis treatment: in silico trial through UISS-TB simulator. In: 2019 IEEE International Conference on Bioinformatics and Biomedicine (BIBM). 2019. p. 2197–201.
 144. Samten B, Wang X, Barnes PF. Immune regulatory activities of early secreted antigenic target of 6-kD protein of *Mycobacterium tuberculosis* and implications for tuberculosis vaccine design. *Tuberculosis*. 2011;91(SUPPL. 1):114–8.
 145. Ottenhoff THM, Kaufmann SHE. Vaccines against tuberculosis: where are we and where do we need to go? *PLoS Pathog*. 2012;8(5):e1002607.
 146. Morel S, Didierlaurent A, Bourguignon P, Delhaye S, Baras B, Jacob V, et al. Adjuvant system AS03 containing α -tocopherol modulates innate immune response and leads to improved adaptive immunity. *Vaccine*. 2011;29(13):2461–73.
 147. McKee AS, Munks MW, Marrack P. How do adjuvants work? Important considerations for new generation adjuvants. *Immunity*. 2007;27(5):687–90.
 148. Achkar JM, Chan J, Casadevall A. B cells and antibodies in the defense against *Mycobacterium tuberculosis* infection. *Immunol Rev*. 2015;264(1):167–81.
 149. Carter MJ, Mitchell RM, Meyer Sauter PM, Kelly DF, Trück J. The Antibody-secreting cell response to infection: kinetics and clinical applications. *Front Immunol*. 2017;8:630.
 150. Dijkman K, Aguilo N, Boot C, Hofman SO, Sombroek CC, Vervenne RAW, et al. Pulmonary MTBVAC vaccination induces immune signatures previously correlated with

- prevention of tuberculosis infection. *Cell reports Med.* 2021;2(1):100187.
151. Thakur A, Rodríguez-Rodríguez C, Saatchi K, Rose F, Esposito T, Nosrati Z, et al. Dual-isotope SPECT/CT imaging of the tuberculosis subunit vaccine H56/CAF01: induction of strong systemic and mucosal IgA and T cell responses in mice upon subcutaneous prime and intrapulmonary boost immunization. *Front Immunol.* 2018;9:2825.
 152. Baldwin SL, Bertholet S, Reese VA, Ching LK, Reed SG, Coler RN. The importance of adjuvant formulation in the development of a tuberculosis vaccine. *J Immunol.* 2012;188(5):2189–97.
 153. Kawahara JY, Irvine EB, Alter G. A Case for Antibodies as mechanistic correlates of immunity in tuberculosis. *Front Immunol.* 2019;10:996.
 154. Van Der Meeren O, Hatherill M, Nduba V, Wilkinson RJ, Muyoyeta M, Van Brakel E, et al. Phase 2b controlled trial of M72/AS01(E) vaccine to prevent tuberculosis. *N Engl J Med.* 2018;379(17):1621–34.
 155. Ning H, Zhang W, Kang J, Ding T, Liang X, Lu Y, et al. Subunit Vaccine ESAT-6:c-di-AMP delivered by intranasal route elicits immune responses and protects against *Mycobacterium tuberculosis* infection. *Front Cell Infect Microbiol.* 2021;11:647220.
 156. Aguilo N, Uranga S, Mata E, Tarancon R, Gómez AB, Marinova D, et al. Respiratory immunization with a whole cell inactivated vaccine induces functional mucosal immunoglobulins against tuberculosis in mice and non-human primates. *Front Microbiol.* 2020;11:1339.
 157. Zimmermann N, Thormann V, Hu B, Köhler A, Imai-Matsushima A, Loch C, et al. Human isotype-dependent inhibitory antibody responses against *Mycobacterium tuberculosis*. *EMBO Mol Med.* 2016;8(11):1325–39.
 158. Christensen D, Mortensen R, Rosenkrands I, Dietrich J, Andersen P. Vaccine-induced Th17 cells are established as resident memory cells in the lung and promote local IgA responses. *Mucosal Immunol.* 2017;10(1):260–70.
 159. Woodworth JS, Christensen D, Cassidy JP, Agger EM, Mortensen R, Andersen P. Mucosal boosting of H56:CAF01 immunization promotes lung-localized T cells and an accelerated pulmonary response to *Mycobacterium tuberculosis* infection without enhancing vaccine protection. *Mucosal Immunol.* 2019;12(3):816–26.
 160. Sudbury EL, Clifford V, Messina NL, Song R, Curtis N. *Mycobacterium tuberculosis*-specific cytokine biomarkers to differentiate active TB and LTBI: A systematic review. *J Infect.* 2020;81(6):873–81.
 161. Ghanavi J, Farnia P, Farnia P, Velayati AA. The role of interferon-gamma and interferon-gamma receptor in tuberculosis and nontuberculous mycobacterial infections. *Int J mycobacteriology.* 2021;10(4):349–57.
 162. Lewinsohn DA, Lewinsohn DM, Scriba TJ. Polyfunctional CD4⁺ T cells as targets for tuberculosis vaccination. *Front Immunol.* 2017;8:1262.
 163. Lyadova I V, Panteleev A V. Th1 and Th17 cells in tuberculosis: protection, pathology, and biomarkers. *Mediators Inflamm.* 2015;2015:854507.
 164. Choi H-G, Kwon KW, Choi S, Back YW, Park H-S, Kang SM, et al. Antigen-specific IFN- γ /IL-17-co-producing CD4⁺ T cells are the determinants for protective efficacy of tuberculosis subunit vaccine. *Vaccines.* 2020;8(2).
 165. Lindenstrøm T, Woodworth J, Dietrich J, Aagaard C, Andersen P, Agger EM. Vaccine-induced th17 cells are maintained long-term postvaccination as a distinct and phenotypically stable memory subset. *Infect Immun.* 2012;80(10):3533–44.

166. Grace PS, Ernst JD. Suboptimal antigen presentation contributes to virulence of *Mycobacterium tuberculosis* in vivo. *J Immunol*. 2016;196(1):357–64.
167. Jang A-R, Choi J-H, Shin SJ, Park J-H. *Mycobacterium tuberculosis* ESAT-6 induces IFN- β gene expression in macrophages via TLRs-mediated signaling. *Cytokine*. 2018;104:104–9.
168. Byun E-H, Kim WS, Kim J-S, Jung ID, Park Y-M, Kim H-J, et al. *Mycobacterium tuberculosis* Rv0577, a novel TLR2 agonist, induces maturation of dendritic cells and drives Th1 immune response. *FASEB J Off Publ Fed Am Soc Exp Biol*. 2012;26(6):2695–711.
169. Nazarova E V, Russell DG. Growing and Handling of *Mycobacterium tuberculosis* for macrophage infection assays. *Methods Mol Biol*. 2017;1519:325–31.